

Superconducting RF cavities for accelerators

Fritz Caspers

slides by: Wolfgang Weingarten, Tobias Junginger, Sarah Aull,
Benedikt Peters, Michael Bartel and Manfred Wendt

CERN

JUAS lecture 2018

OUTLINE OF LECTURE

- Basics of superconductivity
- Basics of RF cavities
- Interaction of the cavity with the beam
- Technological issues
- Diagnostics
- State of the art SRF research

Basics of superconductivity

- Recommended literature
- Historical remarks
- Surface impedance and plane waves in normal conductors
- Basics of RF superconductivity
 - Meissner effect
 - Two kinds of superconductors
 - Materials
 - Two fluid model
 - London equations and penetration depth
 - Complex conductivity, surface impedance and BCS theory
 - How to measure the surface impedance
 - Critical fields
- Summary

Recommended literature

Literature

W. Buckel and R. Kleiner, « Superconductivity: Fundamentals and applications, Wiley VCH 2004

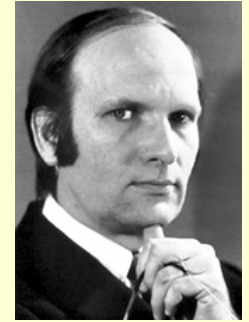
V. V. Schmidt « The physics of superconductors », Springer 1997

M. Tinkham, « Introduction to superconductivity », McGraw-Hill 1996, and many others

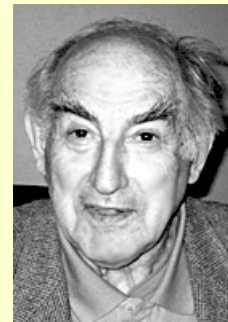
Nobel lectures (http://nobelprize.org/nobel_prizes/physics/laureates/)

Historical remarks ^{1/4}

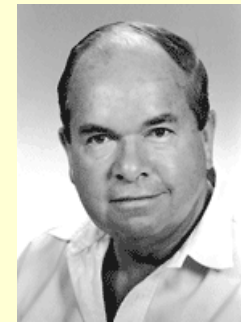
- 1908 Liquefaction of helium (4.2 K)
- 1911 Zero resistance
- 1933 Meissner effect
- 1935 Phenomenological theory of H & F. London
- 1950 Ginzburg – Landau theory
- 1951 – 2 TYPE II superconductors (Abrikosov)
- 1957 Bardeen – Cooper – Schrieffer theory
- 1960 Magnetic flux quantisation
- 1962 Josephson effect
- 1986 High temperature superconductors (Bednorz – Müller)



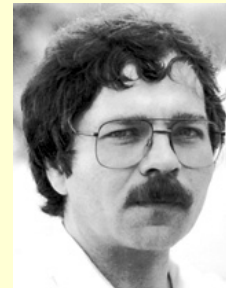
Bardeen – Cooper – Schrieffer (BCS)



Ginzburg



Abrikosov



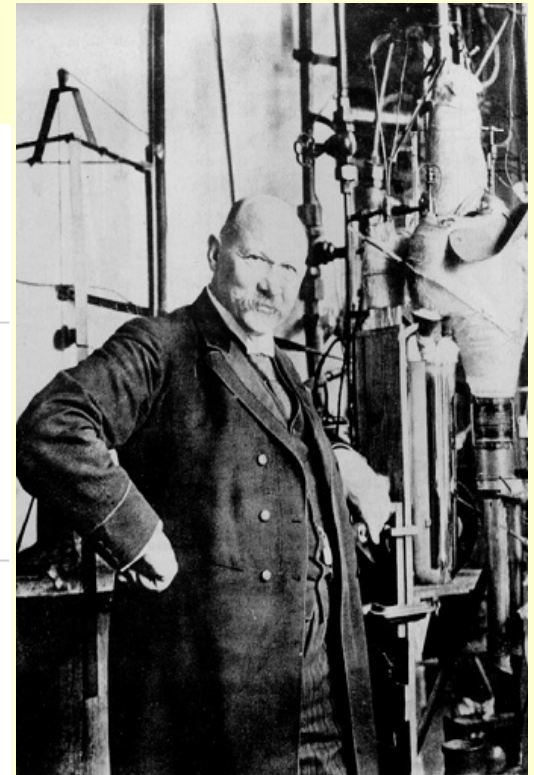
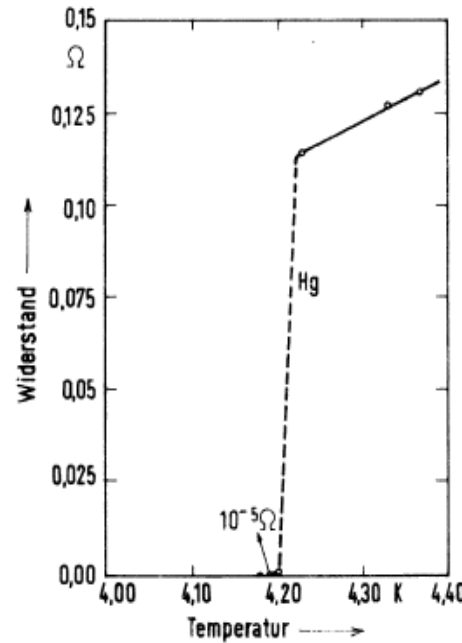
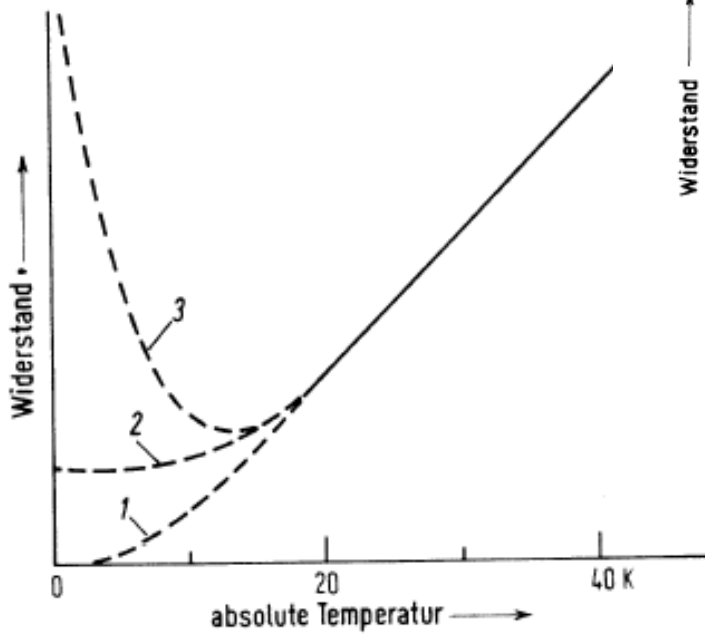
Bednorz



Müller

Historical remarks 2/4

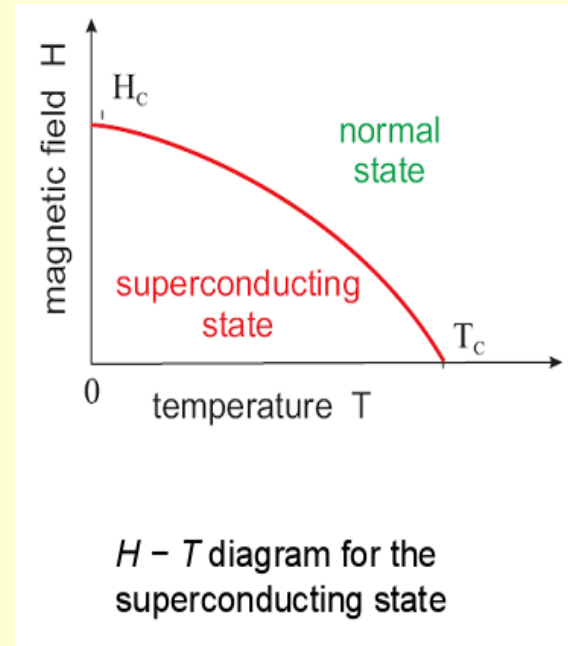
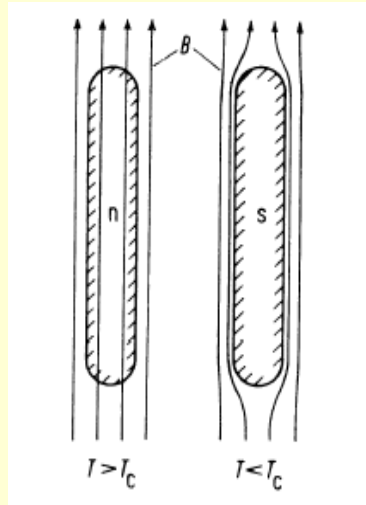
Nobel prize for « his investigations on the properties of matter at low temperatures which led, inter alia, to the production of liquid helium »



H. Kamerling – Onnes
in his laboratory at Leiden (NL)

Historical remarks 3/4

- Zero resistivity
- Meissner effect

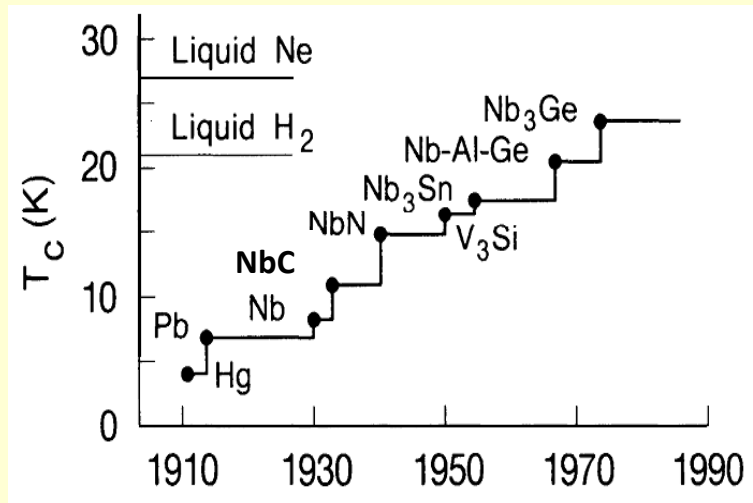


Superconductivity is destroyed:

- by increasing temperature at $T > T_c$
- by large magnetic field $H > H_c$

$$\frac{H_c(T)}{H_c(0)} = \left[1 - \left(\frac{T}{T_c} \right)^2 \right]$$

Historical remarks 4/4



Development of the superconducting transition temperatures after the discovery of the phenomenon in 1911. The materials listed are metals or inter-metallic compounds and reflect the respective highest T_c 's - Adapted from G. Bednorz – Nobel lecture

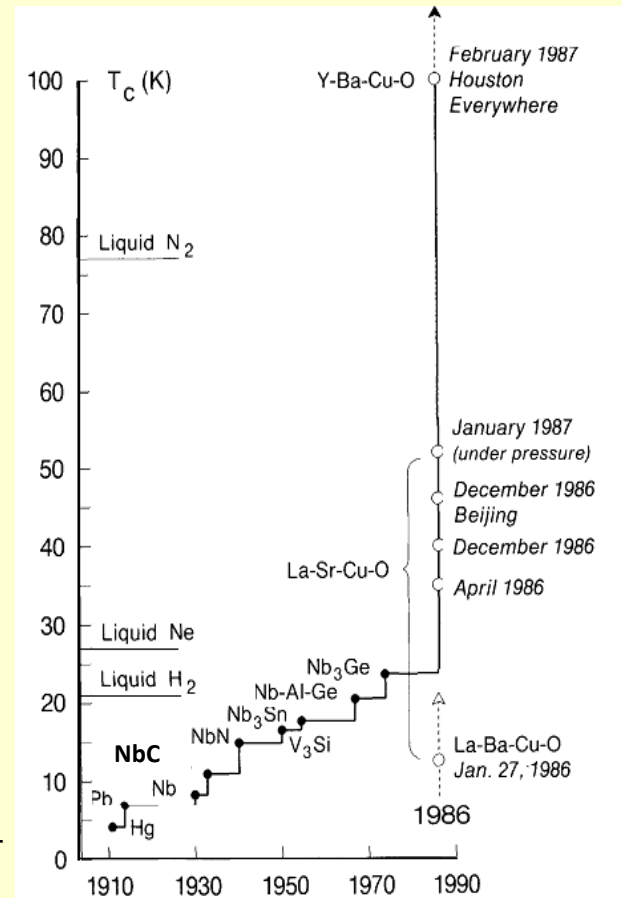


Figure 1.13. Evolution of the superconductive transition temperature subsequent to the discovery of the phenomenon. From [1.29], © 1987 by the American Association for the Advancement of Science.

Surface Impedance

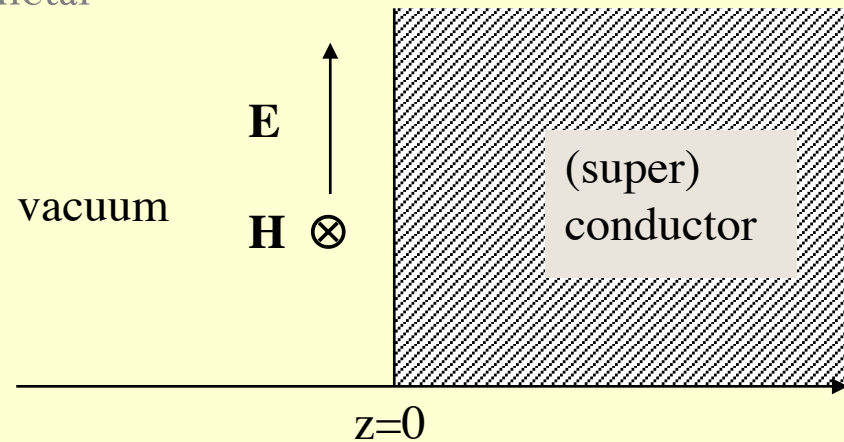
For a plane EM wave incident on a semi-infinite flat metallic surface:

$$Z_S = R_S + iX_S = \frac{E_{\parallel}(0)}{H_{\parallel}(0)}$$

- E , H always in complex notation
- E , H parallel to the surface

Reference frame coordinates:

- x , y parallel to the surface of the metal
- z perpendicular to the surface
 - $z=0$: on the surface



Plane Waves in Vacuum

From Maxwell's equations:

$$E = E_0 e^{i(kz - \omega t)} \quad H = H_0 e^{i(kz - \omega t)} \quad \text{and:} \quad H = E_0 \frac{k}{\omega \mu_0} e^{i(kz - \omega t)}$$

with the wavenumber: $k = \frac{2\pi}{\lambda} = \frac{\omega}{c} = \omega \sqrt{\epsilon_0 \mu_0}$

follows the wave equation in free space: $E = E_0 e^{i(kz - \omega t)} \quad H = E_0 \sqrt{\frac{\epsilon_0}{\mu_0}} e^{i(kz - \omega t)}$

with the free space impedance: $Z = \frac{|\mathbf{E}|}{|\mathbf{H}|} = \sqrt{\frac{\mu_0}{\epsilon_0}} = 376.7 \Omega$

Plane Waves in Metals

Generalized wavenumber: $k^2 = \omega^2 \varepsilon \mu + i \omega \sigma \mu$ $Z = \frac{|\mathbf{E}|}{|\mathbf{H}|} = \sqrt{\frac{\mu}{\varepsilon}} = \frac{\omega \mu}{k}$

Local current density and E-field: $\mathbf{J}(\vec{x}, t) = \sigma \mathbf{E}(\vec{x}, t)$

Conductivity in the metal: $\sigma(\omega) = \frac{\sigma_0}{(1 + i \omega \tau)}$ with: $\sigma_0 = \frac{ne^2 \ell}{m_e v_F} = \frac{ne^2 \tau}{m_e}$

In practice σ is assumed to be frequency independent ($\omega \tau \ll 1$): $\omega \sigma \mu \gg \omega^2 \varepsilon \mu \Rightarrow k^2 = i \omega \sigma \mu$

Wave equation in metals: $E = E_0 e^{i(kz - \omega t)} = E_0 e^{i(\alpha z - \omega t)} e^{-\beta z}$

with: $\frac{1}{\beta} = \sqrt{\frac{2}{\sigma \omega \mu}} = \delta$ being the field penetration or skin depth

Surface Impedance in “normal” Metals

- The **surface impedance** Z_s is defined at the **interface** between two media. It can be calculated in a similar way as for continuous media.
- You take Maxwell's equation, set the appropriate **boundary conditions** for the continuity of the waves (incident, reflected, transmitted), and you get:

$$Z_S = \frac{E_{\parallel}(0)}{H_{\parallel}(0)} = \sqrt{\frac{i\omega\mu_0}{\sigma}} = \sqrt{\frac{\omega\mu_0}{2\sigma}} + i\sqrt{\frac{\omega\mu_0}{2\sigma}} = R_S + iX_S$$

- Introducing appropriate numbers, e.g. for copper at $f = 1 \text{ GHz}$:

$$\sigma_{Cu} = 58.5\text{e}6 \text{ S/m}$$

$$R_S = 8.2 \text{ m}\Omega$$

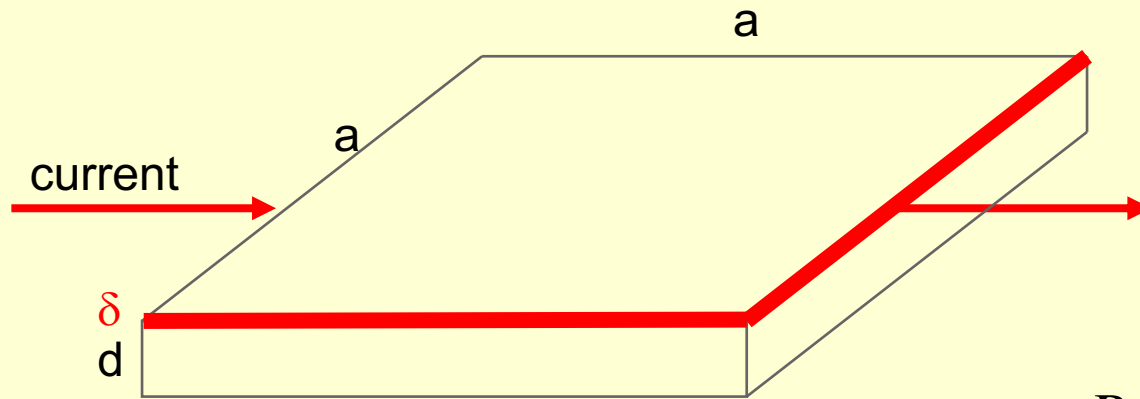
What is the skin depth?

Surface Resistance

Since we will deal a lot with the surface resistance R_s ,

here is a **simple DC model** that gives a rough idea of what it means:

Consider a square sheet of metal and calculate its **resistance to a transverse current** flow:

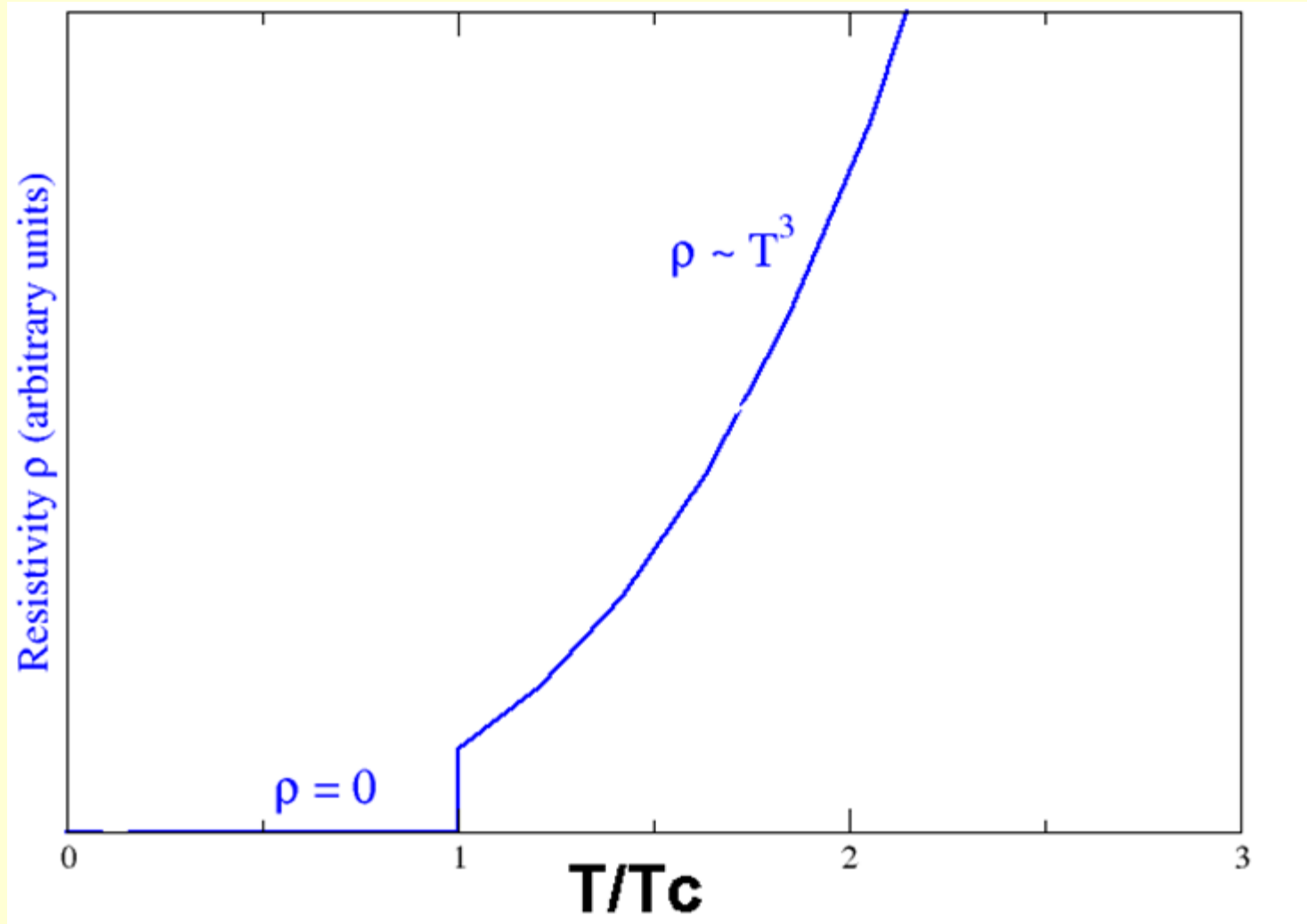


$$R = \frac{\rho \cancel{a}}{d \cancel{a}} = \frac{\rho}{d}$$

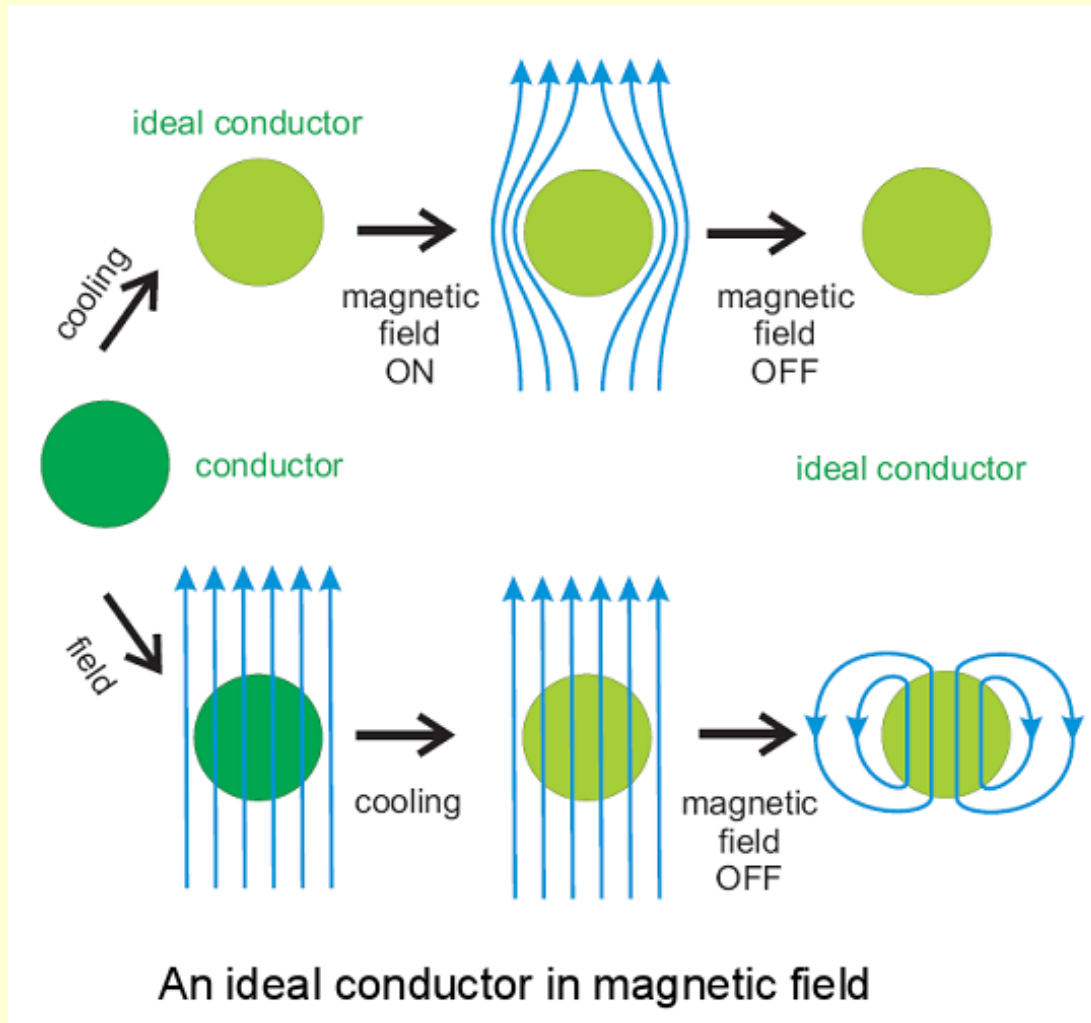
$$R_s = \sqrt{\frac{\mu_0 \omega}{2\sigma}} = \frac{1}{\sigma \delta} = \frac{\rho}{\delta}$$

- The surface resistance R_s is the **resistance** that a **square piece of conductor** opposes to the flow of the currents induced by the RF wave, **within a layer δ**
- ρ is the specific electrical resistance, given in [Ωm].
 - For copper: $\rho_{\text{Cu}} = 17 \cdot 10^{-3} \Omega \cdot \text{mm}^2/\text{m} = 17 \text{ n}\Omega \text{ m}$ (1 m long Cu-wire of 1 mm² cross-section)

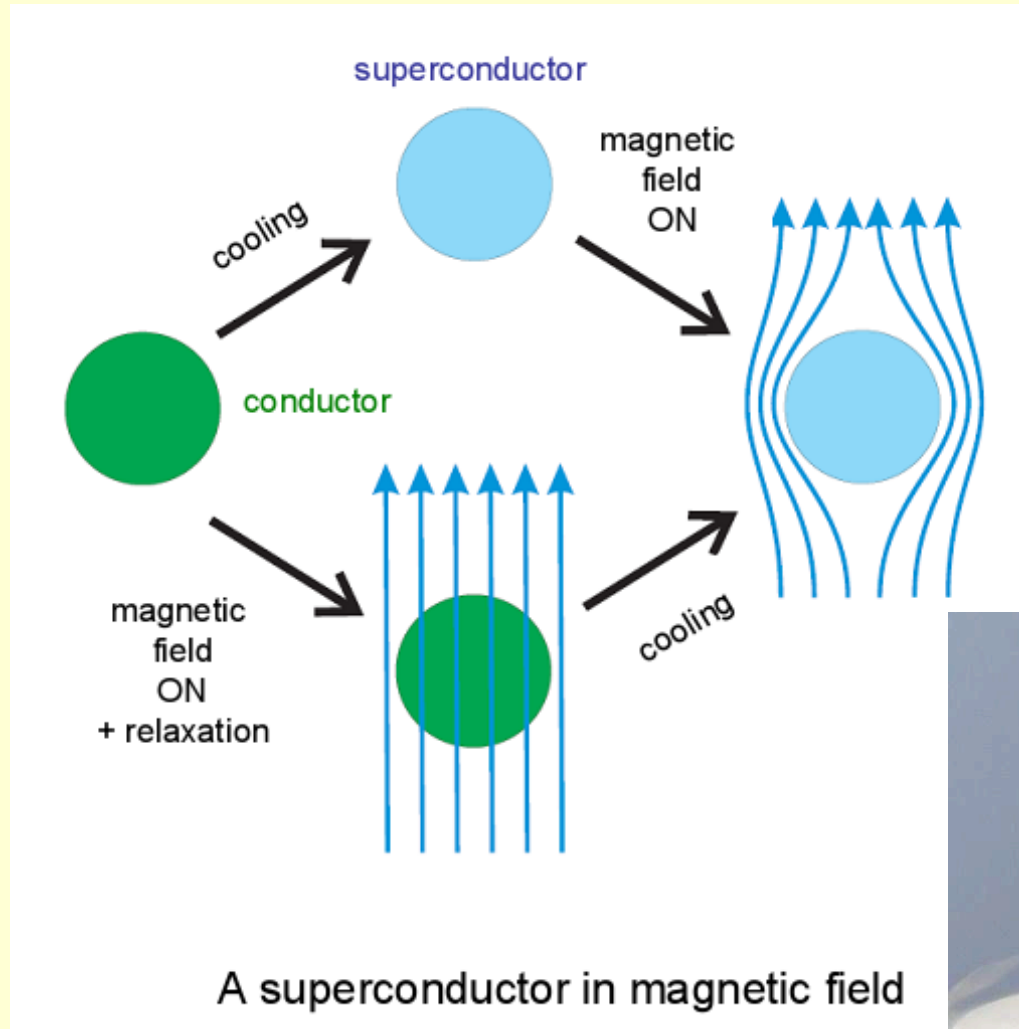
Superconductivity



Meissner effect 1/3



Meissner effect 2/3



Meissner effect 3/3

1. Magnetic lines of force outside a superconductor are always tangential to its surface

$$\operatorname{div} \vec{B} = 0;$$

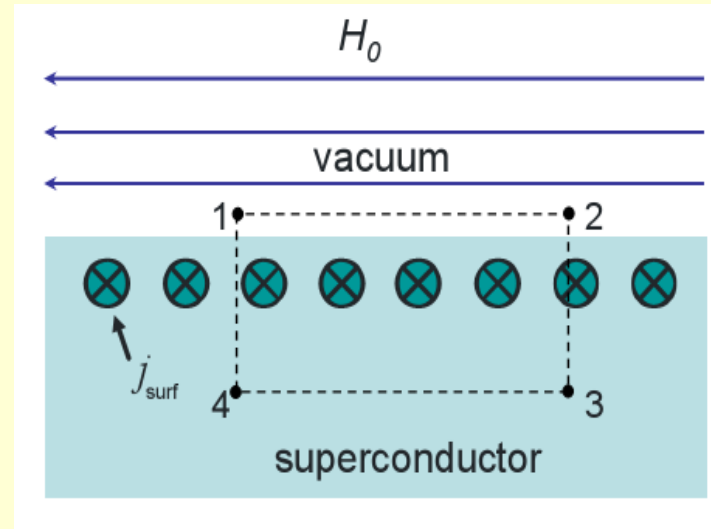
$$\text{Since } \vec{B}_n^{(i)} = 0 \Rightarrow \vec{B}_n^{(e)} = 0$$

2. A superconductor in an external magnetic field always carries an electric current near its surface

$$\vec{\nabla} \times \vec{B} = \mu_0 \vec{j} \Rightarrow \vec{j} = 0 \text{ inside the superconductor}$$

$$\oint \vec{B} \cdot d\vec{l} = \mu_0 j_{\text{surf}} \cdot l_{1-2}$$

$$\oint \vec{B} \cdot d\vec{l} = \mu_0 H_0 \cdot l_{1-2} \Rightarrow \vec{j}_{\text{surf}} = \vec{n} \times \vec{H}_0$$



Thus, the surface current is completely defined by the magnetic field at the surface of a superconductor.

Theories of Superconductors

- Gorter & Casimir two fluid model
 - London Equations
 - Pippard's Coherence length ξ
- Ginzburg-Landau
 - Second order phase transition of complex order parameter Ψ
- BCS (Bardeen-Cooper-Schrieffer)
 - Microscopic theory
 - Two Fluid Model revised
- (Strong coupling – Elihasberg)

Two kinds of superconductors 1/3

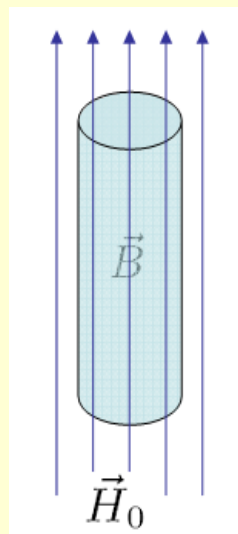
Magnetic properties of a **type I superconductor**

Magnetic properties of a superconductor can be derived from $\rho = 0$ and $B = 0$

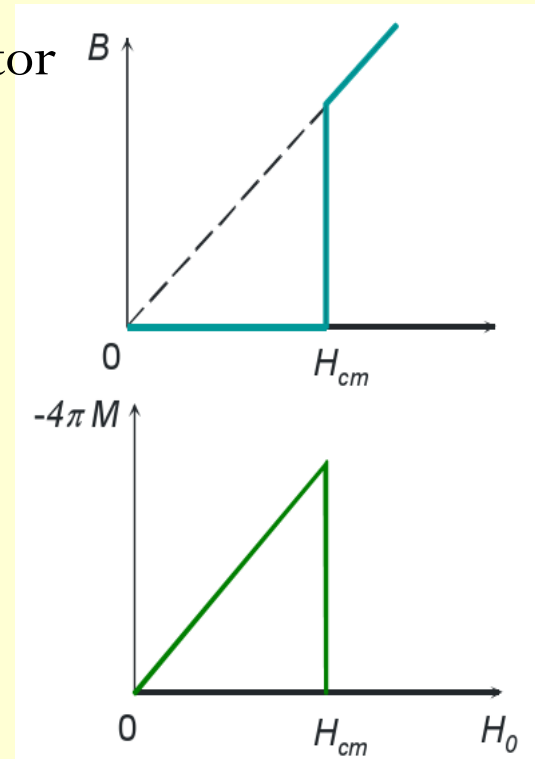
Type I superconductors are all elemental superconductors (except niobium)

$$\vec{B} = \mu_0 \cdot \left(\vec{H}_0 + \vec{M} \right)$$

The magnetization \vec{M} compensates the external field H_0 , thus the SC bulk is field free.



Magnetization curve



H_{cm} ... critical field

Two kinds of superconductors 2/3

- Type II superconductor

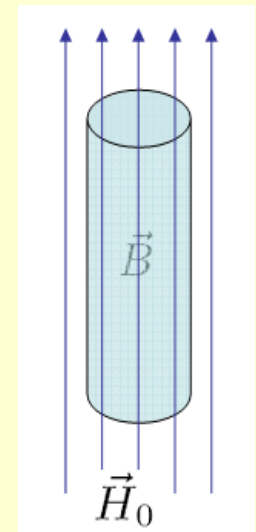
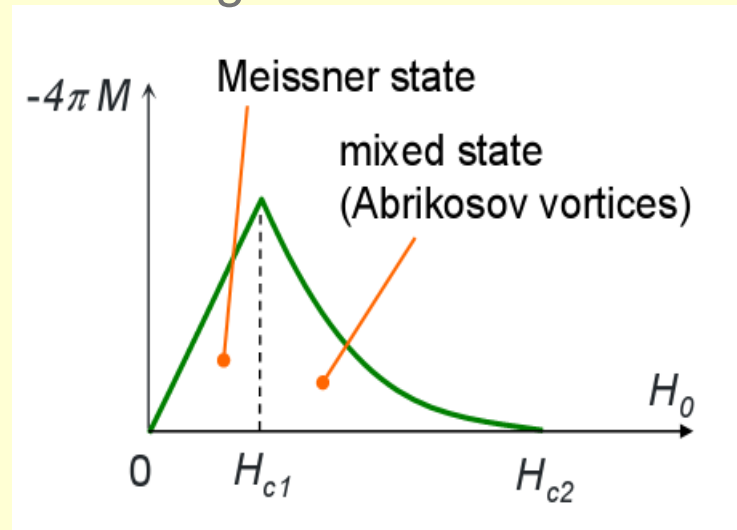
Magnetic properties of a **type II superconductor**

Above the 1st critical field H_{c1} magnetic flux penetrates into the bulk

Above the 2nd critical field H_{c2} the material is normal conducting (except for a thin surface layer that remains superconducting until the 3rd critical field H_{c3})

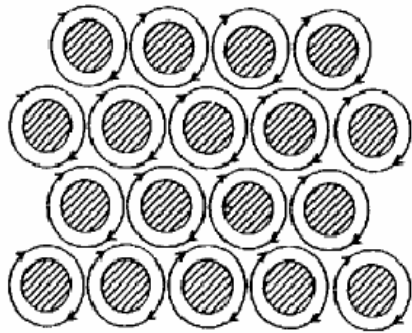
$$\vec{B} = \mu_0 \cdot \left(\vec{H}_0 + \vec{M} \right)$$

Magnetization curve



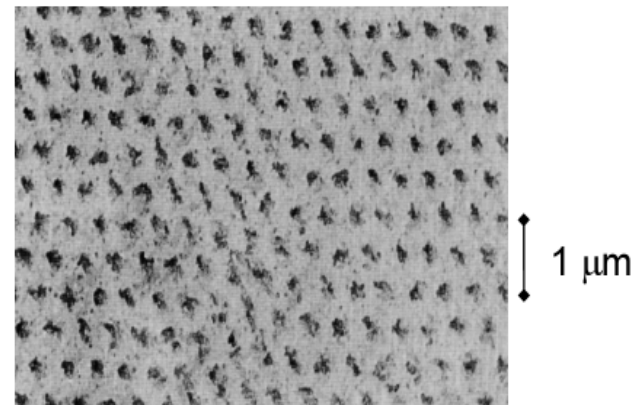
Two kinds of superconductors 3/3

Mixed state of a type II superconductor



Mixed state (Shubnikov phase) of a type II superconductor consists of a regular lattice of Abrikosov vortices.

Magnetic decoration
image of a vortex lattice



Materials _{1/2}

pure
metals

material	T_c, K	H_c, Oe	year
Al	1.2	105	1933
In	3.4	280	
Sn	3.7	305	
Pb	7.2	803	1913
Nb	9.2	2060	1930

alloys

NbN	15	$1.4 \cdot 10^5$	1940
Nb ₃ Ge	23	$3.7 \cdot 10^5$	1971

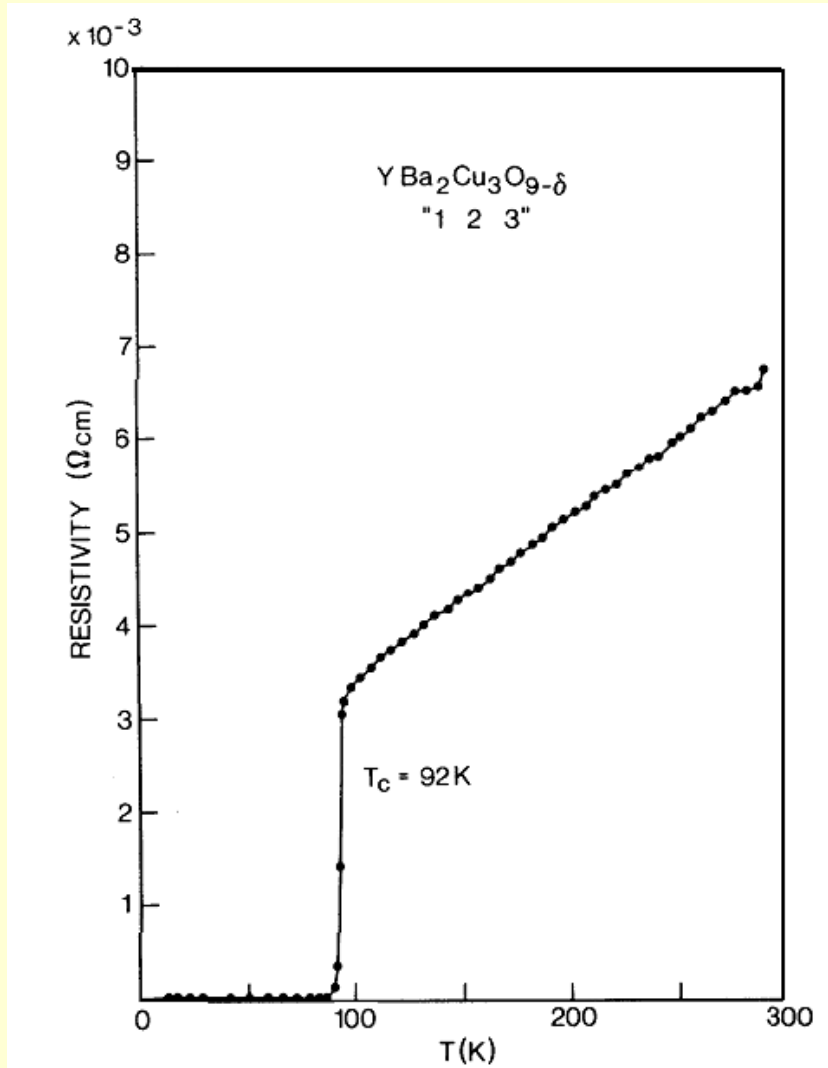
Cold liquids required for reaching low temperatures:

helium ⁴He (4.2 K)
hydrogen H₂ (20 K)
neon Ne (27 K)
nitrogen N₂ (77 K)

ceramics

material	T_c, K	year
La _{1.85} Ba _{0.15} CuO ₄	35	1986
YBa ₂ Cu ₃ O ₇	93	1987
Bi ₂ Sr ₂ CaCu ₂ O _{8+x}	94	1988
Ta ₂ Ba ₂ Ca ₂ Cu ₃ O _{10+x}	125	1988

Materials 2/2



Resistivity of a single-phase $YBa_2Cu_3O_7$ sample as a function of temperature.

Two fluid model

Basic ingredients for RF superconductivity

Two fluid model (Gorter-Casimir)
Maxwell electrodynamics

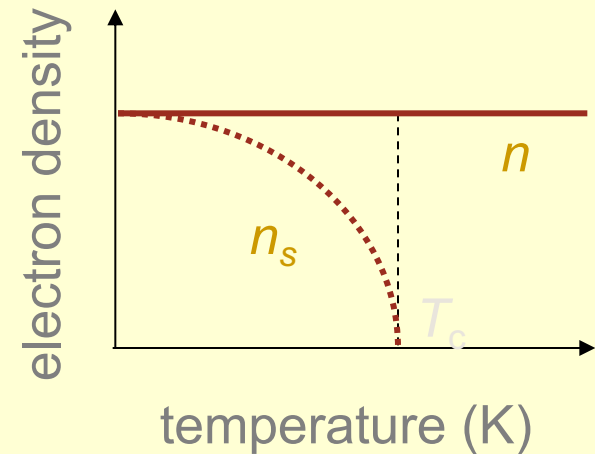
Basic assumptions of two fluid model

- all free electrons of the superconductor are divided into two groups
 - superconducting electrons of density n_s
 - normal electrons of density n_n

The total density of the free electrons is

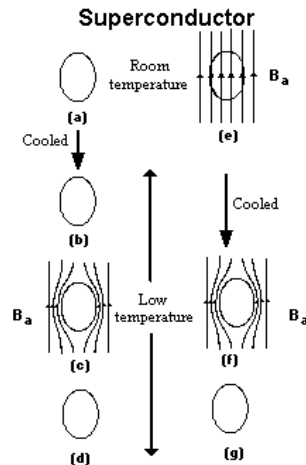
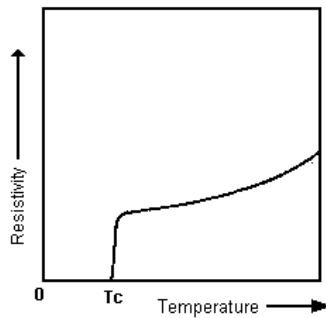
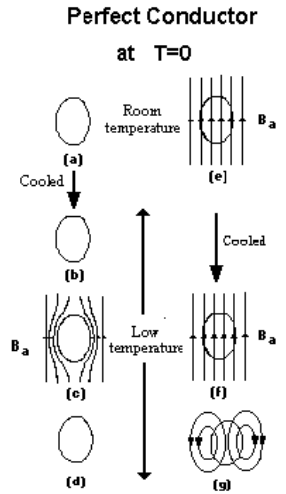
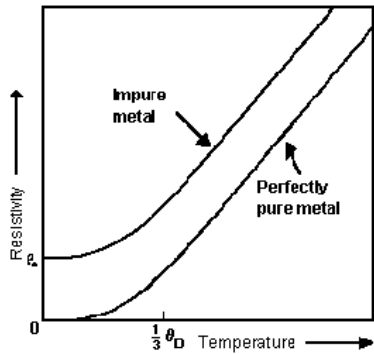
$$n = n_s + n_n.$$

As the temperature increases from 0 to T_c , the density n_s decreases from n to 0.



$$n_s/n = 1 - (T/T_c)^4$$

London Equations



Postulated on plausibility arguments

$$\frac{\partial \mathbf{j}_s}{\partial t} = \frac{n_s e^2}{m} \mathbf{E} \quad \nabla \times \mathbf{j}_s = -\frac{n_s e^2}{m} \mathbf{B}$$

Applying $\mathbf{B} = \nabla \times \mathbf{A}$
on the vector potential \mathbf{A}

$$\mathbf{j}_s = -\frac{n_s e^2}{m} \mathbf{A} = -\Lambda^{-1} \mathbf{A}$$

Applying Ampere's law
to London's 2nd eq gives:

$$\nabla^2 \mathbf{B} = \frac{1}{\lambda_L^2} \mathbf{B} \quad \lambda_L = \sqrt{\frac{m}{\mu_0 n_s e^2}}$$

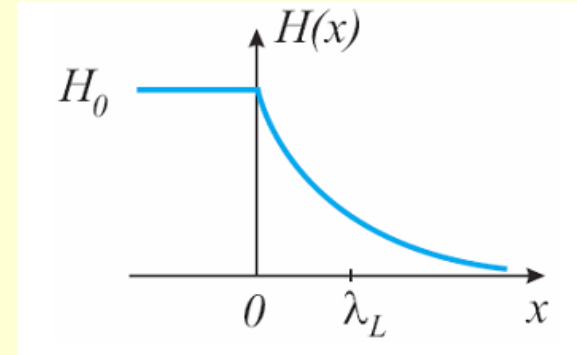
Exponential decay of the B-field
inside the superconductor

London penetration depth

On introducing the vector potential \mathbf{A} via $\mathbf{B} = \nabla \times \mathbf{A}$

one obtains a relationship between the supercurrent and the vector potential, very similar to Ohm's law $\mathbf{j} = \sigma \mathbf{E}$

$$\Rightarrow \mathbf{j}_s = -\frac{1}{\Lambda} \mathbf{A} = -\frac{n_s e^2}{m} \mathbf{A}$$



with the London penetration depth $\lambda_L^2 = \Lambda / \mu_0 = m / (n_s e^2 \mu_0)$

Element	Al	Nb (crystal)	Nb (film)	Pb	Sn	YBCO
λ_L [nm]	50	47	90	39	51	170

Compare to
NC Cu skin depth:
2 μm @ 1 GHz

Complex Conductivity _{1/3}

- You will probably be only half surprised to hear that a superconductor at $T > 0$ has a $R_s \neq 0$.
- This can be understood in the framework of the previous **two fluids model**, where a population of normal electrons of density n_n and a population of “superconducting electrons” of density $n_s = n_0(1 - T^4/T_c^4)$ coexist such as $n_n + n_s = 1$ and both give a response to the varying EM fields.
- Let’s “invent” the conductivity of superconducting electrons:

$$\sigma(\omega) = \frac{ne^2\tau}{m_e(1+i\omega\tau)} \quad \lim_{\tau \rightarrow \infty} \sigma(\omega) = -i \frac{ne^2}{m_e\omega}$$

Complex Conductivity _{2/3}

- Do you think the previous formula looks like a joke: conductivity of a perfect conductor is an imaginary number?
- There is indeed real physics behind it. Recall London equations, from which we can set-up the following equivalence, in the “dirty” limit:

Normal metal	Superconductor (London theory)
$\mathbf{j} = \sigma_0 \mathbf{E} = \frac{n_n e^2 \ell}{m v_F} \mathbf{E}$	$\mathbf{j}_s = -\Lambda^{-1} \mathbf{A} = -\frac{n_s e^2}{m} \mathbf{A}$

- The value of Λ is the expression of the kinetic inductivity of the “superconducting electrons”: basically, the electron pairs have a mass, and they get accelerated by the RF wave. This is the same as what happens with the magnetic field produced inside an inductor.

London&London Proc. Roy. Soc A149 (1935) 71

Pippard Proc. Roy. Soc. A216 (1953) 547

Complex Conductivity 3/3

- The conductivity of superconductors then becomes:

$$\sigma_s = \frac{n_0 e^2 \tau}{m} \left(\frac{T^4}{T_c^4} \right) - i \frac{n_0 e^2}{m \omega} \left(1 - \frac{T^4}{T_c^4} \right) = \sigma_1 - i \sigma_2$$

conductivity of
"normal electrons"

conductivity of
"superconducting electrons"

- Where $n_s = n_0(1 - T^4/T_c^4)$ and $n_n = n_0(T^4/T_c^4)$ with n_0 total electron density
- Note:

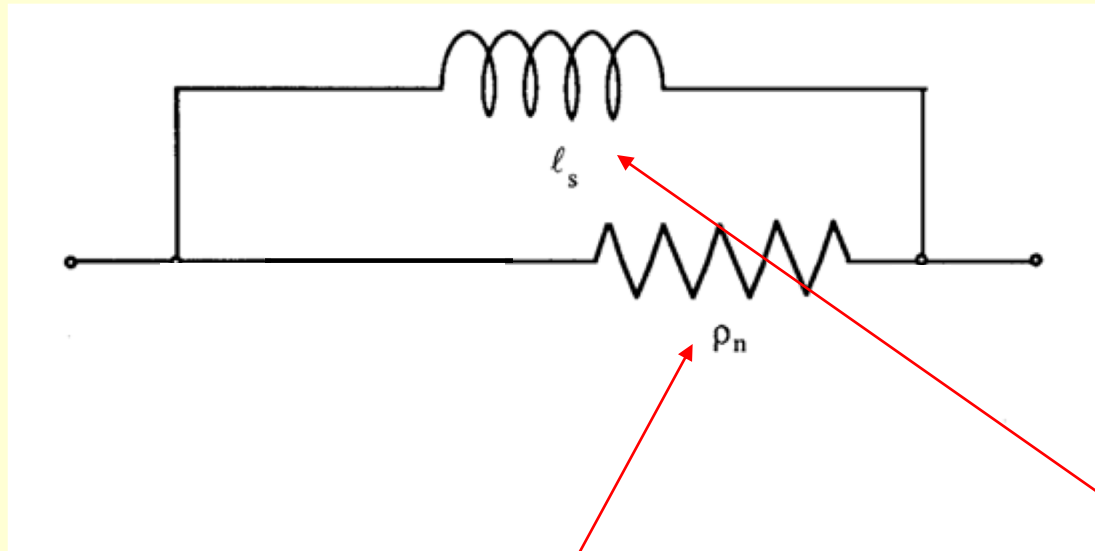
$$\sigma_2 = \frac{\sigma_0}{\omega \tau} = \frac{1}{\mu_0 \omega \lambda_L^2} = \frac{1}{\Lambda \omega} \quad \text{with} \quad \lambda_L^2 = \frac{\Lambda}{\mu_0}$$

Equivalent Circuit

Indeed if you take the time derivative of $\mathbf{j}_s = -\Lambda^{-1} \mathbf{A}$ you get the 1st London eq:

$$-\frac{\partial \mathbf{A}}{\partial t} = \mathbf{E} = \Lambda \frac{\partial \mathbf{j}_s}{\partial t}$$

Λ is interpreted as a specific inductance. This justifies representing the complex conductivity of a superconductor with an equivalent circuit of parallel conductors:



$$\sigma_s = \sigma_1 - i\sigma_2 = \sigma_n \left(\frac{T^4}{T_c^4} \right) - i \frac{\sigma_n}{\omega\tau} \left(1 - \frac{T^4}{T_c^4} \right)$$

Surface Impedance ^{1/2}

- It is now possible, within the basic **approximations** we have made, to calculate the **surface impedance of a superconductor**.

- Take the formula for normal metals:

$$Z = (1 + i) \sqrt{\frac{\mu_0 \omega}{2\sigma_n}}$$

- Perform the substitution: $\sigma_n \rightarrow \sigma_s = \sigma_1 - i\sigma_2$

- Calculate:
$$R_s = \sqrt{\frac{\mu_0 \omega}{\sigma_n}} \frac{\left[(\sigma_1^2 + \sigma_2^2)^{1/2} - \sigma_2 \right]^{1/2}}{(\sigma_1^2 + \sigma_2^2)^{1/2}} \quad X_s = \dots\dots$$

- In the approximation of small ℓ (small $\omega\tau \rightarrow \sigma_1 < \sigma_2$)

- and $0 < T < 0.5T_c$ ($n_n < n_s \rightarrow \sigma_1 < \sigma_2$) it gives:

$$R_s = \frac{R_N}{\sqrt{2}} \frac{\sigma_1/\sigma_n}{(\sigma_2/\sigma_n)^{3/2}} = \frac{1}{2} \mu_0^2 \omega^2 \sigma_1 \lambda_L^3 \quad X_s = X_N \frac{\sqrt{2}}{(\sigma_2/\sigma_n)^{1/2}} = \sqrt{\frac{\mu_0 \omega}{\sigma_2}} = \mu_0 \omega \lambda_L$$

- Which is a good description of the experimental data, but...

Surface Impedance _{2/2}

- How to **generalize** to larger ℓ ? Take:
(Pippard Proc. Roy. Soc. A216 (1953) 547) $\mathbf{j}_s = -\Lambda^{-1} \mathbf{A} = -\frac{ne^2}{m} \mathbf{A}$

- Introduce a parameter ξ
in some way proportional to ℓ : $\mathbf{j}_s = -\frac{\xi}{\xi_0} \Lambda^{-1} \mathbf{A}$

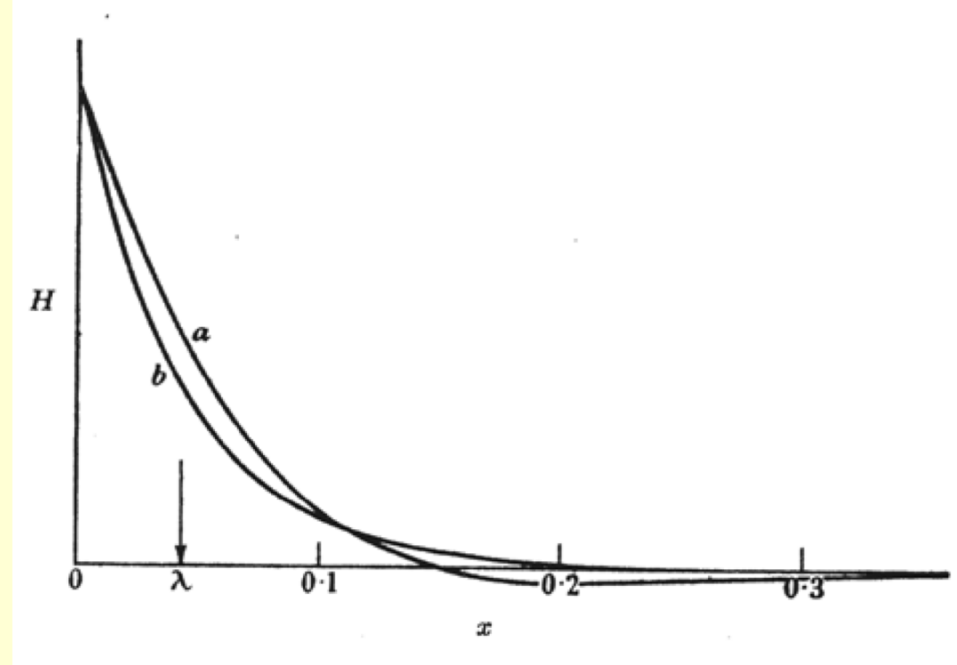
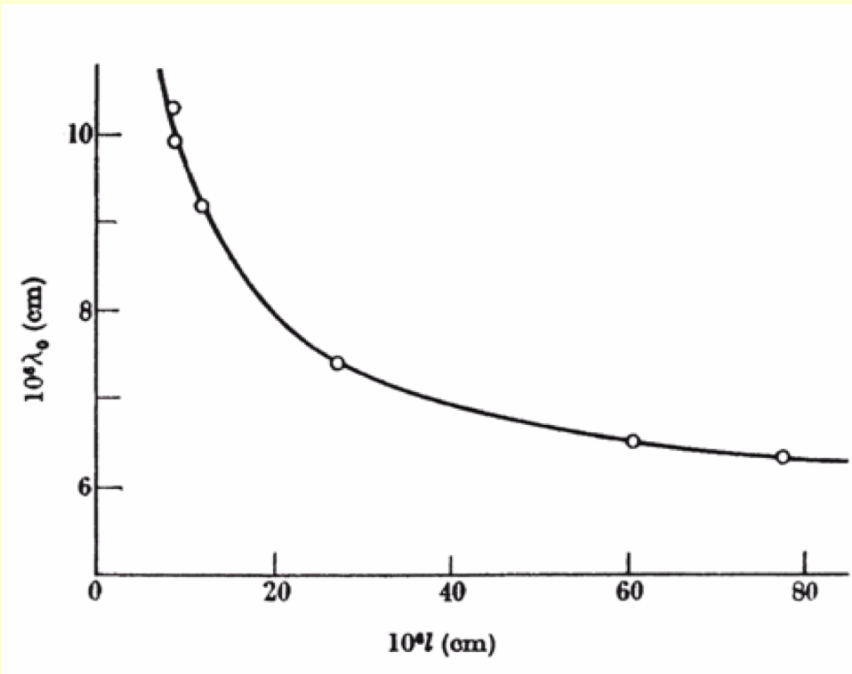
- Then substitute corresponding quantities into Chambers' formula:

$$\mathbf{J}(\mathbf{r}, t) = -\frac{3}{4\pi\xi_0\Lambda} \int_V \frac{\mathbf{R}[\mathbf{R} \cdot \mathbf{A}(\mathbf{r}', t - R/v_F)] e^{-R/\xi}}{R^4} d\mathbf{v}'$$

- Pippard used this formula to fit his experimental data, and found: $\frac{1}{\xi} = \frac{1}{\xi_0} + \frac{1}{\ell} \quad \xi_0 = 0.15 \frac{\hbar v_F}{kT_c}$

- This was the first definition ever of the coherence length ξ_0

Pippard's Data



We are now ready to go into the real (“heavy”) stuff: the BCS formulation.

- In BCS theory the values for σ_1 / σ_n and σ_2 / σ_n can be calculated.
- These are then used to **calculate** the surface impedance

BCS Theory 1/2

1st step:

$$\mathbf{j}(\mathbf{r}, t) = \sum_{\omega} \frac{e^2 N(0) v_0}{2\pi^2 \hbar c}$$

Mattis & Bardeen, Phys. Rev. 111 (1958) 412

$$\times \int \frac{\mathbf{R}[\mathbf{R} \cdot \mathbf{A}_{\omega}(\mathbf{r}')] I(\omega, R, T) e^{-R/l}}{R^4} d\mathbf{r}', \quad (3.3)$$

is

$$I(\omega, R, T) = \int_{-\infty}^{\infty} \int_{-\infty}^{\infty} \left\{ L(\omega, \epsilon, \epsilon') - \frac{f(\epsilon) - f(\epsilon')}{\epsilon' - \epsilon} \right\} \\ \times \cos[\alpha(\epsilon - \epsilon')] d\epsilon d\epsilon', \quad (3.4)$$

2nd step:

$$\frac{\sigma_1 - i\sigma_2}{\sigma_N} = \frac{I(\omega, 0, T)}{-\pi i \hbar \omega}.$$

3rd step:

$$\frac{\sigma_1}{\sigma_N} = \frac{2}{\hbar \omega} \int_{\epsilon_0}^{\infty} [f(E) - f(E + \hbar \omega)] g(E) dE \\ + \frac{1}{\hbar \omega} \int_{\epsilon_0 - \hbar \omega}^{-\epsilon_0} [1 - 2f(E + \hbar \omega)] g(E) dE, \quad (3.9)$$

$$\frac{\sigma_2}{\sigma_N} = \frac{1}{\hbar \omega} \int_{\epsilon_0 - \hbar \omega, -\epsilon_0}^{\epsilon_0} \frac{[1 - 2f(E + \hbar \omega)] (E^2 + \epsilon_0^2 + \hbar \omega E)}{(\epsilon_0^2 - E^2)^{\frac{1}{2}} [(E + \hbar \omega)^2 - \epsilon_0^2]^{\frac{1}{2}}} dE. \quad (3.10)$$

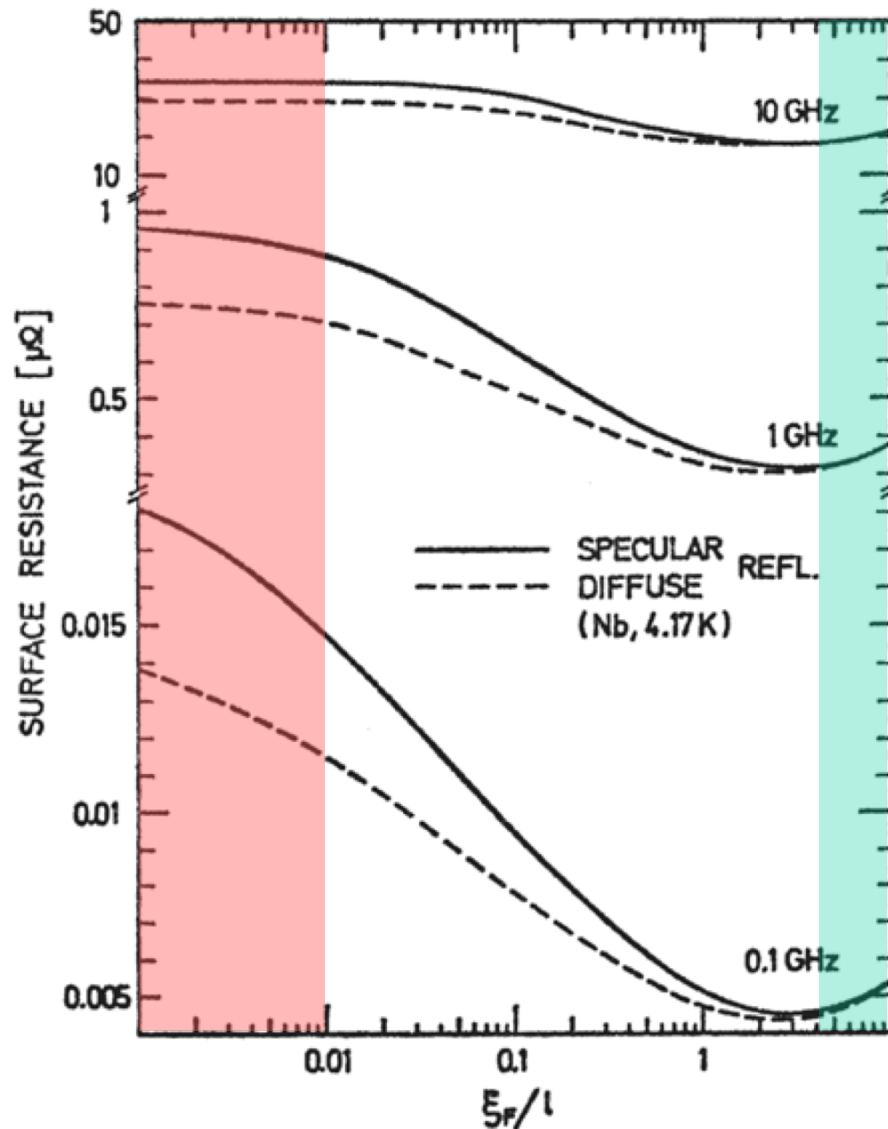
BCS Theory 2/2

- (3.9) and (3.10) can be approximated for low frequencies $h\nu \ll 2\Delta$ as:

$$\frac{\sigma_1}{\sigma_n} = 2f(\Delta) \left\{ 1 + \frac{1}{kT} \ln \left(\frac{2\Delta}{\hbar\omega} \right) [1 - f(\Delta)] \right\} \quad \frac{\sigma_2}{\sigma_n} = \frac{\pi\Delta}{\hbar\omega} \tanh \left(\frac{\Delta}{2kT} \right)$$

- The surface impedance Z can be calculated from σ_1/σ_n and σ_2/σ_n
- However the formulas seen until now are approximate valid only in a very specific limit.
- Calculations can be done having a full validity range (but only for $H_{RF} \ll H_c$)
 - Abrikosov Gorkov Khalatnikov, JETP 35 (1959) 182
 - Miller, Phys. Rev. 113 (1959) 1209
 - Nam, Phys. Rev. A 156 (1967) 470
 - Halbritter, Z. Phys. 238 (1970) 466 and KFK Ext. Bericht 3/70-6

Halbritter's theoretical Predictions



In the **green** region (small l):

$$\frac{Z_s}{Z_n} = \left(\frac{\sigma_1}{\sigma_n} - i \frac{\sigma_2}{\sigma_n} \right)^{1/2}$$

$$R_s \propto \frac{\omega^2}{T\sqrt{\sigma}} \exp\left(-\frac{\Delta}{kT}\right)$$

In the **red** region (large l):

$$\frac{Z_s}{Z_n} = \left(\frac{\sigma_1}{\sigma_n} - i \frac{\sigma_2}{\sigma_n} \right)^{1/3}$$

$$R_s \propto \frac{\omega^{3/2}}{T} \exp\left(-\frac{\Delta}{kT}\right)$$

BCS Surface Resistance

- Material parameter dependence of $R_s(T, f)$

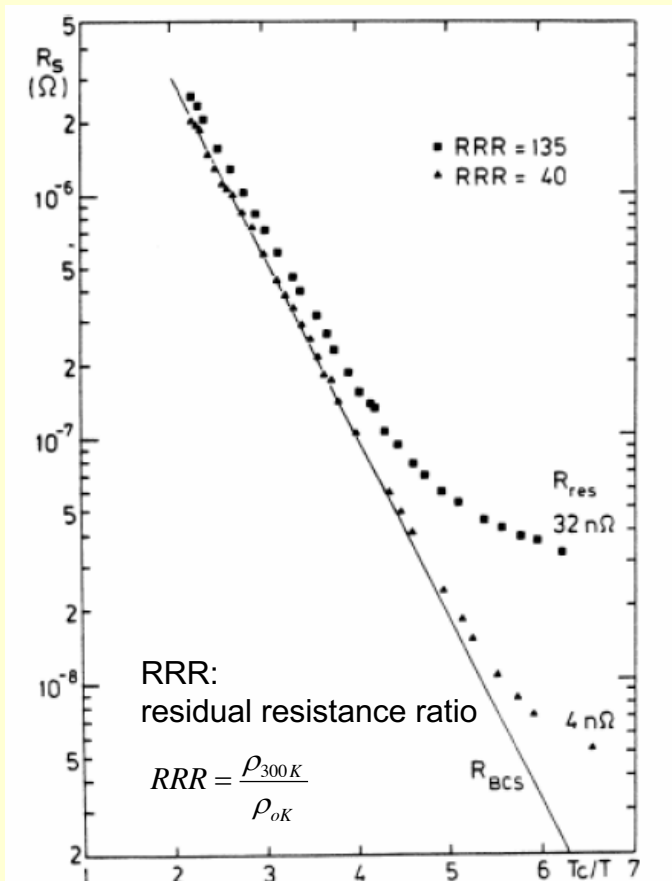


Fig. 2: Surface resistance $R_s(T)$ of two 3 GHz cavities, fabricated from niobium of different purity. $R_s(T)$ is the sum of the temperature dependent part R_{BCS} and the residual resistance R_{res} .

$$R_s^{BCS}(\omega, T) = \frac{A}{T} \omega^2 \exp\left(-\frac{\Delta}{kT}\right)$$

$$2\Delta \approx 3.5 \cdot kT_c$$

A depends on the material

$$R_s = R_s^{BCS} + R_{res}$$

An approximate expression for Niobium:

$$R_s^{BCS} \approx 3 \times 10^{-4} \Omega \cdot \left(\frac{f[\text{MHz}]}{1500 \text{ MHz}}\right)^2 \cdot \frac{\exp\left(-\frac{17.67 \text{ K}}{T[\text{K}]}\right)}{T[\text{K}]}$$

Developed by *Mattis* and *Bardeen*, based on the SC theory of *Bardeen*, *Cooper* and *Schrieffer* (BCS theory).

How to measure RF Surface Impedance ^{1/7}

- Normally some kind of resonator is applied for the samples
- You **MUST** avoid any contacts since they have usually an undefined contact resistance and spoil the Q of the cavity and you should avoid any radiation losses
- Often a TE₀₁₁ mode type resonator is used..works very well not sensitive to contact resistance due to azimuthal wall current only
- But if you would like to go to lower frequencies then the quadrupolar resonator is a good choice
- For even lower frequencies the shielded two wire coaxial resonator has been used (for the LHC beam screen)

How to measure RF Surface Impedance ^{2/7}

- Small samples can be exposed to RF using a pill box cavity with demountable endplate
- Two possible techniques
 - Replacement
 - **Calorimetric**

Replacement = Q-measurement with copper cover/DUT

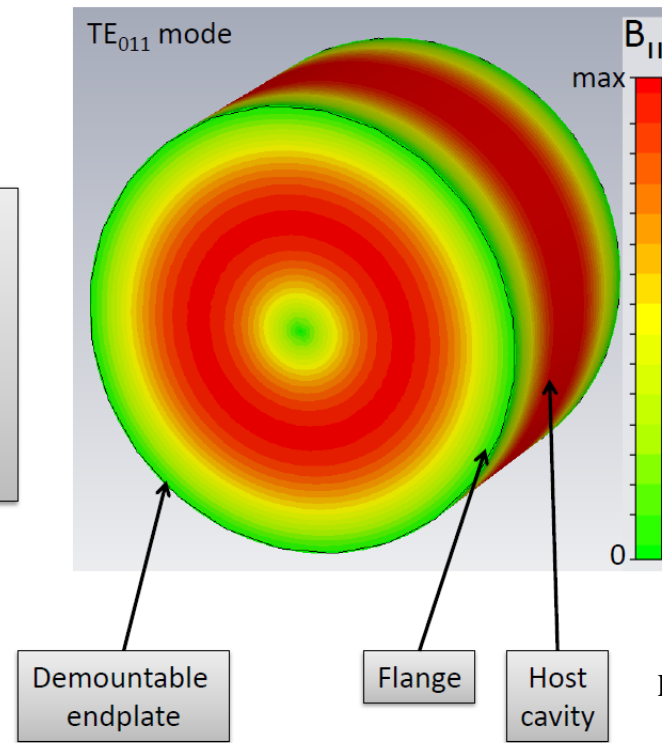


Figure by T. Junginger

How to measure RF Surface Impedance ^{3/7}

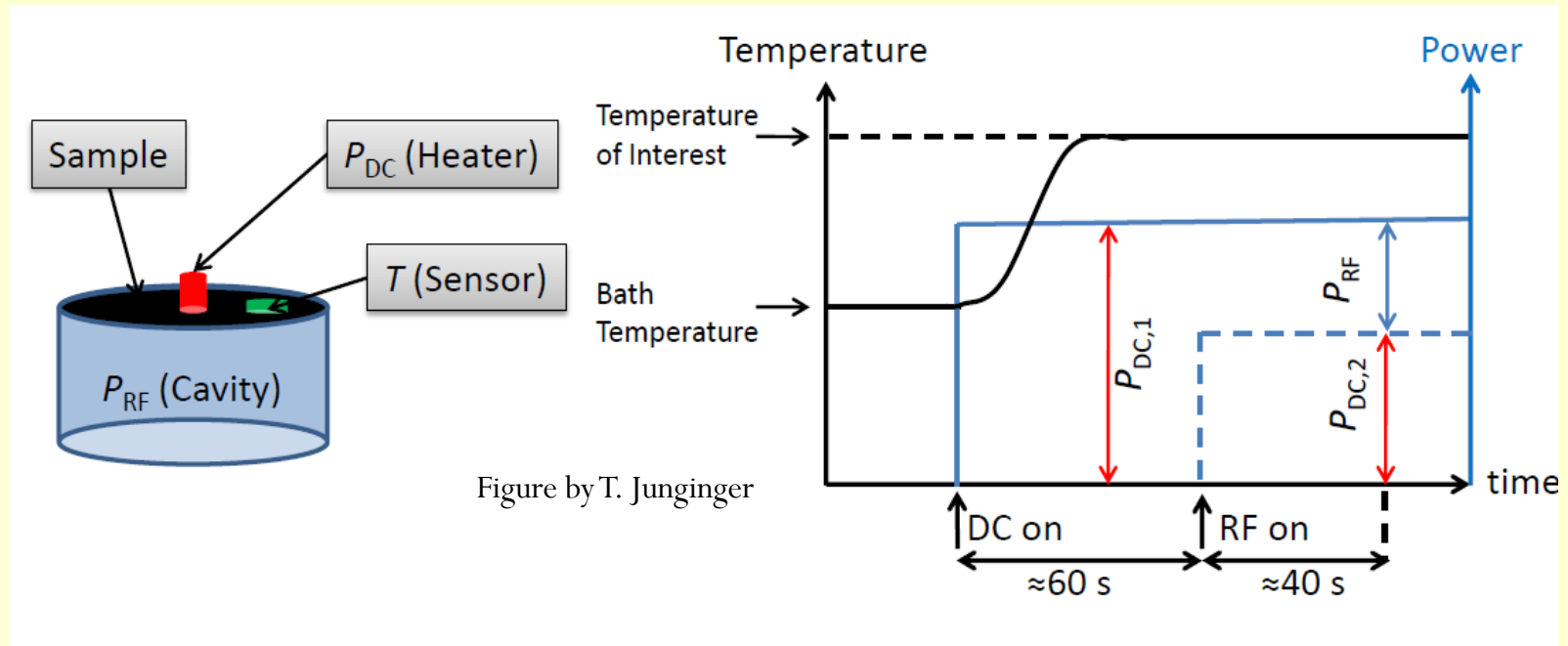


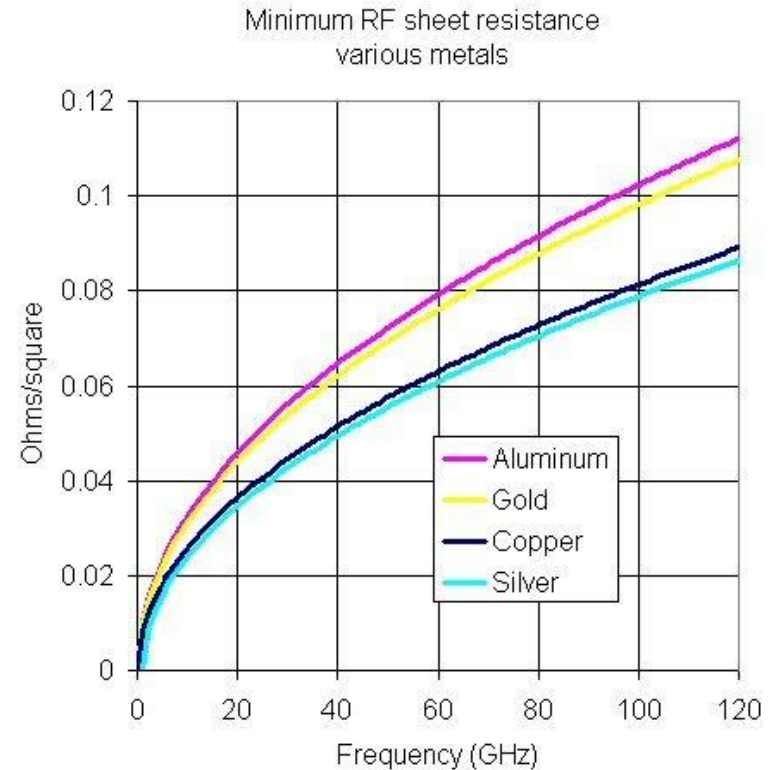
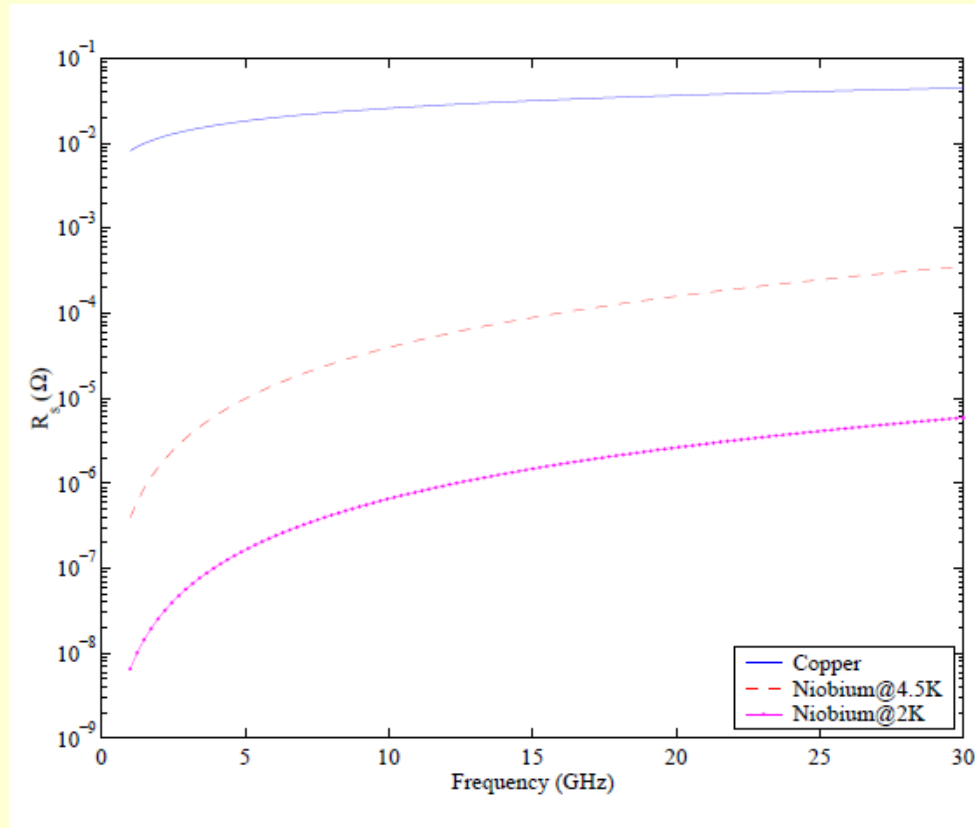
Figure by T. Junginger

$$P_{RF} = P_{DC,1} - P_{DC,2} \approx 1/2 R_{Surface} \int_{Sample} H^2 dS$$

$$R_{Surface} = \frac{2(P_{DC,1} - P_{DC,2})}{\int_{Sample} H^2 dS} \rightarrow \text{Direct Measurement}$$

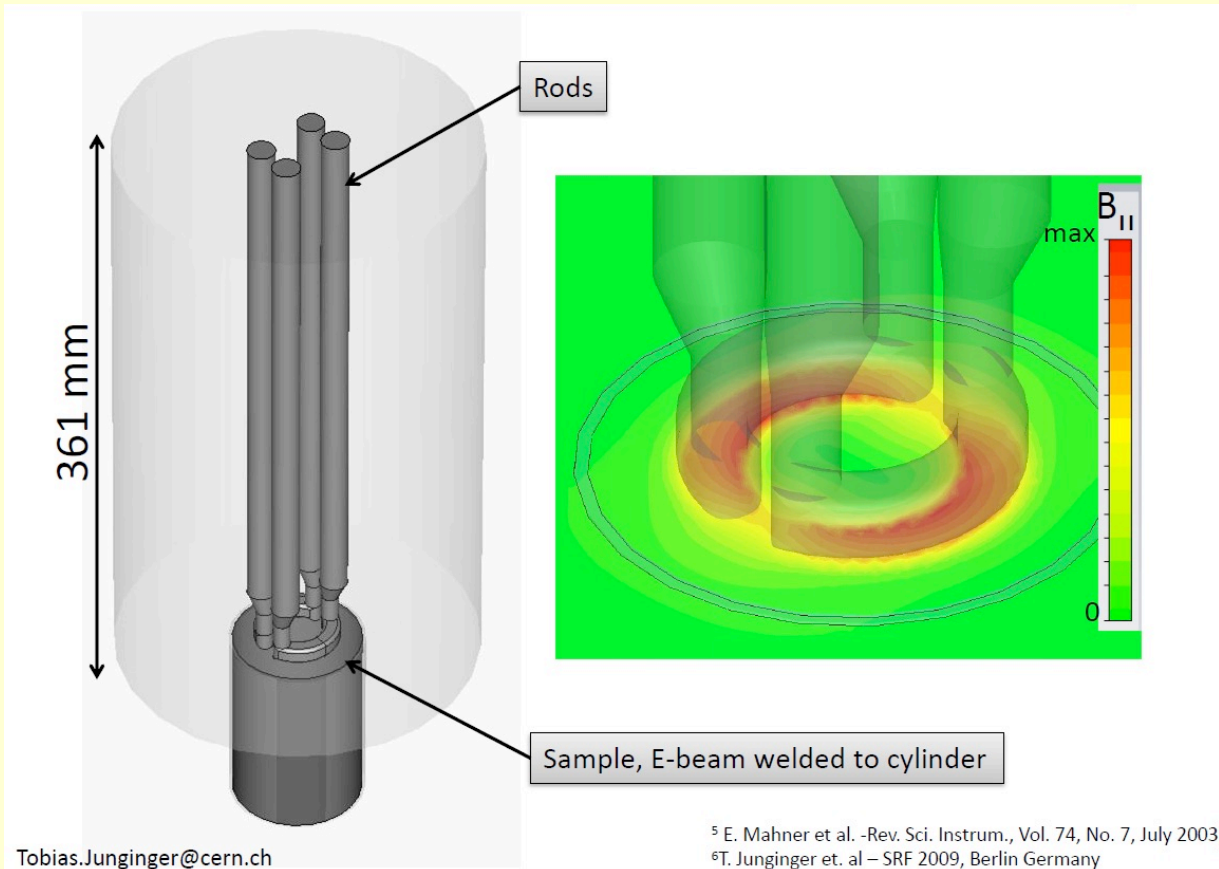
- Measurement of transmitted power P_t
- $P_t = c \int H^2 ds$, c from computer code

How to measure RF Surface Impedance 4/7



Surface resistance vs frequency for copper and Niobium at @2K and 4.5 K respectively (left graph by B.Tenenbaum)

How to measure RF Surface Impedance ^{5/7}



Why should we use this kind of resonator when we have the nice TE₀₁₁ type pillbox?

Answer: It allows for lower frequencies or a smaller sample size compared to the pillbox resonator

How to measure RF Surface Impedance ^{6/7}

The measurement principle is based on the so-called shielded pair technique [7], which consists of a one metre long cylindrical TEM cavity with two cylindrical inner conductors (see Figure 1). A detailed description of the experimental set-up is given in ref. [6]. Basically, processing of the loaded quality factors measured in the even and odd mode excitations, in steps of ~ 150 MHz, yields the surface resistance of the outer tube and of the inner conductors, assuming that the latter have an identical copper coating.

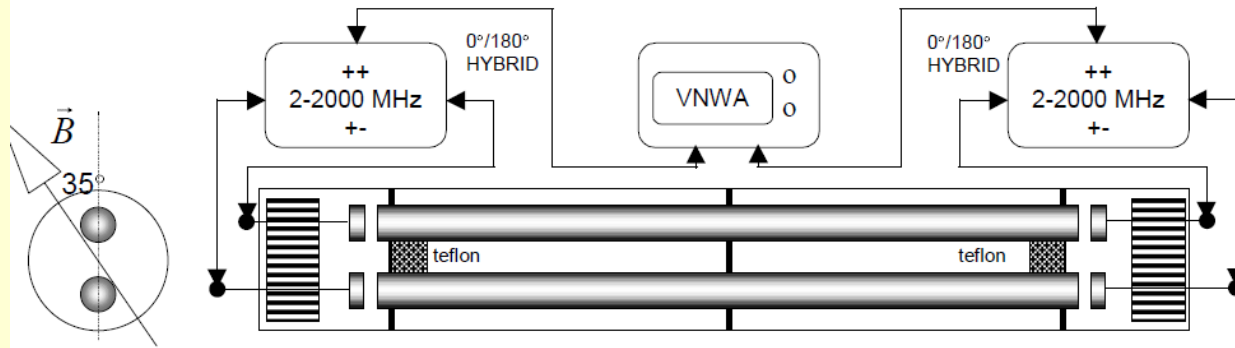


Figure 1: Cross section and side view of the experimental setup: a vector network analyser (VNA) is used in conjunction with two hybrids, yielding either even (++) or odd (+-) mode excitation for a 1 m long cylindrical cavity with 2 inner conductors, held by 3 Teflon supports. The near degeneracy of even and odd modes is removed by 2 teflon blocks (splitters) placed between the inner conductors.

This setup has been intensively used for measurements of the normal conducting copper losses of the LHC beam screen at cryo temperature at with a strong static magnetic field; it now again under discussion for the FCC beam screen evaluation which may have high T_c superconducting coating (compatible with the strong DC magnetic field)

From: F. Caspers et al; Surface resistance measurements... LHC project report 307

How to measure RF Surface Impedance ^{7/7}

- The examples shown so far are by no means exhaustive
- For the design of new measurement setups e.g. related to the evaluation of surface roughness impact, one may have to take anisotropy issues into account, depending on the structure of the surface roughness (e.g. laser erosion for multipactor reduction)
- For very high frequencies confocal resonator (Fabry Perot type) setups were used.
- For tube-like (beam-pipe style) samples the first resonance frequency is often too high to cover the frequency range of interest. In this case one may insert a sapphire rod which at cryo has extremely low RF losses and an epsilon around 10 (caveat: anisotropic)

Critical field (s)

Critical field of superconductors studied for RF

Material	T_c [K]	B_{cth0} [mT]	B_{c10} [mT]	B_{c20} [mT]	B_{sh0} [mT]	B_{exp0} [mT]
Sn	3.7	30.9	–	–	68	30.6
In	3.4	29.3	–	–	104	28.4
Pb	7.2	80.4	–	–	105	112
Nb	9.2	200	185	420	240	160
Nb ₃ Sn	18.2	535	≈ 20	2400	400	106

Critical fields in DC and RF superconductivity

B_c	Critical magnetic field of type-I superconductor
B_{c1}	Lower critical magnetic field of type-II superconductor
B_{c2}	Upper critical magnetic field of type-II superconductor
B_{cth}	Thermodynamic critical field
B_{sh}	Superheating critical field
B_{exp}	Experimentally obtained maximum field in RF
An index “0” following any of the above symbols refers to the temperature $T = 0$ K, tacitly assuming $B(T) = B_0 [1 - (T/T_c)^2]$.	

Other deterministic parameters for cavity performance

Until till now we discussed the role of the RF frequency, lHe bath temperature, and sc material with its characteristic critical field and temperature. There are still other (less important) parameters that determine the performance of the cavity as well:

Influencing quantity	Impact quantity	Physical explanation	Cure
External static magnetic field B_{ext}	Residual surface resistance	Creation of vortices	Shielding of ambient magnetic field by Mu-metal / Cryoperm
Residual resistivity ratio RRR	BCS surface resistance	Mean free path dependence of R_{res}	Annealing steps during ingot production/after cavity manufacture
Ratio peak magnetic field to accelerating gradient B_p/E_a	Max. accelerating gradient	Critical magnetic field as ultimate gradient limitation	Optimization of cavity shape
Nb-H precipitate	Q-value / acc. gradient (Q-disease)	Lowering of T_c/B_c at precipitates of Nb-H	T-control during chemical polishing Degassing @ 700 °C Fast cool-down

Summary

Superconducting materials:

- are characterized by zero resistivity (in DC) and the Meissner effect;
- Show the (thermodynamic) phase transition into the superconducting state below a critical temperature and below a critical field;
- have a non-zero surface resistance for RF which can be understood by the two-fluid model and the London theory
- are subdivided into type I and type II, depending on the value of the Ginzburg-Landau parameter κ ;
- may be alloys or elements, for which they are of type I, except Nb, the technically most important one, which is type II and has the largest critical temperature and critical field;

Basics of RF cavities

- Variety of RF cavities (examples)
- Cavity characteristics
 - Cavity characteristics (peak fields, stored energy, ...)
 - Pillbox resonator –basics, field distribution
 - Computer codes to determine the cavity parameters
 - Different mode families
- Transmission line
- Response of a sc cavity to RF (determination of Q_0 , E_{acc} , ...)
- Measuring setup ($Q(E_{\text{acc}})$ curve, ...)
- Pass-band modes
- Typical example of storage ring cavity (LEP)
- Summary

Examples of RF cavities



Fig. 1 A spectrum of superconducting cavities.

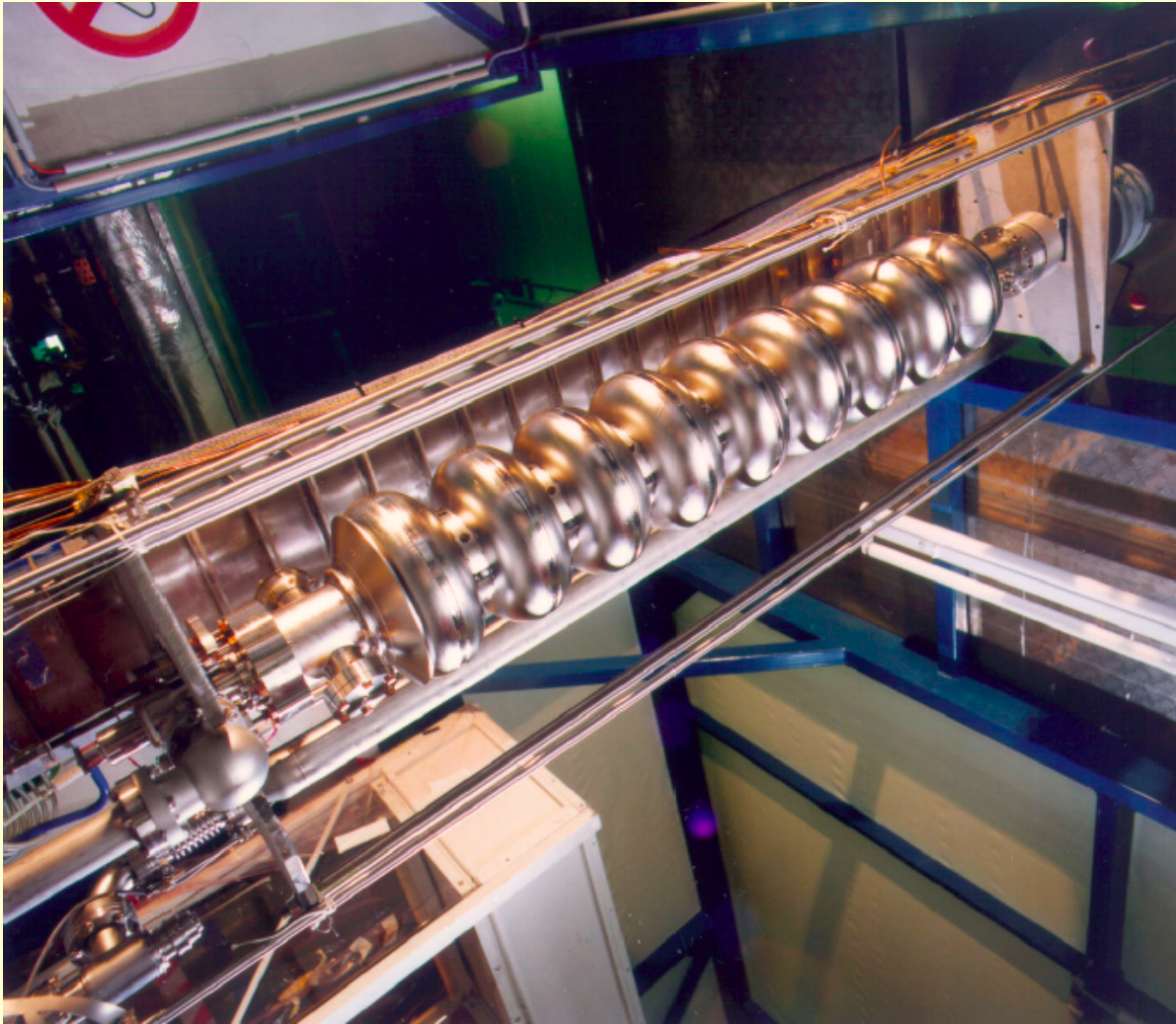
(from H. Padamsee, CERN-2004-008)

LHC - CERN



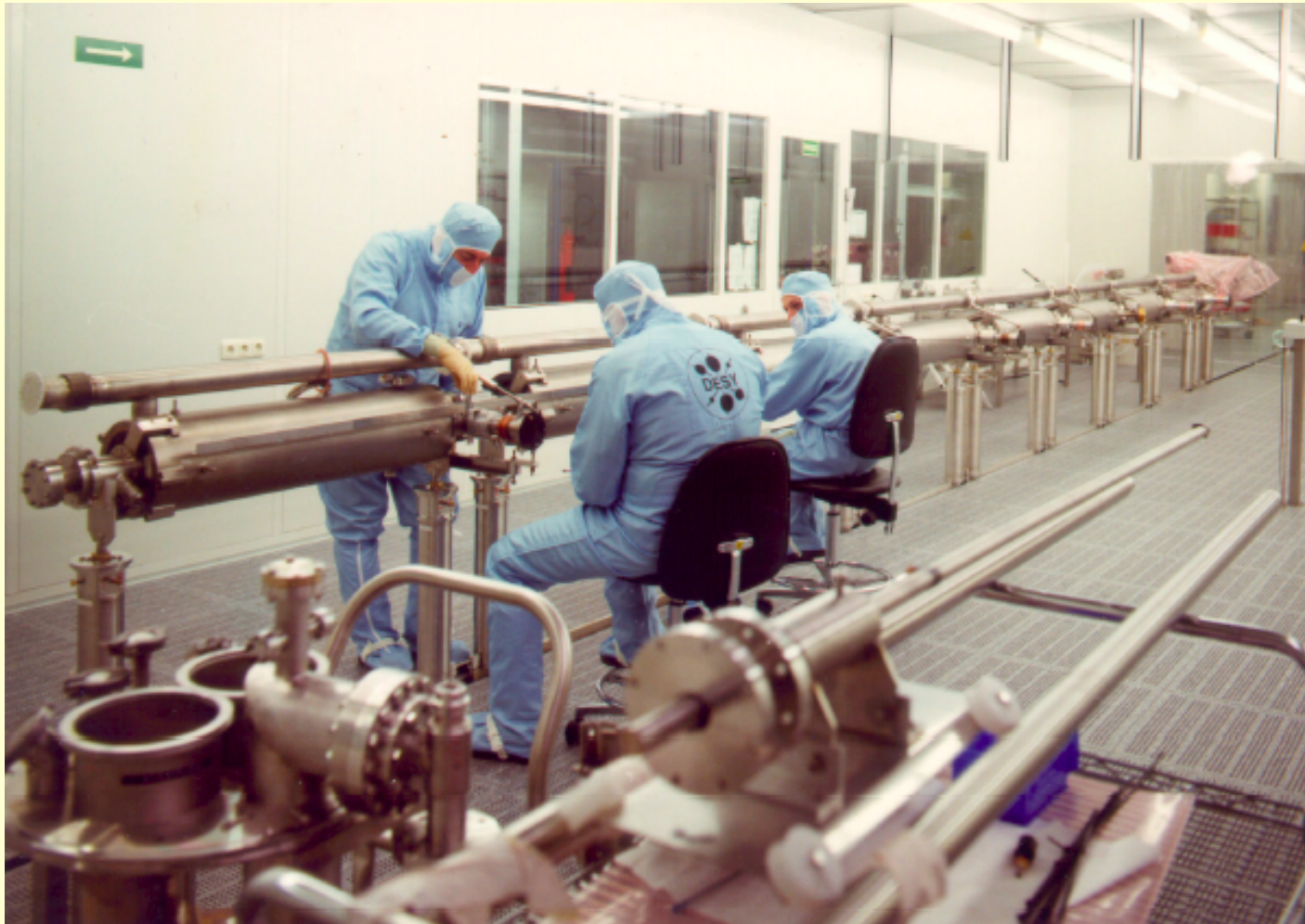
- $f_{res} = 400 \text{ MHz}$
 - $R/Q = 89 \Omega$
 - $Q_0 = 2 \times 10^9$
 - $E_{acc} = 5.33 \text{ MV/m}$
 - $P_{in} = 116 \text{ kW (CW)}$
- Niobium-film on Cu
 - 1-2 μm thickness
- 4 single-cell cavities per cryomodule
 - Each resonator delivers 2 MV
 - Blade tuner
 - «Doorknob» power coupler, 75 Ω coaxial
- Total of 8 cavities per beam: 16 MV

XFEL – DESY 1/3



- $f_{res} = 1300 \text{ MHz}$
 - $R/Q = 89 \Omega$
 - $Q_0 = 2 \times 10^9$
 - $E_{acc} = 5.33 \text{ MV/m}$
 - $P_{in} = 116 \text{ kW (CW)}$
- Niobium-film on Cu
 - 1-2 μm thickness
- 4 single-cell cavities per cryomodule
 - Each resonator delivers 2 MV
 - Blade tuner
 - «Doorknob» power coupler, 75 Ω coaxial
- Total of 8 cavities per beam: 16 MV

XFEL - DESY 2/3



XFEL cryomodule assembly of eight 9-cell cavities, quadrupole and BPM in a cleanroom

XFEL - DESY 3/3



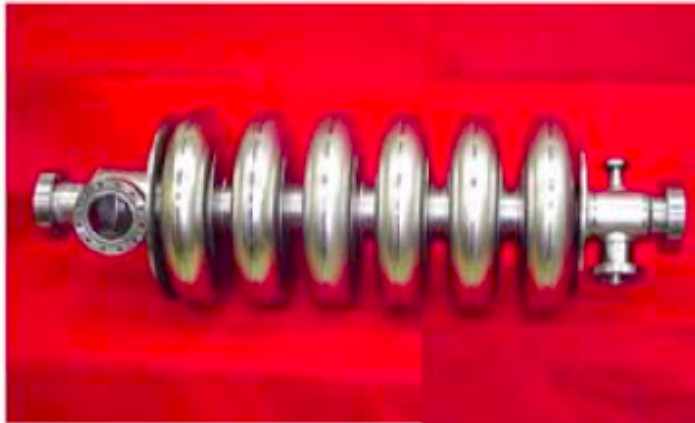
Cryomodule installation in the tunnel (the XFEL consists out of 101 cryomodules)

CEBAF - JLAB



SPL - CERN/ SNS - ORNL

Prototype Beta 0.61 and .81 Cavities



Development led by P. Kneisel with aid from colleagues all over the world

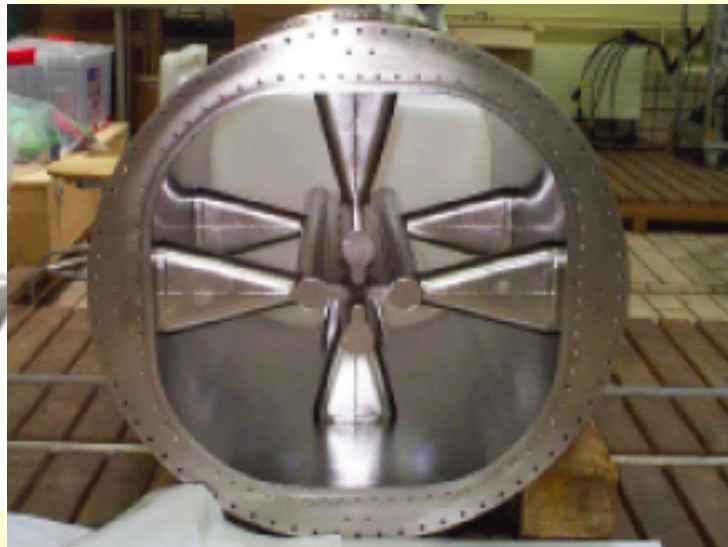
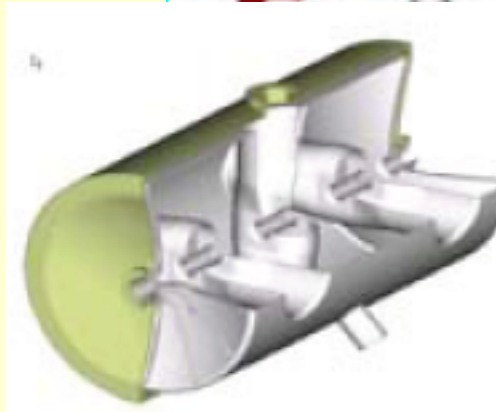
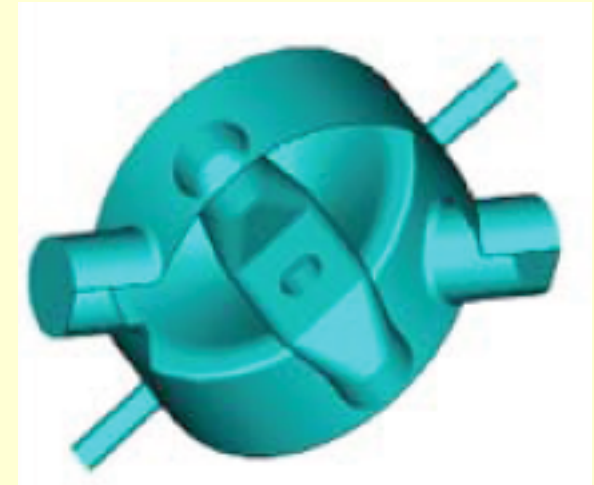
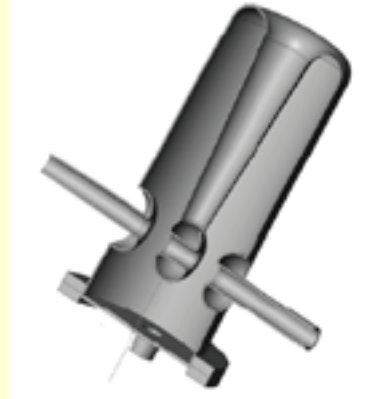
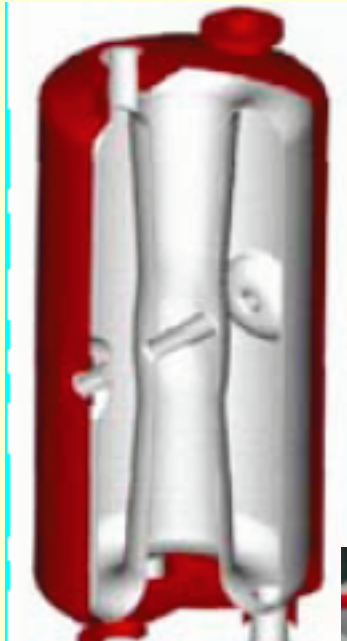
704 MHz SRF cavity R&D study to upgrade the CERN injectors with a high intensity superconducting RF proton linac (SPL)



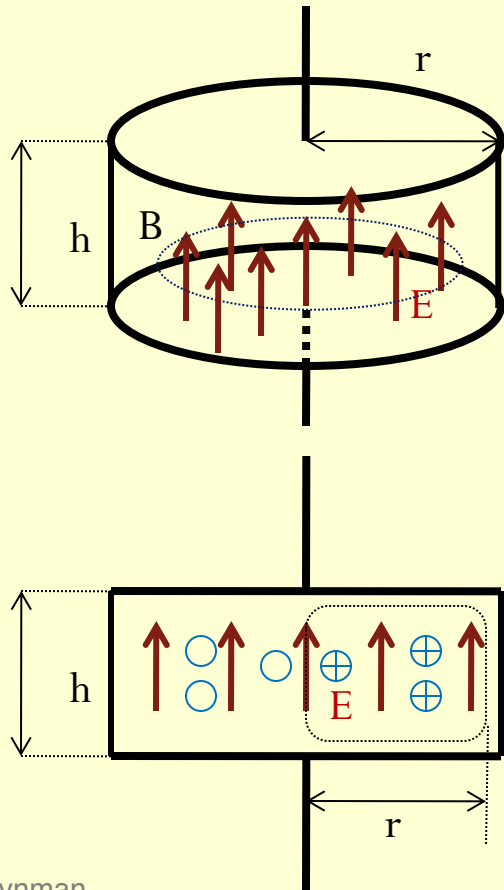
Heavy Ion accelerators ATLAS - ANL



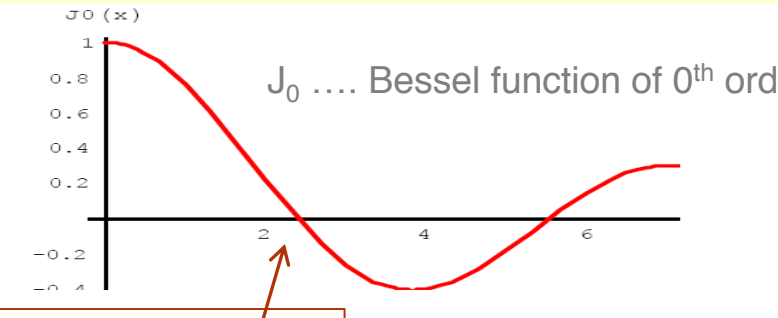
Shapes of heavy ion accelerator cavities



Pill box resonator

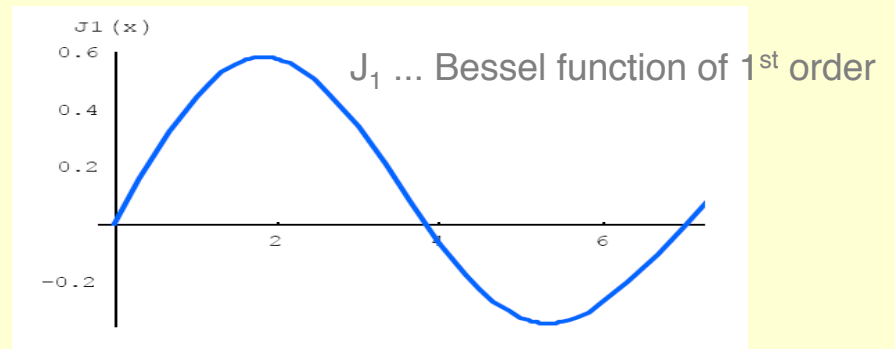


Field distribution TM_{010} mode:



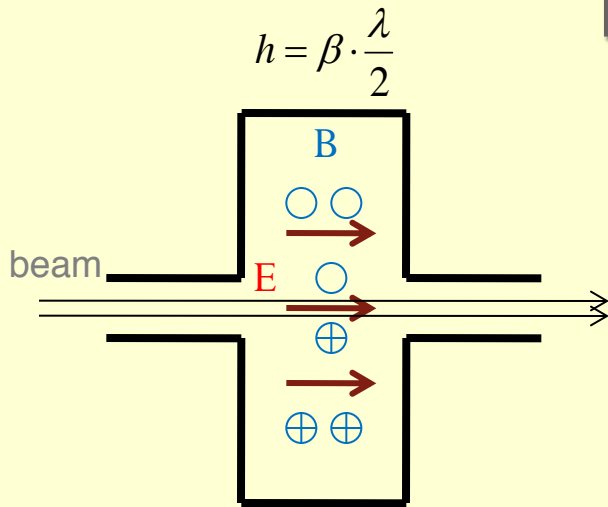
$$\frac{\omega_0 \cdot R}{c} = 2.405$$

Resonance-condition



Source: The Feynman Lectures on Physics, Vol. II

Pill box resonator



$$E(r, t) = J_0\left(\frac{2.405 \cdot r}{R}\right) \cdot E_0 \sin(\omega_0 \cdot t) \quad B_\varphi(r) = \frac{i}{c} J_1\left(\frac{2.405 \cdot r}{R}\right) \cdot E_0 e^{i\omega_0 t}$$

$$t(z) = z / (\beta \cdot c)$$

Stored energy U:

$$U = \frac{\epsilon_0}{2} \int_0^{2\pi} d\varphi \int_0^h dz \int_0^R r dr \cdot |E(r)|^2 = \frac{\epsilon_0}{2} \cdot \underbrace{\pi R^2 h}_V |E_0|^2 \cdot \left| \underbrace{J_1(2.405)}_{0.581865} \right|^2$$

$\eta = \sqrt{\frac{\mu_0}{\epsilon_0}}$

Dissipated power P:

$$P = \frac{R_s}{2\mu_0^2} \int_0^{2\pi} d\varphi \cdot \left(\int_0^h dz |B_\varphi(R)|^2 + 2 \cdot \int_0^R r dr |B_\varphi(r)|^2 \right) = R_s \frac{1}{\eta^2} |E_0|^2 \cdot \pi R \cdot (h + R) \cdot \left| \underbrace{J_1(2.405)}_{0.581865} \right|^2$$

Q factor:

$$Q = \frac{\text{Stored energy } U}{\text{Energy lost during 1 RF period}} = \omega \frac{U}{P} \quad Q = \omega \cdot \frac{\epsilon_0 \cdot \eta^2}{2R_s \cdot \left(\frac{1}{R} + \frac{1}{h}\right)}$$

Cavity characteristics

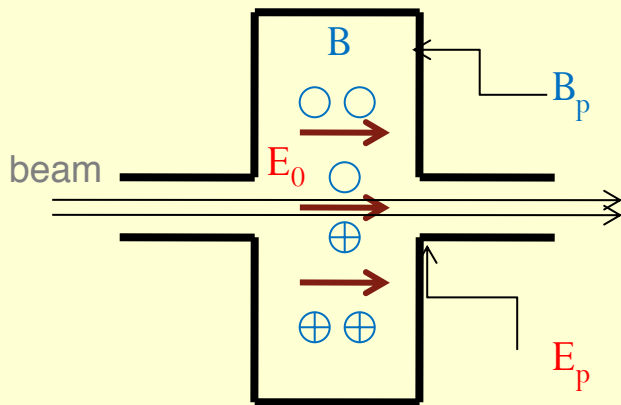
shunt impedance R :

$$R = \frac{V_a^2}{2 \cdot P}$$

R/Q measures the interaction of the cavity with the beam:

$$\frac{R}{Q} = \frac{V_a^2}{\underbrace{2 \cdot P}_R} \cdot \frac{P}{\underbrace{\omega \cdot U}_{1/Q}} = 7.10 \frac{4}{\pi^3} \cdot \frac{h}{R} \cdot \eta$$

The **peak surface electric and magnetic fields** constitute the ultimate limit for the accelerating gradient \Rightarrow minimize the ratio E_p/E_a and B_p/E_a .



$$E_a = \frac{2E_0}{\pi}$$

$$\frac{B_p}{E_a} = 3.07 \left[\frac{\text{mT}}{\text{MV/m}} \right]$$

$$\frac{E_p}{E_a} = \frac{\pi}{2} \approx 1.57$$

Cavity characteristics - Summary

Symbol	Name	Definition	Pillbox cavity [0.35 GHz, 4.2 K, Nb]	Accelerating cavity [0.35 GHz, 4.2 K, Nb]
E_p/E_a	Peak normalized surface electric field	n/a	1.6	2
B_p/E_a [mT/(MV/m)]	Peak normalized surface magnetic field	n/a	3.1	4
R_s [n Ω]	Surface resistance	E_x/H_y	40	40
h [m]	Cavity length	$h=\lambda/2$	0.43	0.43
E_a [MV/m]	Accelerating gradient	$(1/e) \cdot \text{Energy gain/length}$	10	10
V [MV]	Accelerating voltage	$V=E_a \cdot h$	4.3	4.3
G [Ω]	Geometry factor	$G=R_s \cdot Q$	260	275
Q [10^9]	Quality factor	$Q=\omega U/P$	6.5	6.9
R/Q [Ω]	(R/Q) factor	$(R/Q)=V^2/(2\omega U)$	450	280
R [M Ω]	Shunt impedance	$R=V^2/(2P)$	$3 \cdot 10^6$	$2 \cdot 10^6$
U [J]	Stored energy	$U=V^2/[2\omega(R/Q)]$	9	15
P [W]	Dissipated power	$P=\omega U/Q$	3	5
h/R	Ratio cavity length to radius	n/a	1.3	0.5

Computer codes for RF cavities

Computer codes to determine the cavity parameters

For real structures with contoured shapes, beam apertures and beam pipes, it is necessary to use field computation codes, such as MAFIA and Microwave Studio. Figure 10 shows the electric and magnetic fields computed by Microwave Studio for the accelerating mode of a pillbox cavity with a beam hole, and for a round wall cavity. Such codes are also necessary for computing the fields in the higher order modes of a cavity that can have an adverse effect on beam quality or cause instabilities. Figure 11 shows the electric and magnetic fields of the first monopole HOM. Beam induced voltages are also proportional to the R/Q of HOMs.

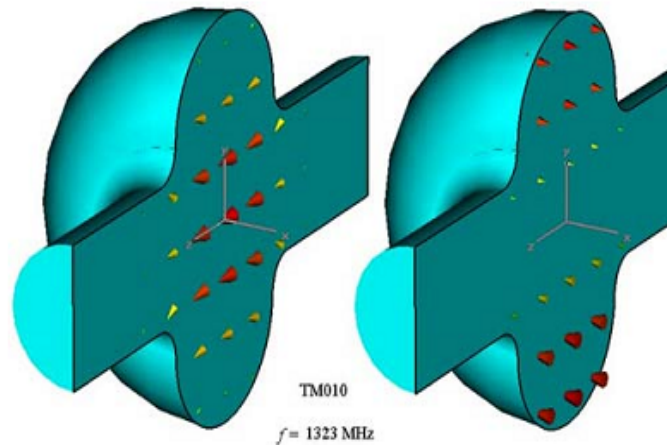


Fig.10 (Left) Electric and (Right) Magnetic fields for a round cavity with beam holes.

Cavity characteristics – Summary table

Table: Equivalence of cavity and lumped-element circuit parameters

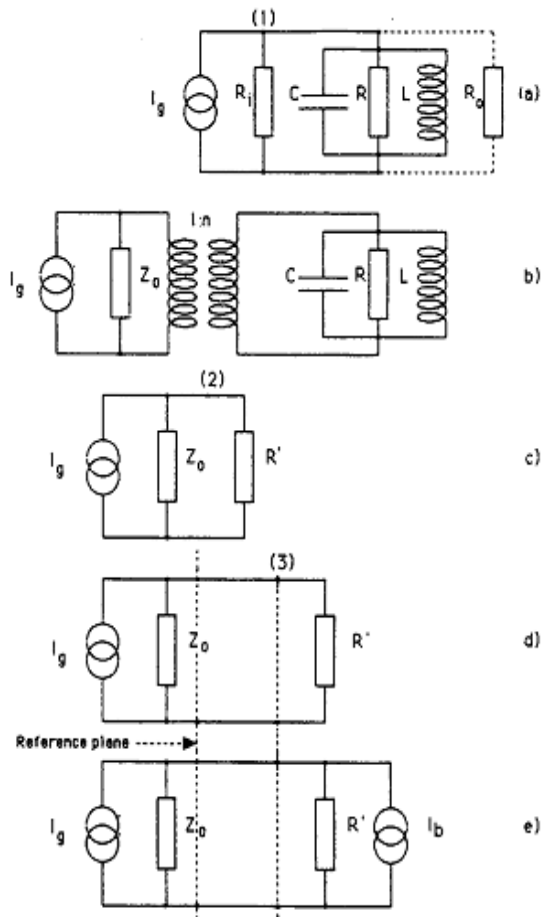


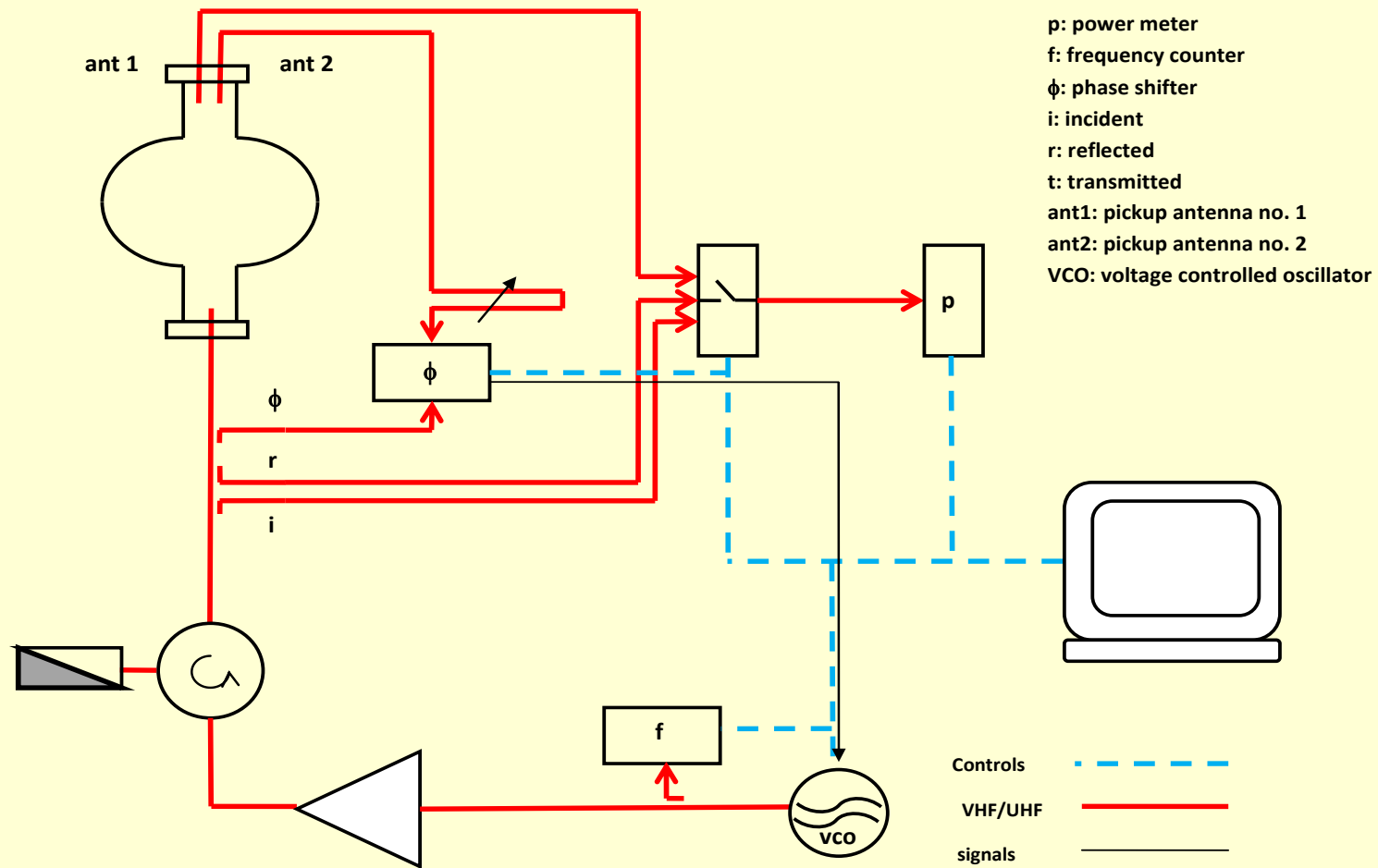
Fig. 8 Lumped element equivalent circuit model of an accelerating cavity resonator

Cavity	Lumped-element circuit
Accelerating voltage V	Peak voltage V
Resonant frequency ω_0	$\omega_0 = 1/\sqrt{LC}$
Stored energy U	$U = (1/2)CV^2$
Dissipated power P_c	$P_c = (1/2) V^2/R$
Radiated power P_{rad}	$P_{\text{rad}} = (1/2) V^2/R_i$
Shunt impedance $R = V^2/(2 \cdot P_c)$	R
Unloaded Q - value $Q_0 = \omega_0 \cdot U/P_c$	$Q_0 = \omega_0 \cdot RC$
External Q - value $Q_{\text{ext}} = \omega_0 \cdot U/P_{\text{rad}}$	$Q_{\text{ext}} = \omega_0 \cdot R_i C = R_i/(R/Q)$
(R/Q) value $R/Q = V^2/(2 \omega_0 \cdot U)$	$R/Q = \sqrt{L/C} = 1/(\omega_0 \cdot C)$
Coupling factor $\beta = Q_0/Q_{\text{ext}}$	$\beta = R/R_i$
Loaded Q - value $Q_L = Q_0/(1 + \beta)$ (because $Q_L^{-1} = Q_0^{-1} + Q_{\text{ext}}^{-1}$)	$Q_L = \omega_0 \cdot RC/(1 + \beta)$
Turns ratio $n = \sqrt{[(R/Q) \cdot Q_{\text{ext}}/Z_0]}$	$n = \sqrt{R_i/Z_0}$
Wave impedance $Z_0 = 50 \Omega$	

From W. Weingarten, CERN-1992-03

Measuring setup

- Q determined by measuring the decay time of the cavity response
- Measurement of Q vs E_{acc}



Q(E_{acc}) curve

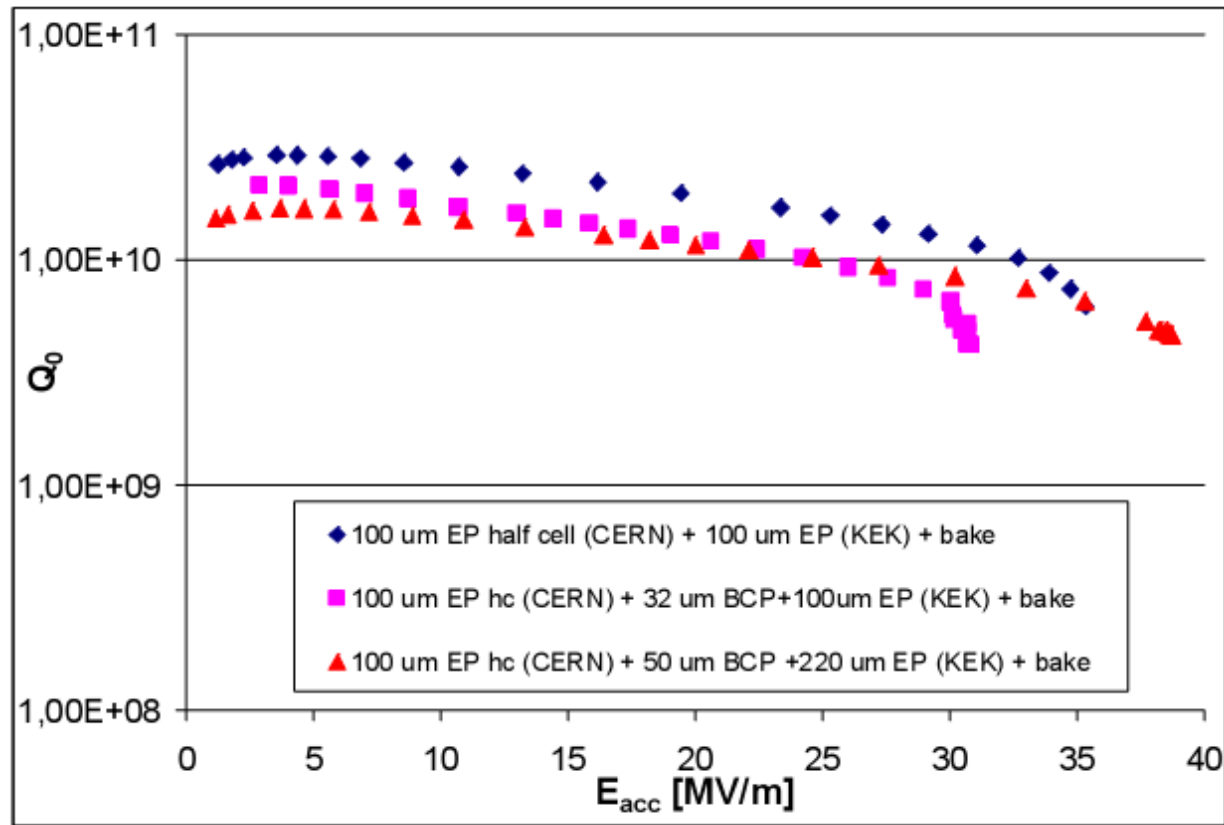
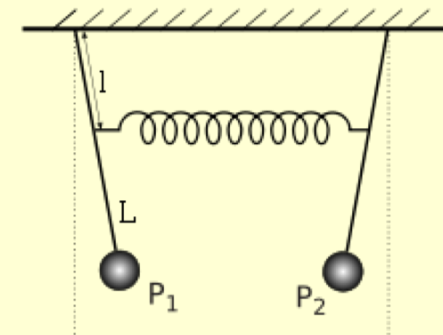
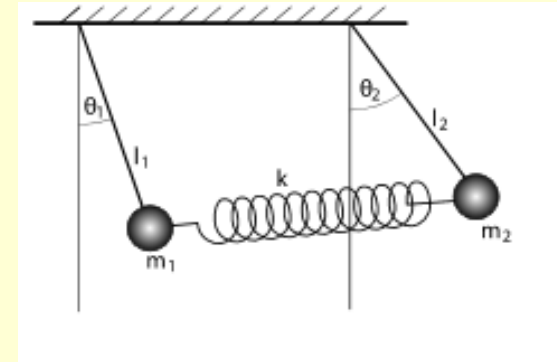
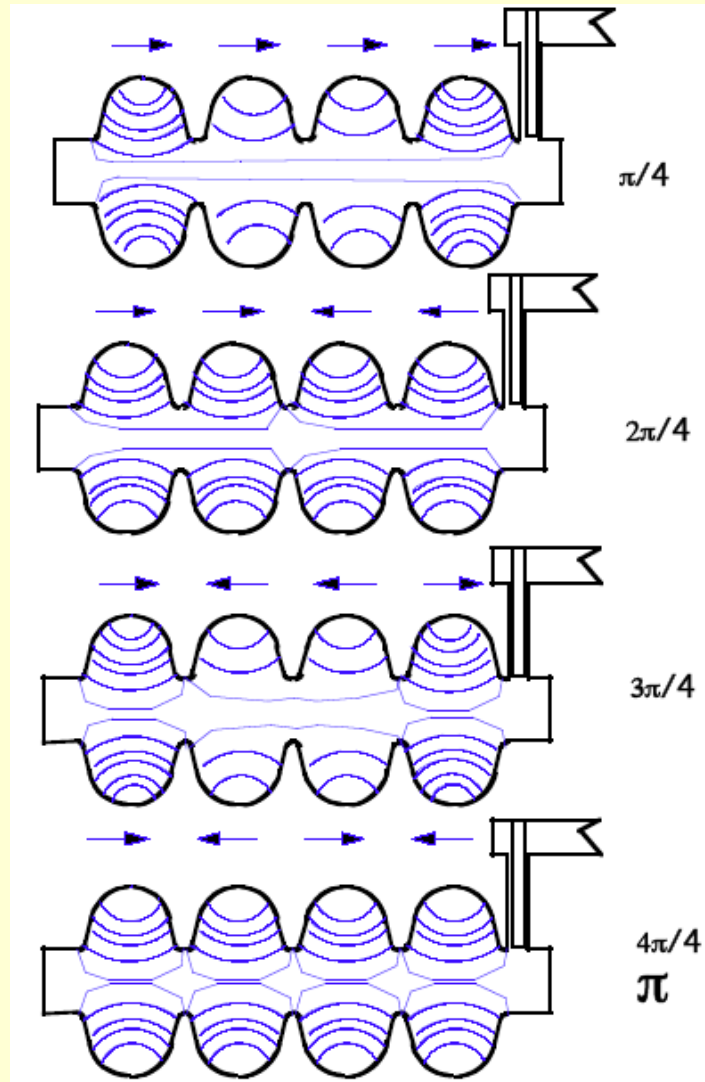


Figure 6: The cavities after bakeout show no Q-drop. One cavity is limited at 30 MV/m due to strong field emission and available RF power.

Passband modes

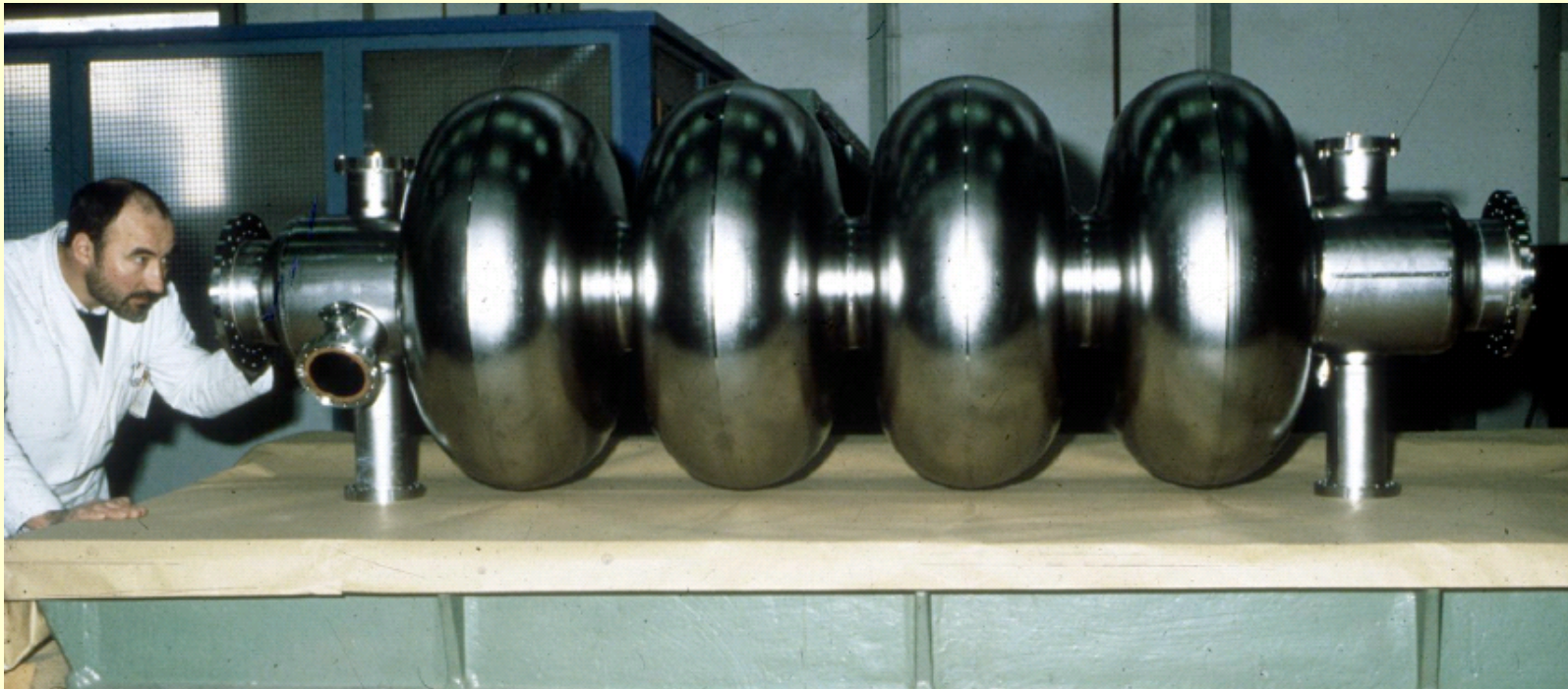


http://de.wikipedia.org/wiki/Gekoppelte_Pendel



- <http://www.youtube.com/watch?v=IAPWpViY19A>

Typical storage ring cavity (LEP)



Summary

- The pillbox resonator (TM_{010} mode) allows – as a paradigm - the analytical description of typical accelerator parameters, such as peak surface fields (E and H), power loss and Q-value, shunt impedance, geometrical shunt impedance, geometry factor, etc.
- « Real » accelerator cavities are designed by making use of computer codes such as Microwave Studio, MAFIA, SUPERFISH, etc.
- The response of a cavity to an RF pulse is well described by lumped circuit networks, in particular by the transmission and reflection of an electromagnetic wave at a discontinuity in the line.
- An algorithm is presented to determine the coupling factor β (or the reflection factor ρ), and finally the unloaded Q-value Q_0 , the accelerating voltage V (accelerating gradient E_a) and the surface resistance R_s .

Interaction of cavity with beam

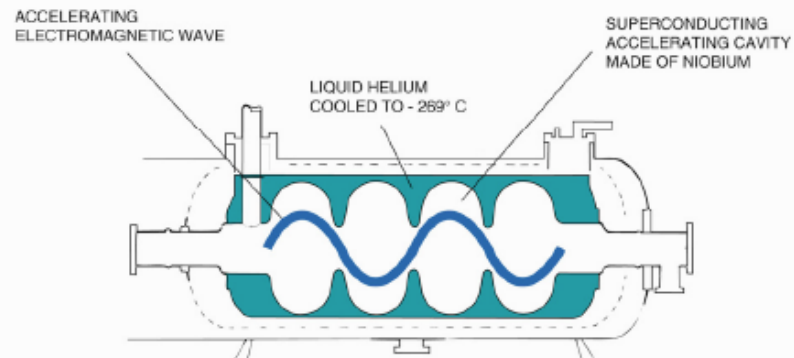
- Descriptive introduction
- Analytical introduction
- Transfer of RF power from the cavity to the beam
 - The fundamental mode power coupler
- Transfer of RF power from the beam to the cavity
 - Higher order modes and their damping
- The frequency tuner
- Summary

Descriptive Introduction

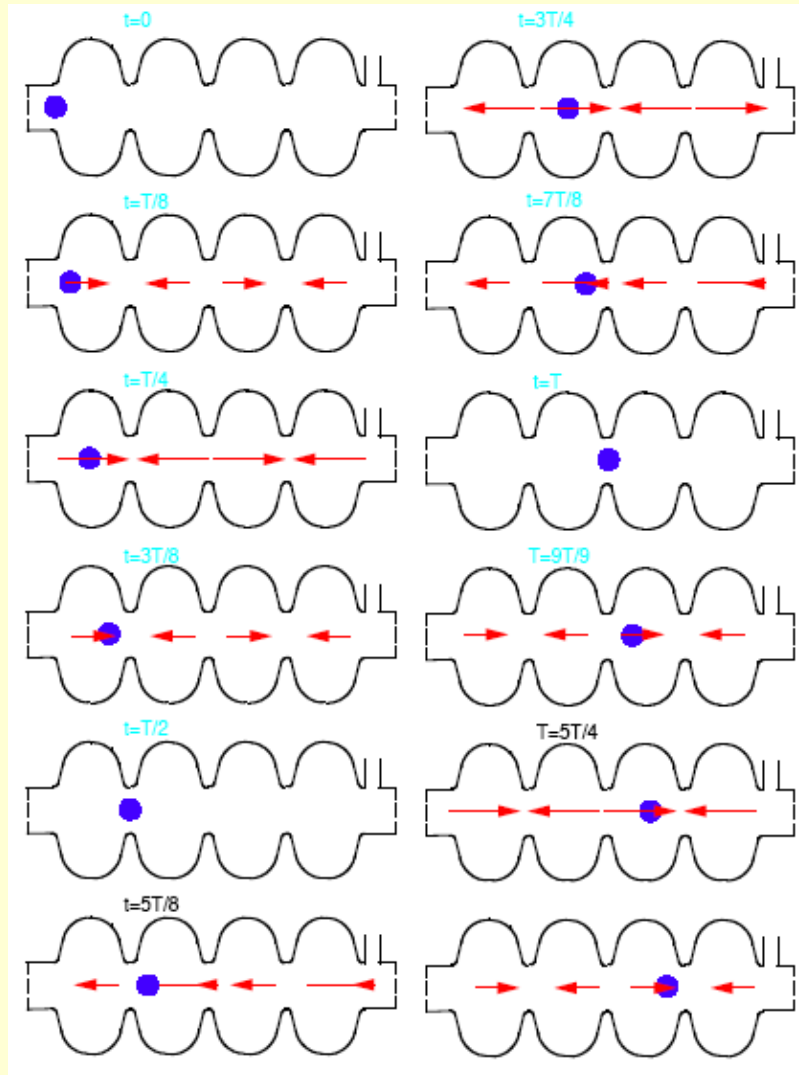
THE SUPRACONDUCTIVITY



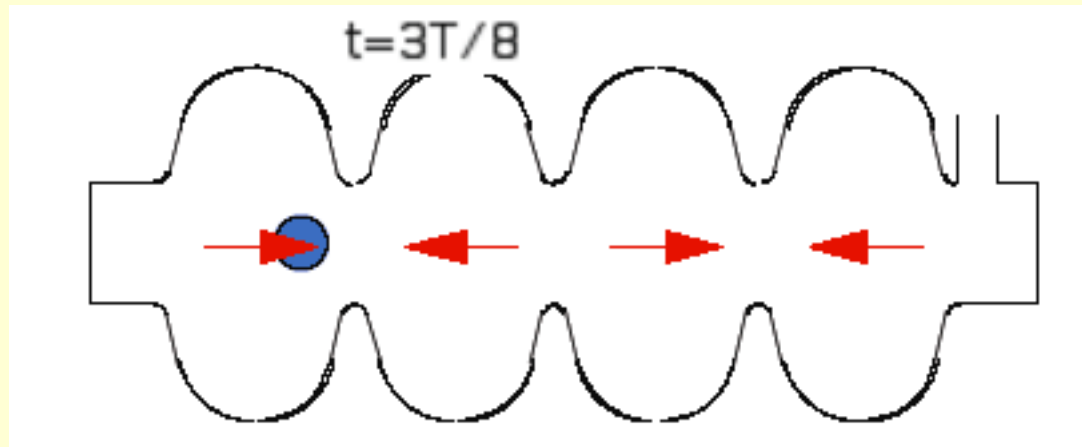
THE USE OF SUPRACONDUCTIVITY TO INCREASE
PERFORMANCES AND CONSIDERABLY REDUCE
ELECTRICITY CONSUMPTION



Particle passing through cavity



Analytical Introduction



$$V = E(z_1, t_1) \Delta z_1 + E(z_2, t_2) \Delta z_2 + \dots$$

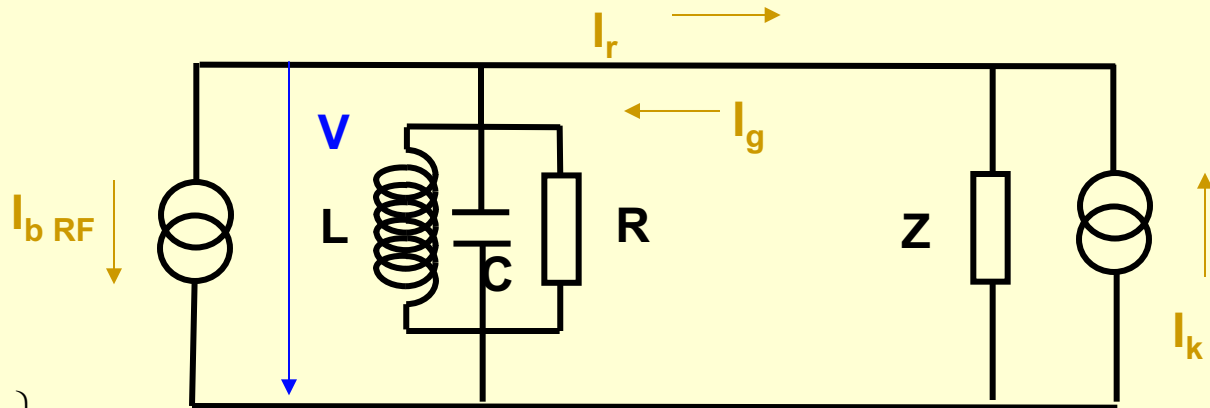
$$\Rightarrow V = \int_{-\infty}^{+\infty} E(z, t(z)) dz$$

$$E(z, t) = E(z) * \cos(\omega t + \varphi)$$

$$t = z/v$$

$$V(\varphi) = \int_{-\infty}^{+\infty} E(z) * \cos(z\omega/v + \varphi) dz$$

Transfer of RF power from the cavity to the beam 1/3



$$\left. \begin{aligned} I_r - I_g + I_k &= \frac{V}{Z} \\ I_k &= 2I_g \end{aligned} \right\} \Rightarrow I_r + I_g = \frac{V}{Z}$$

A circulator guarantees that under no circumstances there is no reflected wave impinging to the RF generator

$$I_{LCR} = I_g - I_r - I_{b,RF} = 2I_g - I_{b,RF} - \frac{V}{Z}$$

$$I_{LCR} = V \left(\frac{1}{i\omega L} + i\omega C + \frac{1}{R} \right)$$

$$\omega_0 = \frac{1}{\sqrt{LC}}$$

With $\omega_0^2 - \omega^2 \approx 2\omega_0\Delta\omega$ and $\Delta\omega \ll \omega$

$$\Rightarrow V \left(-\frac{2\Delta\omega}{\omega} + \frac{1}{i\omega C} \left(\frac{1}{R} + \frac{1}{Z} \right) \right) = \frac{2I_g - I_{b,RF}}{i\omega C}$$

Transfer of RF power from the cavity to the beam ^{2/3}

Re-write preceding equation

$$V \left(-\frac{2\Delta\omega}{\omega} + \frac{1}{i\omega C} \left(\frac{1}{R} + \frac{1}{Z} \right) \right) = \frac{2I_g - I_{b,RF}}{i\omega C}$$

in cavity parameters

$$V \left(\frac{1}{2(R/Q)} \left(\frac{1}{Q_{ext}} + \frac{1}{Q_0} \right) - i \frac{\Delta\omega}{\omega(R/Q)} \right) = I_g - \frac{1}{2} I_{b,RF}$$

Transfer of RF power from the cavity to the beam 3/3

$$V \left(\frac{1}{2(R/Q)} \left(\frac{1}{Q_{ext}} + \frac{1}{Q_0} \right) - i \frac{\Delta\omega}{\omega(R/Q)} \right) = I_g - \frac{1}{2} I_{bRF}$$

- Minimize reflected power

$$\Rightarrow I_g = \frac{V}{2(R/Q)} \left(\frac{1}{Q_{ext}} + \frac{1}{Q_0} \right) + I_{DC} \cos\Phi - i \left(I_{DC} \sin\Phi + \frac{V\Delta\omega}{\omega(R/Q)} \right)$$

$\frac{1}{Q_0} \ll \frac{1}{Q_{ext}}$ for sc cavities

$$I_r = \frac{V}{Q_{ext} \cdot (R/Q)} - I_g = \frac{V}{2 \cdot (R/Q)} \left(\frac{1}{Q_{ext}} - \frac{1}{Q_0} \right) - I_{DC} \cos\Phi - i \left(I_{DC} \sin\Phi + \frac{V\Delta\omega}{\omega(R/Q)} \right)$$

Actions: 1) compensate « reactive beam loading » to zero by detuning $\Delta\omega$

$$\Delta\omega = -\omega \frac{(R/Q) \cdot I_{DC} \sin\Phi}{V}$$

2) define optimum Q_{ext} for nominal beam current for $I_r = 0$

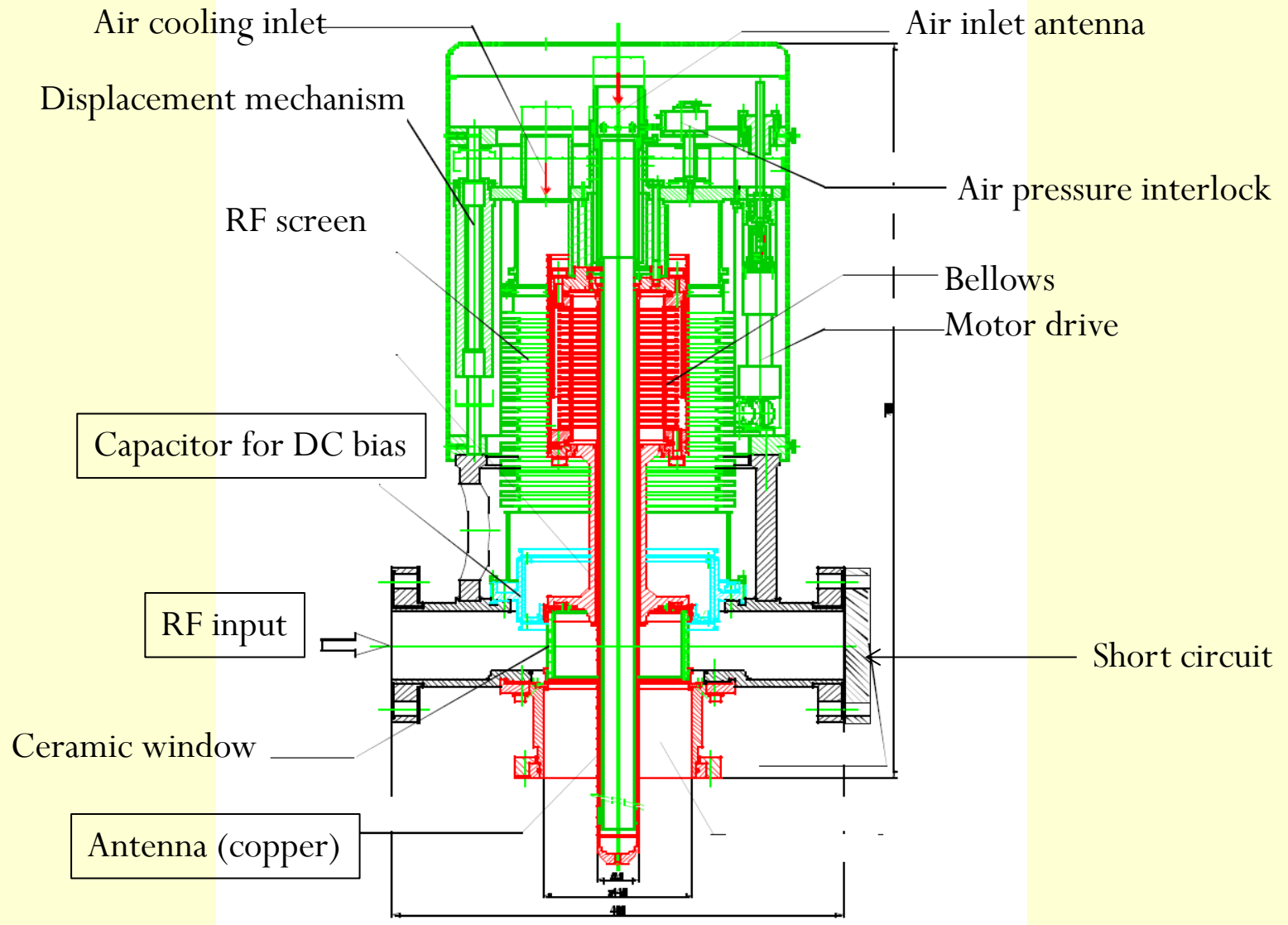
$$Q_{ext,opt} = \frac{V}{2 \cdot (R/Q) I_{DC} \cos\Phi}$$

RF power $P_{g,r} = \frac{1}{2} Z |I_{g,r}|^2 = \frac{1}{2} (R/Q) \cdot Q_{ext} \cdot |I_{g,r}|^2$

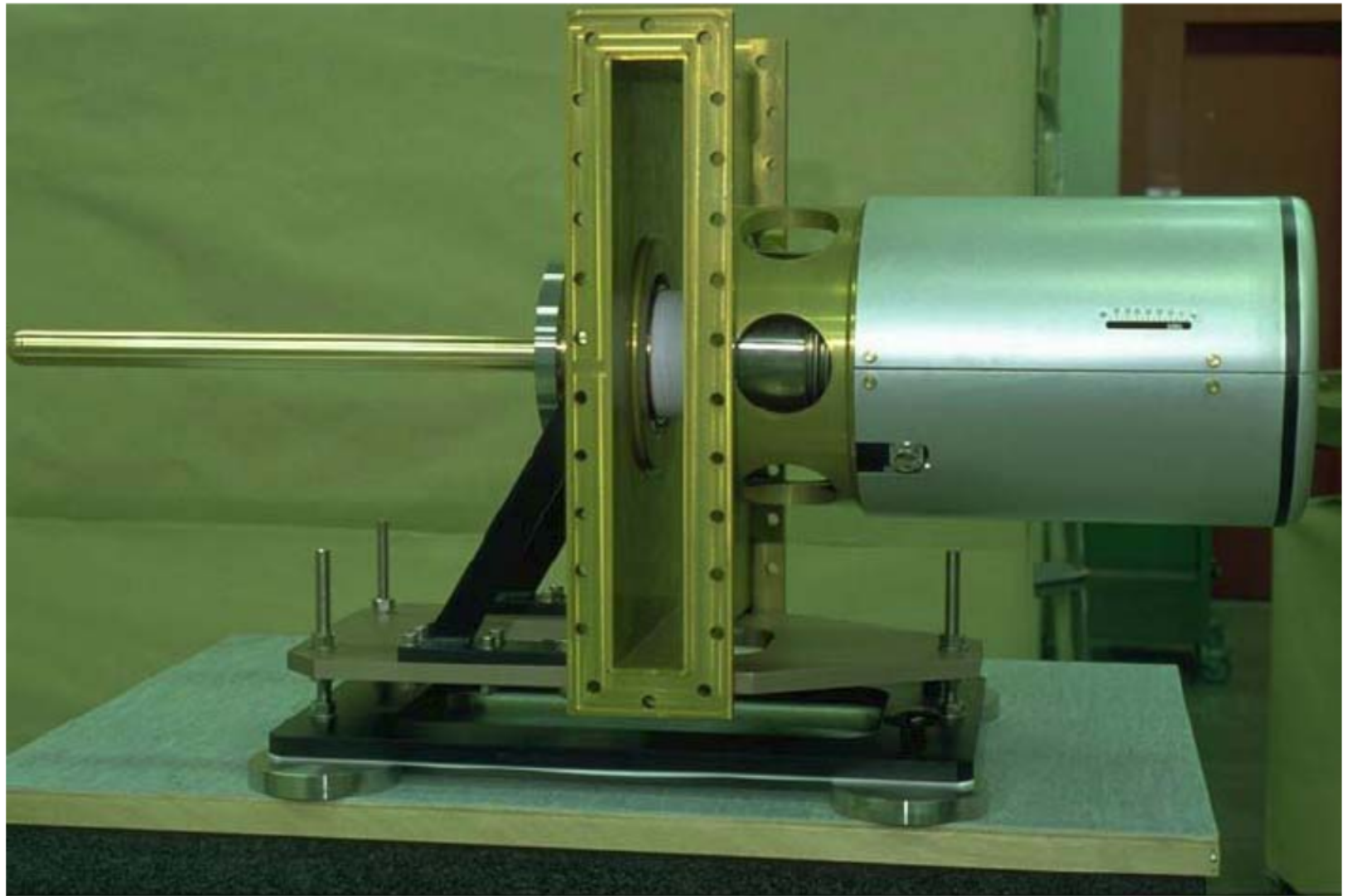
Check:

$$P_{beam,r} = P_{g,r} - P_{r,r} = V \cdot I_{DC} \cdot \cos\Phi$$

The fundamental mode power coupler



LHC solution of the power coupler



Transfer of RF power from the beam to the cavity

- Need for Higher Order Mode (HOM) coupler

Imagine worst case

1. the cavity resonant frequency is « tuned » to a spectral line of the beam
2. Generator switched off, $I_g=0$.

$$V \left(\frac{1}{2(R/Q)} \left(\frac{1}{Q_{ext}} + \frac{1}{Q_0} \right) - i \frac{\Delta\omega}{\omega(R/Q)} \right) = I_s - \frac{1}{2} I_{b,RF} \quad \Rightarrow \Delta\omega = 0; \Phi = 0$$

$$\Rightarrow V = -I_{b,RF} \cdot (R/Q) \cdot Q_{ext} = -2 \cdot I_{DC} \cdot (R/Q) \cdot Q_{ext}$$

This means that the beam is decelerated.

Remedy: keep Q_{ext} as low as possible.

Output power (reflected):

$$P_r = \frac{V^2}{2 \cdot Z} = \frac{V^2}{2 \cdot (R/Q) \cdot Q_{ext}} = 2 \cdot (R/Q) \cdot Q_{ext} \cdot I_{DC}^2$$

1st example (LEP); RF Generator trip.

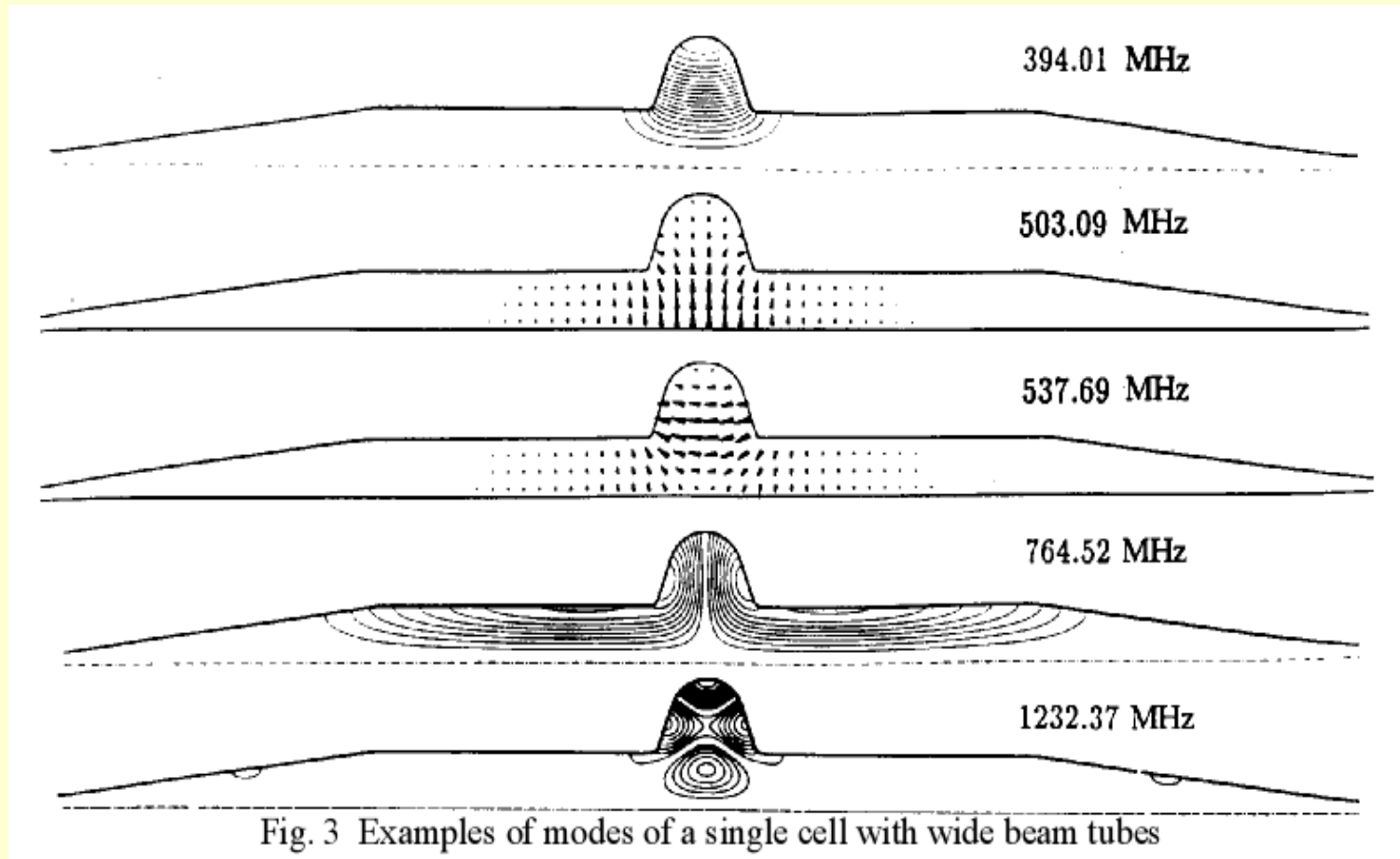
We obtain for the **accelerating mode** $R/Q = 232 \Omega$; $Q_{ext} = 2 \cdot 10^6$; $I_{DC} = 6 \text{ mA}$; $P_r = 33 \text{ kW}$

2nd example;

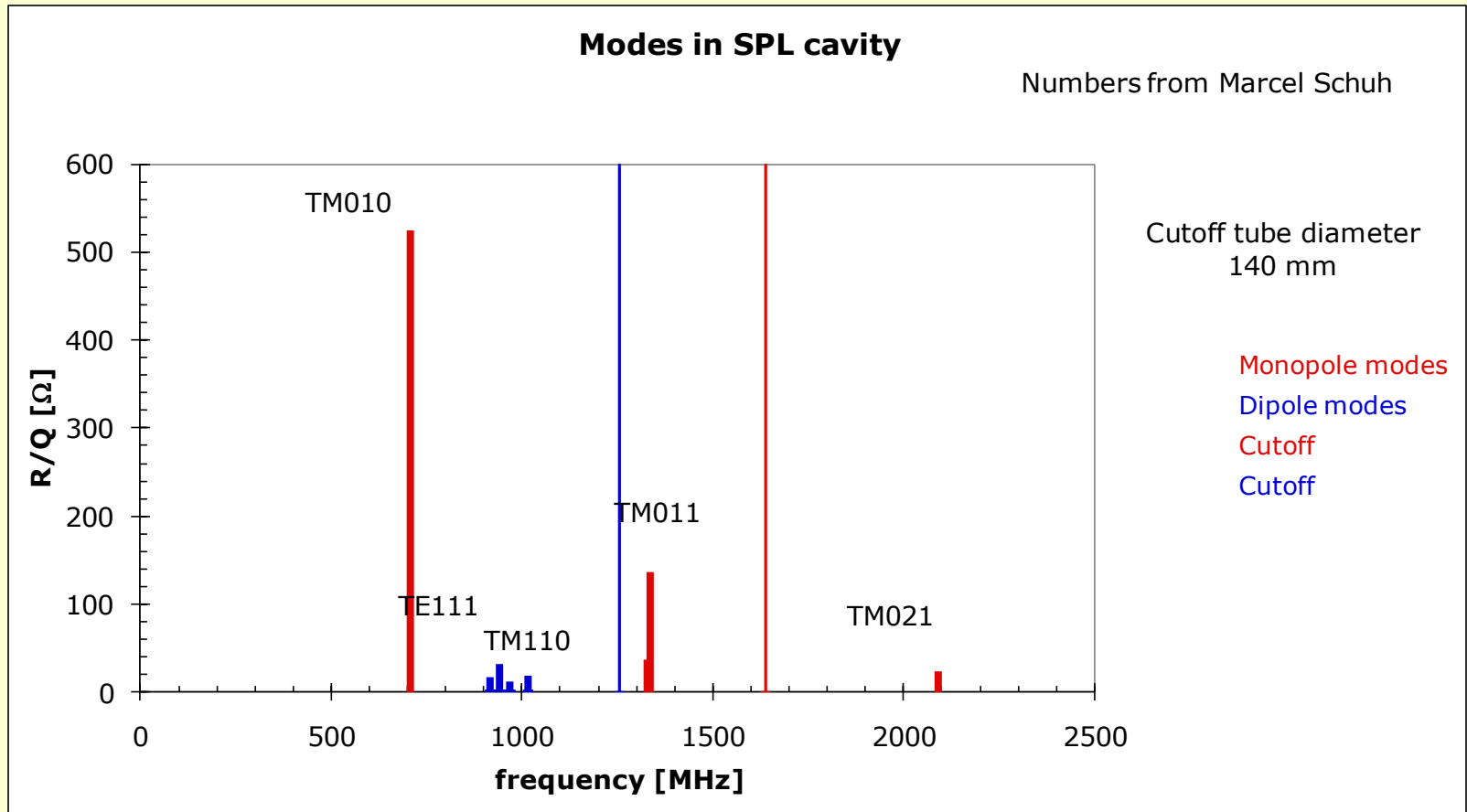
We obtain for the **higher order mode** with $(R/Q) = 10 \Omega$, $Q_{ext} = 20000$

$$V = -2.4 \text{ kV} \Rightarrow P_r = 14.4 \text{ W}$$

Higher order modes



A typical HOM spectrum



How to deconfine HOMs¹

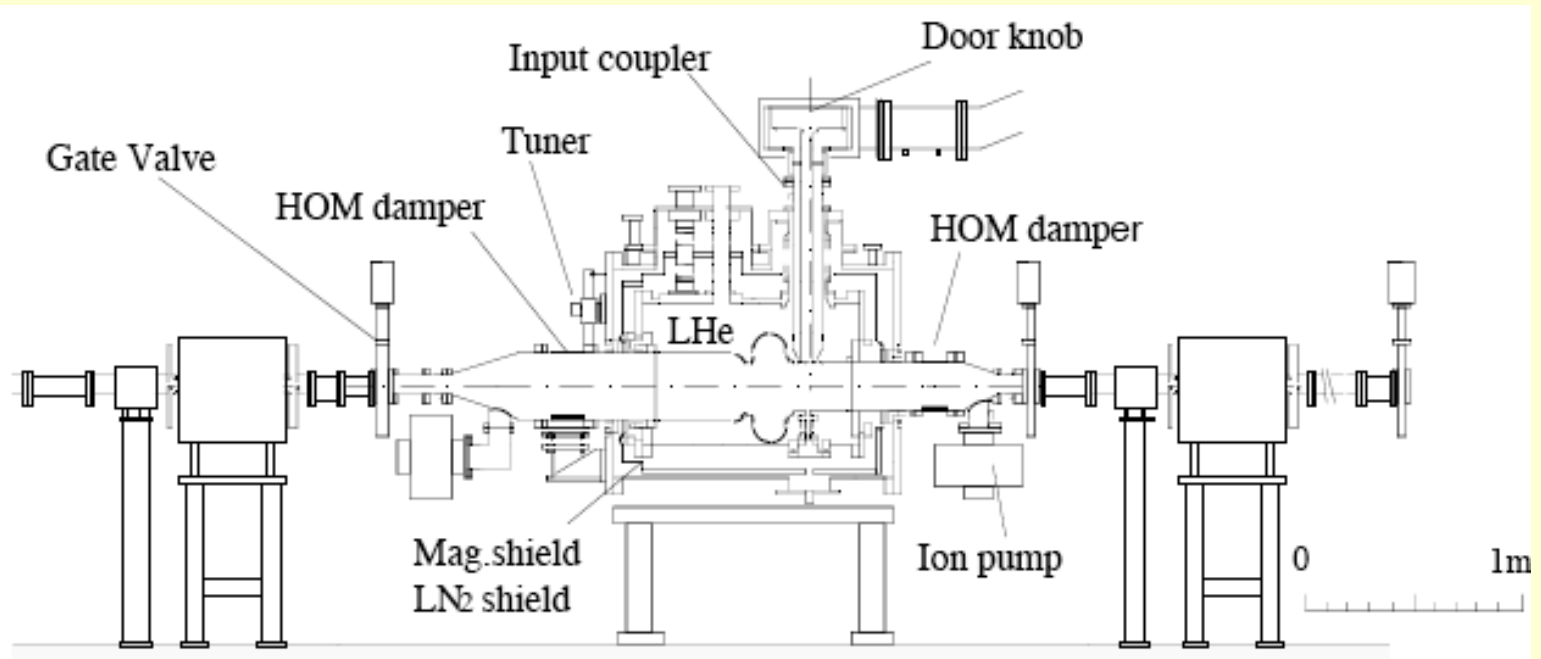


Figure: 1 A sketch of the prototype module in TRISTAN Accumulation Ring.

Open beam tube

OK for single cell cavity, but high cryo-load by thermal radiation

¹<http://www.lns.cornell.edu/Events/HOM10/Agenda.html>

Damping HOMs ^{1/2}: Beam tube loads

Ferrites

low power handling capacity if cold
higher power handling capacity if warm
mechanical and vacuum design not easy

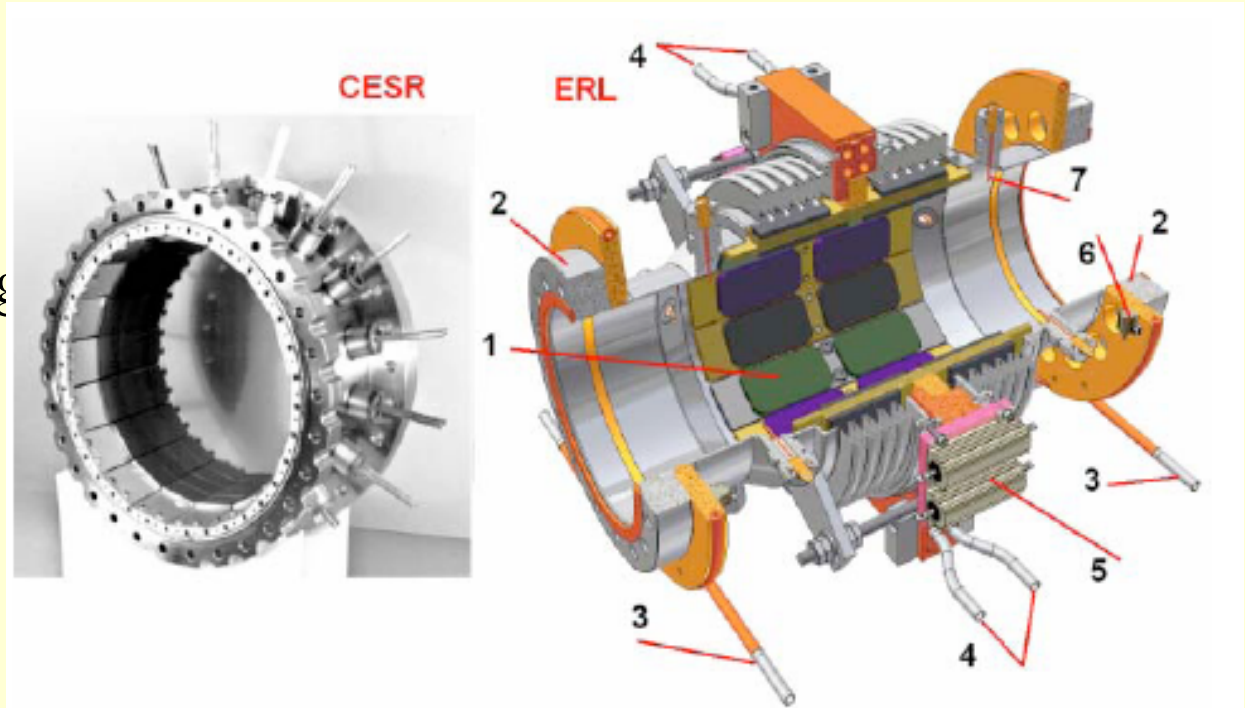


Figure 1: CESR and ERL HOM loads. 1 – absorber plates, 2 – flange to cavity, 3 – 5 K He cooling loop, 4 – 80 K cooling loop, 5 – 80 K heater, 6 – 5 K heaters, 7 – HOM pickup.

Damping HOMs 2/2: Resonant coaxial transmission line dampers

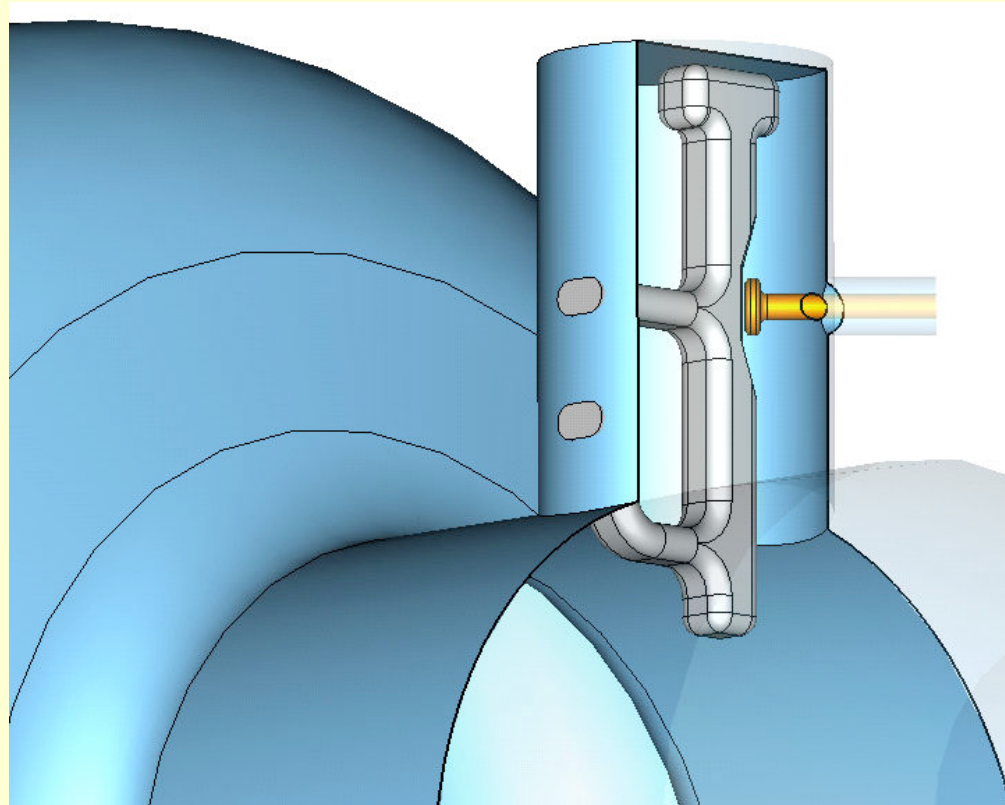
- Compensate internal impedances: The HOM coupler becomes a resonator coupled to the cavity resonator. It may have two eigenfrequencies.
Obtainable Q_{ext} : 50
- Pros:
 - Couplers with several resonances possible (HERA, LEP, LHC, ILC are of this type)
 - Demountability
 - Fundamental mode rejection:
 - LEP: Fundamental mode E-field rejected by stop-filter in front of HOM coupler
 - Fundamental mode H-field rejected by loop plane perpendicular to cavity axis
 - Risk of detuning of notch filter
- BUT: High currents request for superconducting material prepared under ultra-clean conditions (like the cavity) and lHe cooling
- Prone to electron emission from inside cavity

Resonant coaxial transmission line dampers: Technical solution $1/3$



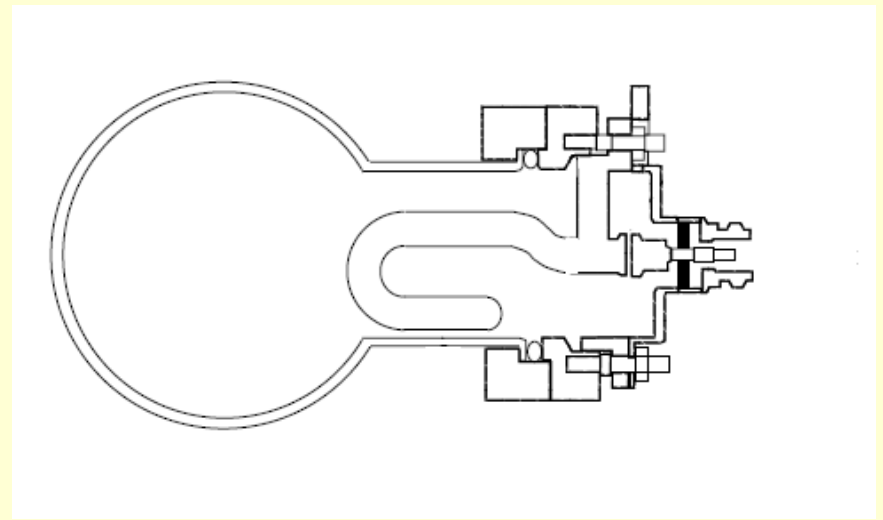
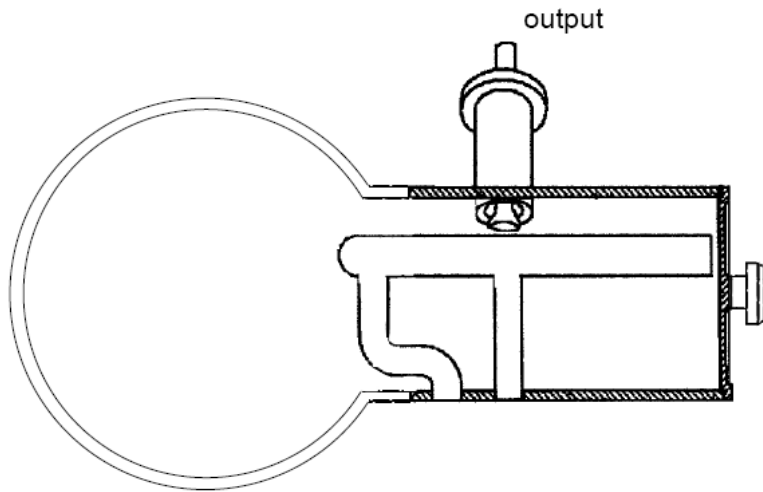
LHC HOM coupler

Resonant coaxial transmission line dampers: Technical solution 2/3



SNS HOM coupler

Resonant coaxial transmission line dampers : Technical solution 3/3



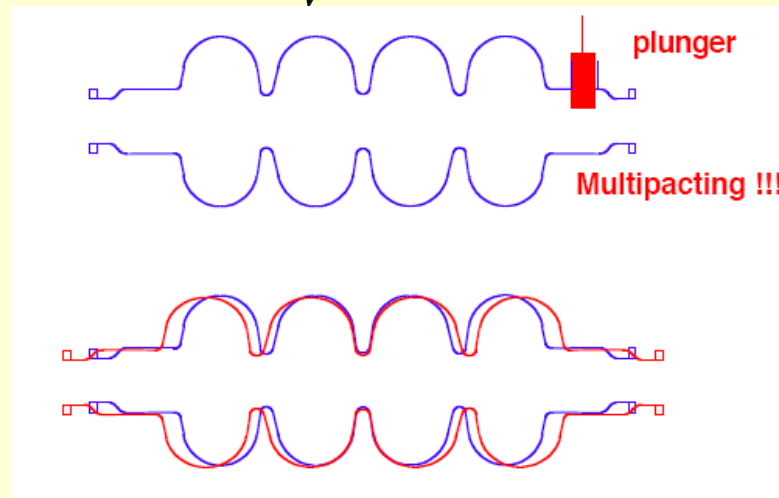
TESLA HOM coupler

The frequency tuner

The frequency of the cavity must be tuned to the harmonic spectral line of the bunched beam => need to develop a frequency tuner. Slater's theorem states that

$$\frac{\Delta f}{f} = \frac{1}{4U} \int_{\Delta V} (\epsilon_0 E^2 - \mu_0 H^2) dV$$

$$U = \frac{1}{4} \int_V (\epsilon_0 E^2 + \mu_0 H^2) dV$$



Mechanical oscillations

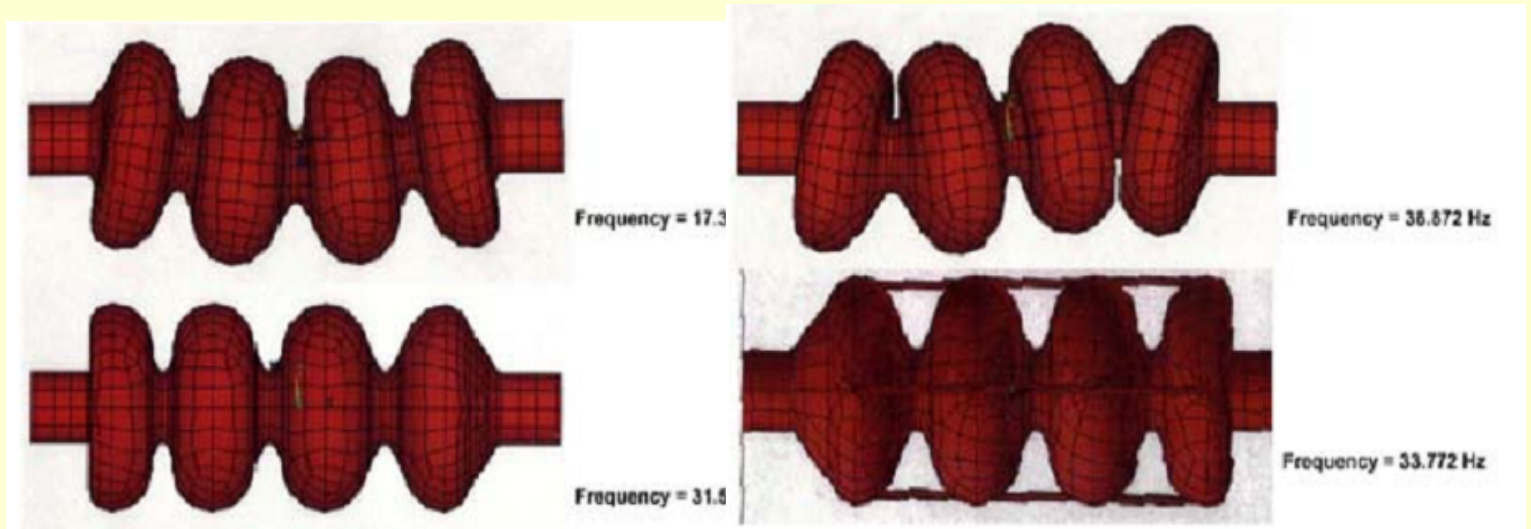
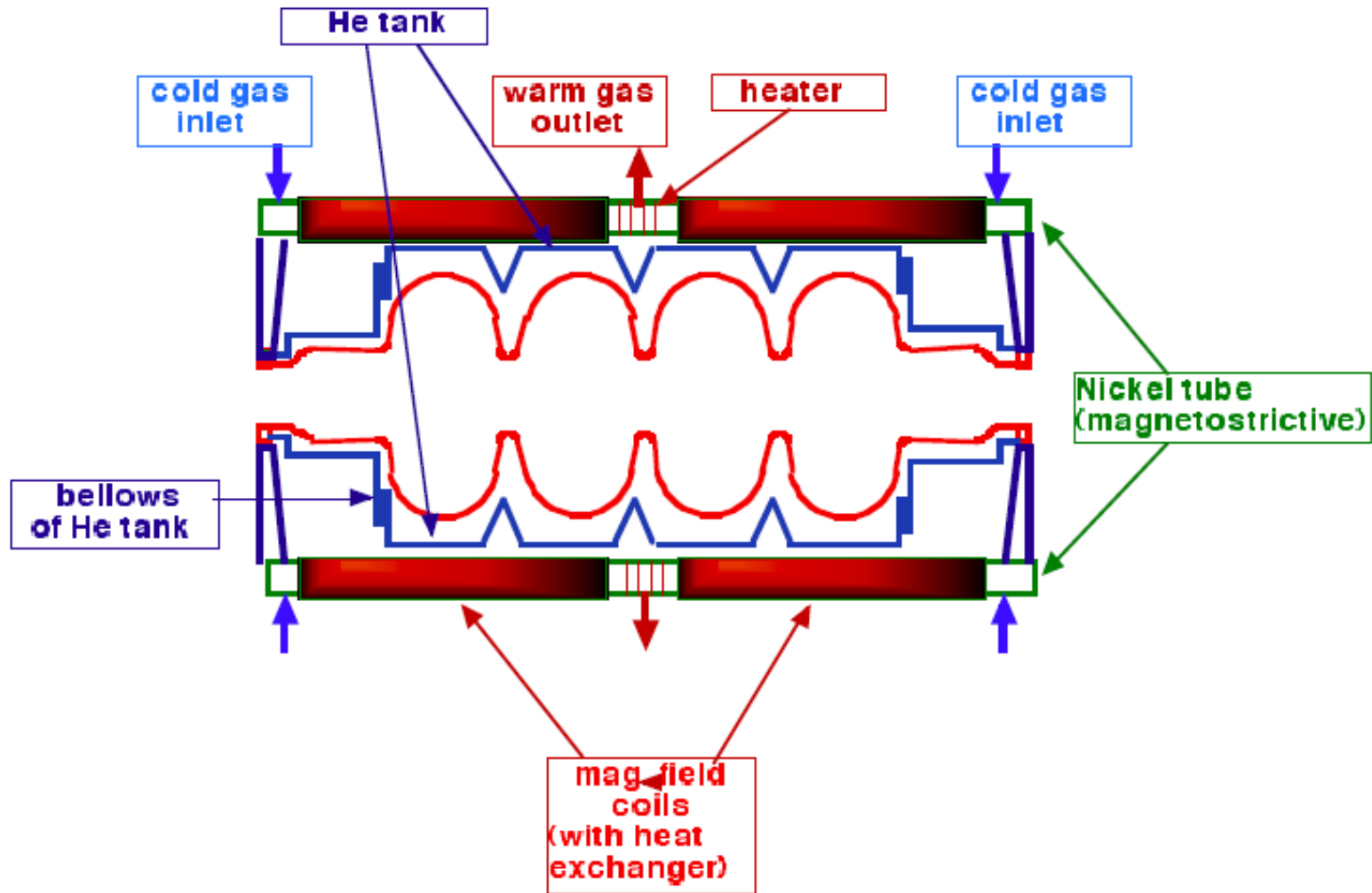


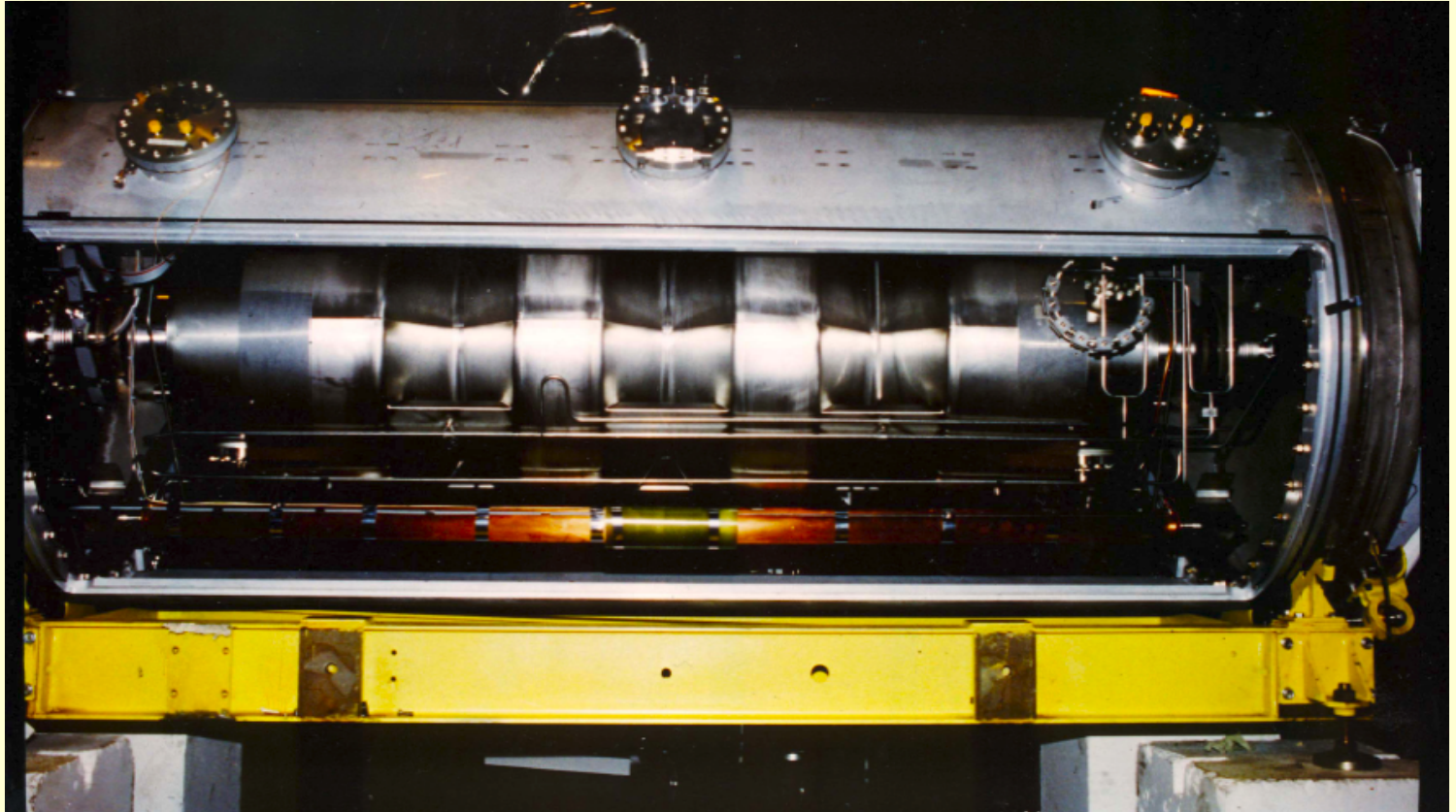
Fig. 20 Mechanical resonant modes of a 4-cell, 200 MHz cavity with 8 mm wall thickness. The low resonant frequencies spell trouble in the form of microphonics. Reducing the number of cells or stiffening is essential.

For example: at LEP, radiation pressure on the cavity walls of about 1000N in total possible

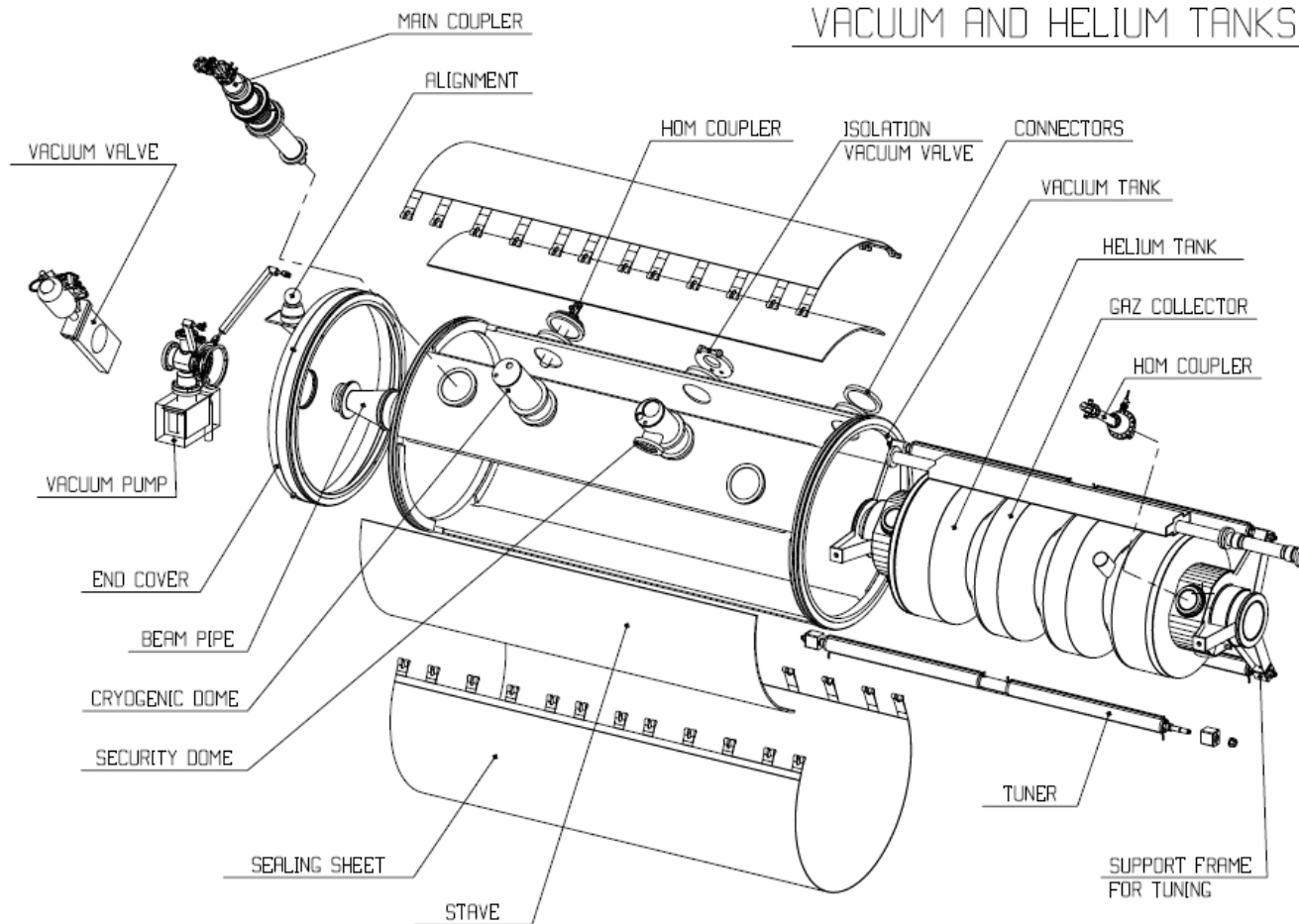
The LEP solution



Integration into LEP cryostat ^{1/2}



Integration into LEP cryostat 2/2



Comments:

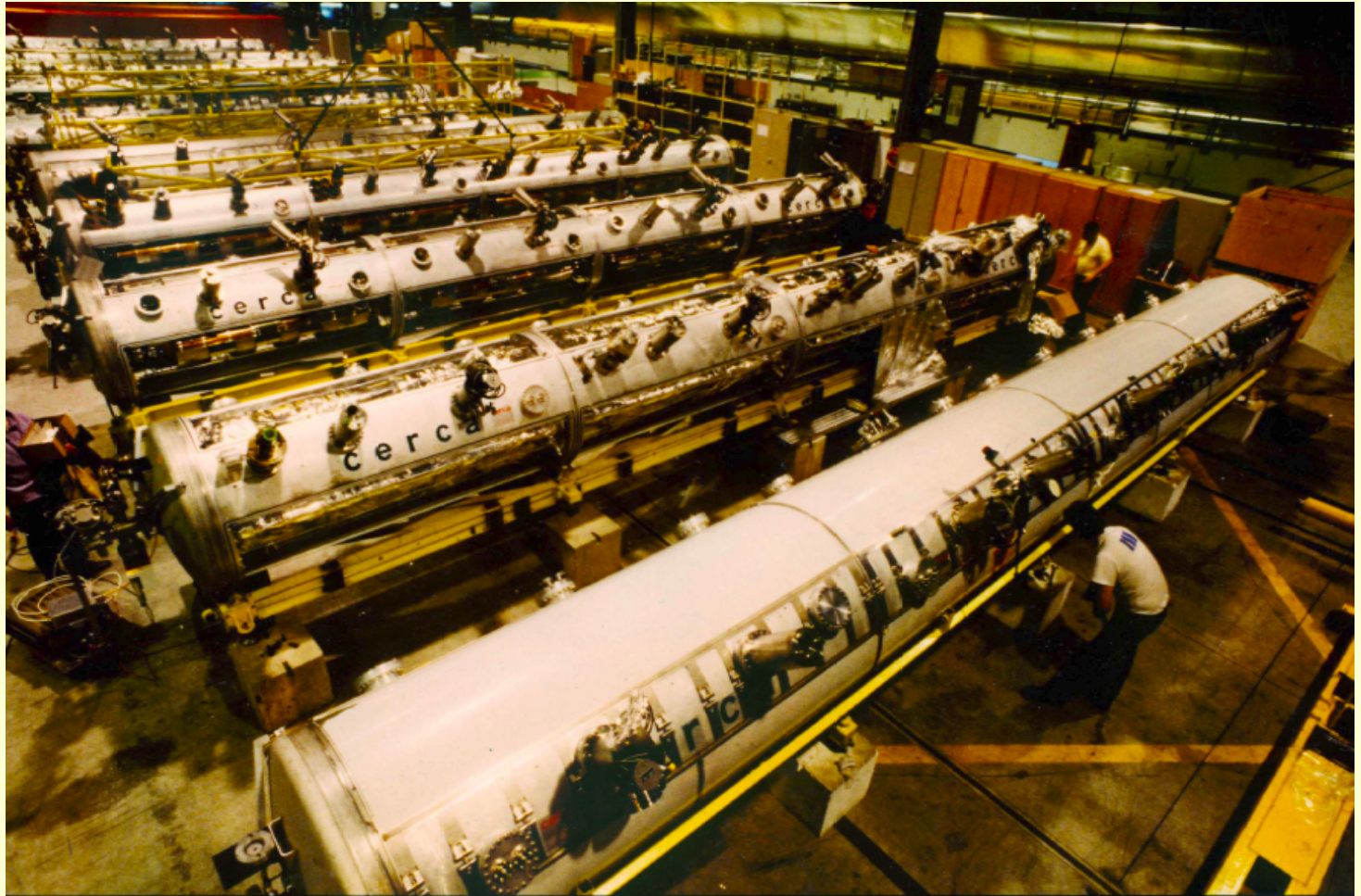
The LEP cryostat could reliably be operated under CW conditions with beam and in pulsed conditions without beam in the present LHC tunnel environment (1.4 % slope).

It is worth noting that the LHe tank, the gas openings, and gHe collector were relatively small.

Pulsed operation: The thermal diffusivity $\kappa = \lambda / (c \cdot \rho)$ is such that it takes ~ 1 ms before the temperature pulse arrives at the niobium helium interface \Rightarrow advantage compared to CW operation.

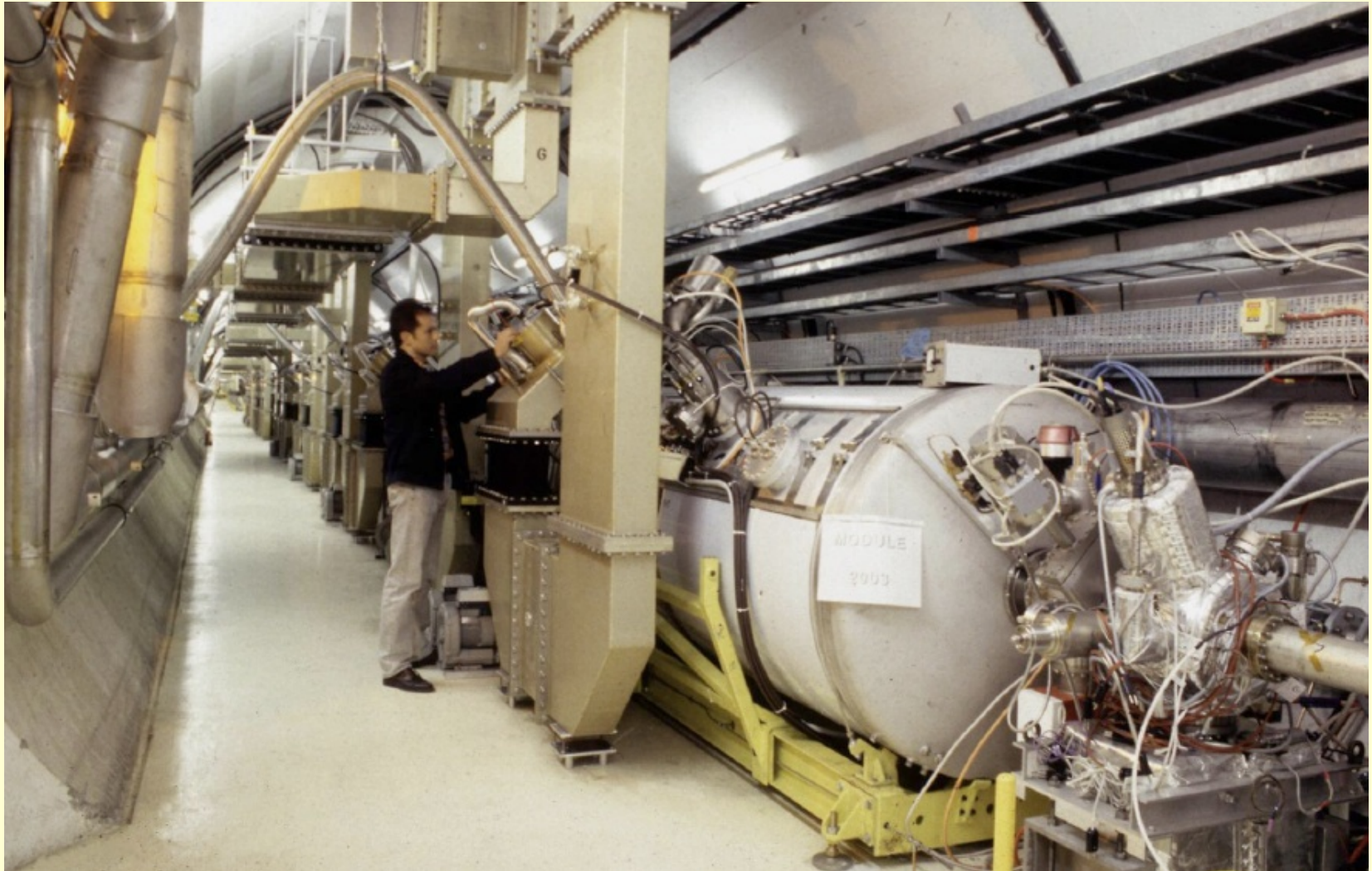
This cryostat was tested under pulsed conditions with beam in the CERN SPS.

Cryomodules $1/2$



Cryomodules 2/2

- installed in LEP tunnel



Summary

- A lumped network circuit diagram allows an analytical description of the interaction of the RF cavity with the beam
- The cavity is designed to minimize the reflected RF power (which would be wasted anyhow in a load) by eliminating the « reactive beam loading » through tuning the frequency of the cavity and by matching the external Q to the nominal beam current.
- The beam consists of bunches passing the cavity in fractions of milliseconds¹ that may excite higher order modes (HOMs) of the cavity to high voltages, if not sufficiently damped by HOM couplers.
- Frequency tuners are in addition needed to damp frequency shifts from mechanical resonances excited by external noise sources (microphonics) or the interaction of the electromagnetic pressure with the cavity wall (Lorentz force detuning).

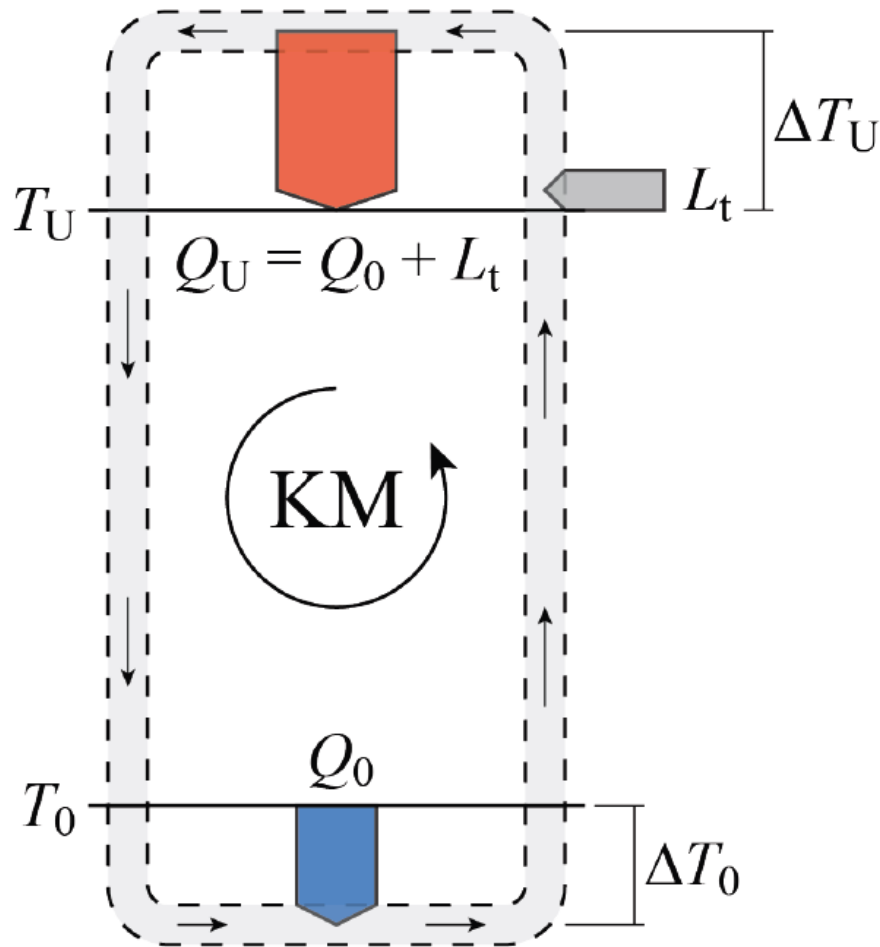
¹ for large storage rings such as LEP

Technological issues

- Cryogenics
- **Anomalous losses:**
 - Residual losses \magnetic shielding
 - Electron field emission
 - Electro polishing
 - Electron Multipacting (dust free assembly)
 - Heat removal (Quench - the role of large thermal conductivity, Coating a copper cavity with a thin niobium film)
 - Quality assurance and stochastic parameters
- Cavity production
- Improvement of cavity performance
- Summary

Basic Cryogenics

Carnot efficiency



- In the ideal case the ΔT 's are zero.
- With the 1st law of thermodynamics the work of the compressor is given by

$$L_t = Q_U - Q_0 = Q_0 (Q_U / Q_0 - 1) \\ = Q_0 (T_U / T_0 - 1)$$

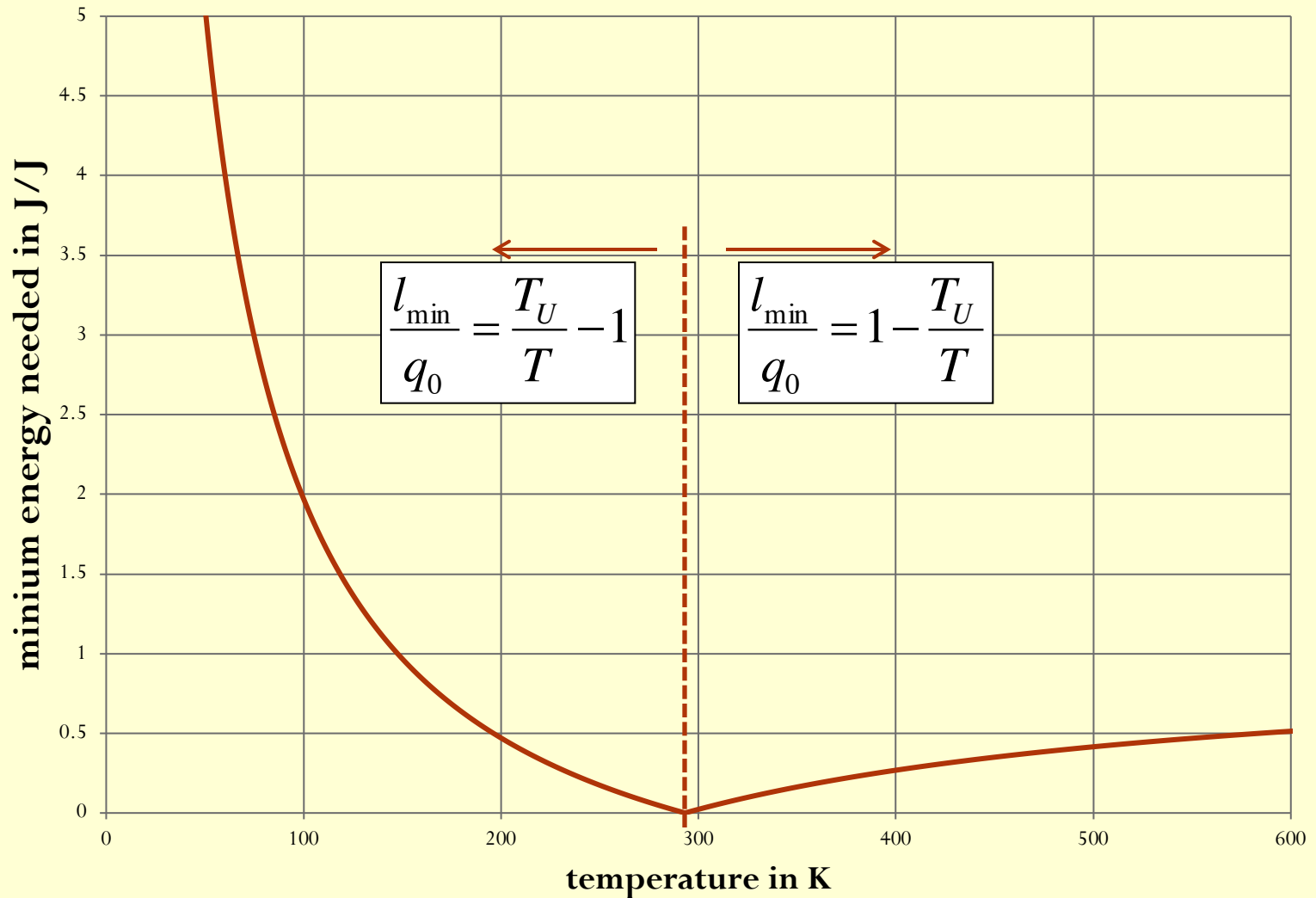
- The Carnot efficiency μ_C for a refrigerator is defined as

$$\mu_C = Q_0 / L_t = T_0 / (T_U - T_0)$$

Schematic of cooling cycle, Kaeltechnik A, S. Grohmann (ITTK, KIT)

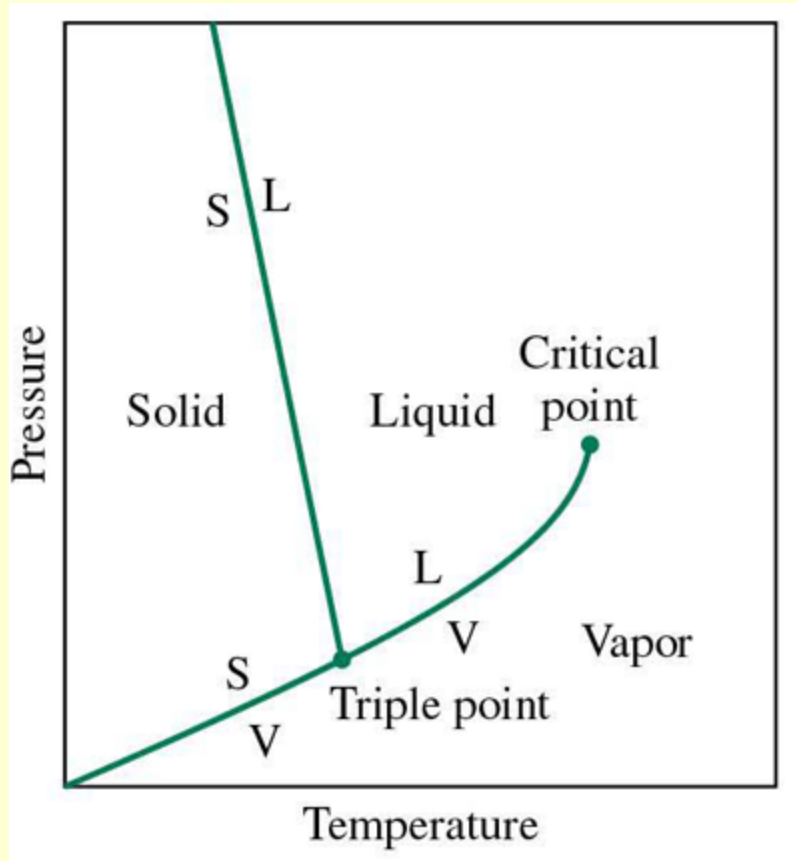
Basic Cryogenics

minimum energy for cooling and heating



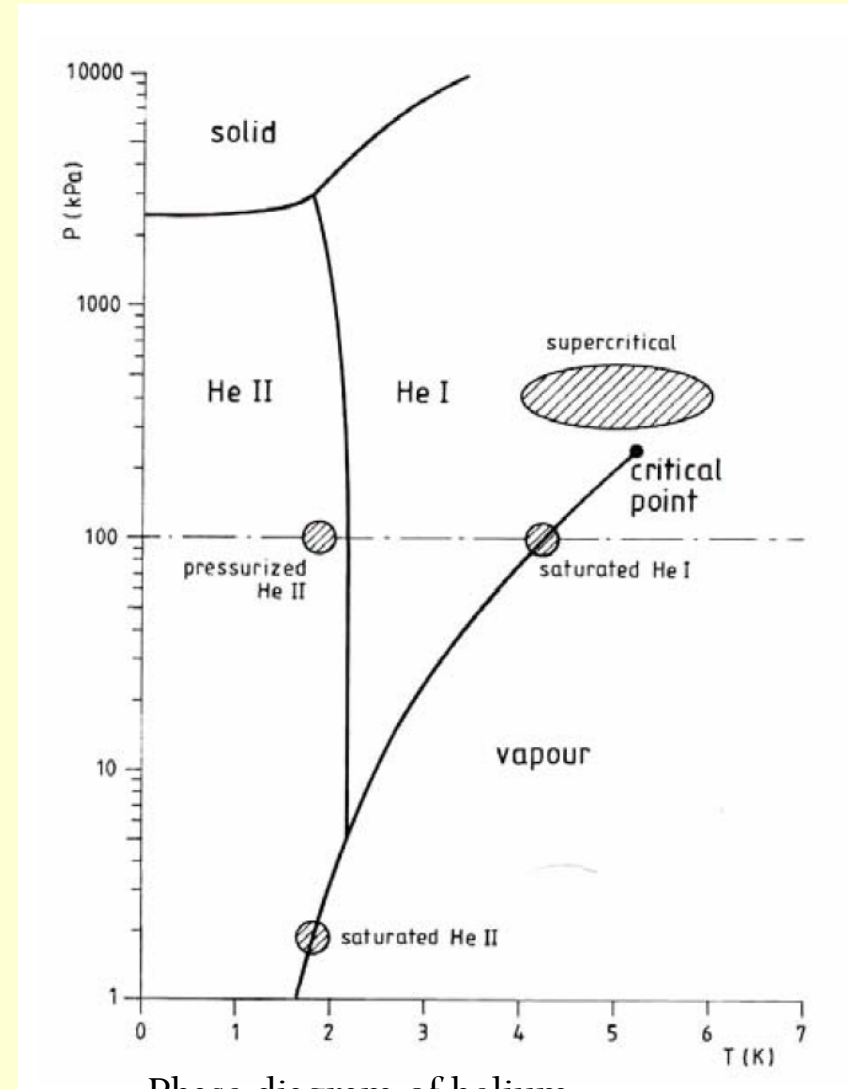
Basic Cryogenics cont.

pT-curve, Material properties



Schematic of a phase diagram,

<http://moodle.zhaw.ch/mod/book/tool/print/index.php?id=63256>



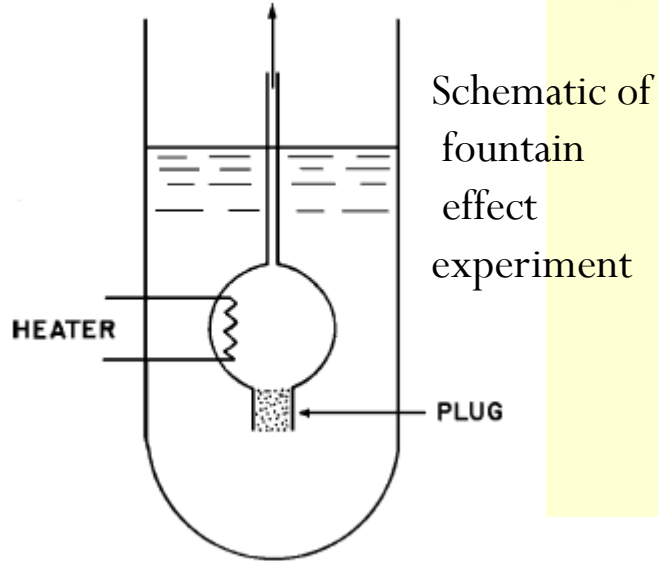
Phase diagram of helium,

CAS 2002, G. Vandoni

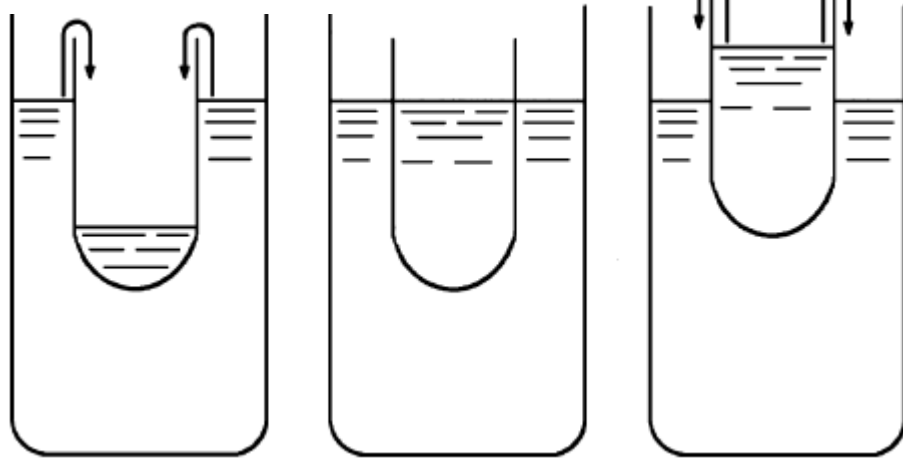
Basic Cryogenics cont.

He II and superfluidity

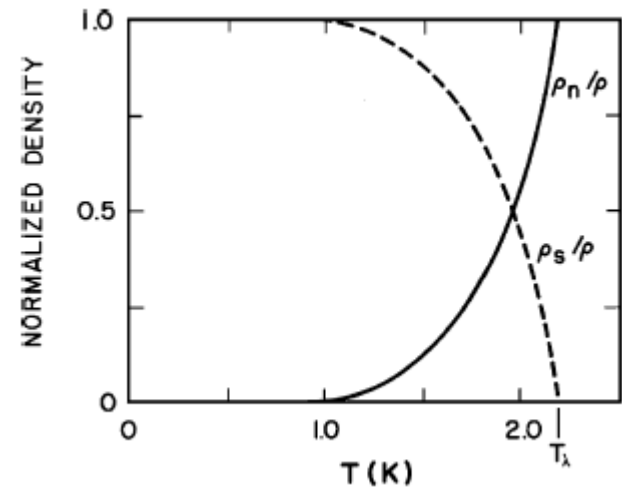
- One of the few macroscopic quantum phenomena
- Special effects
- Extremely low viscosity in thin channels
- Very high heat transport capability
- Can be described by two-fluid theory



Schematic of fountain effect experiment

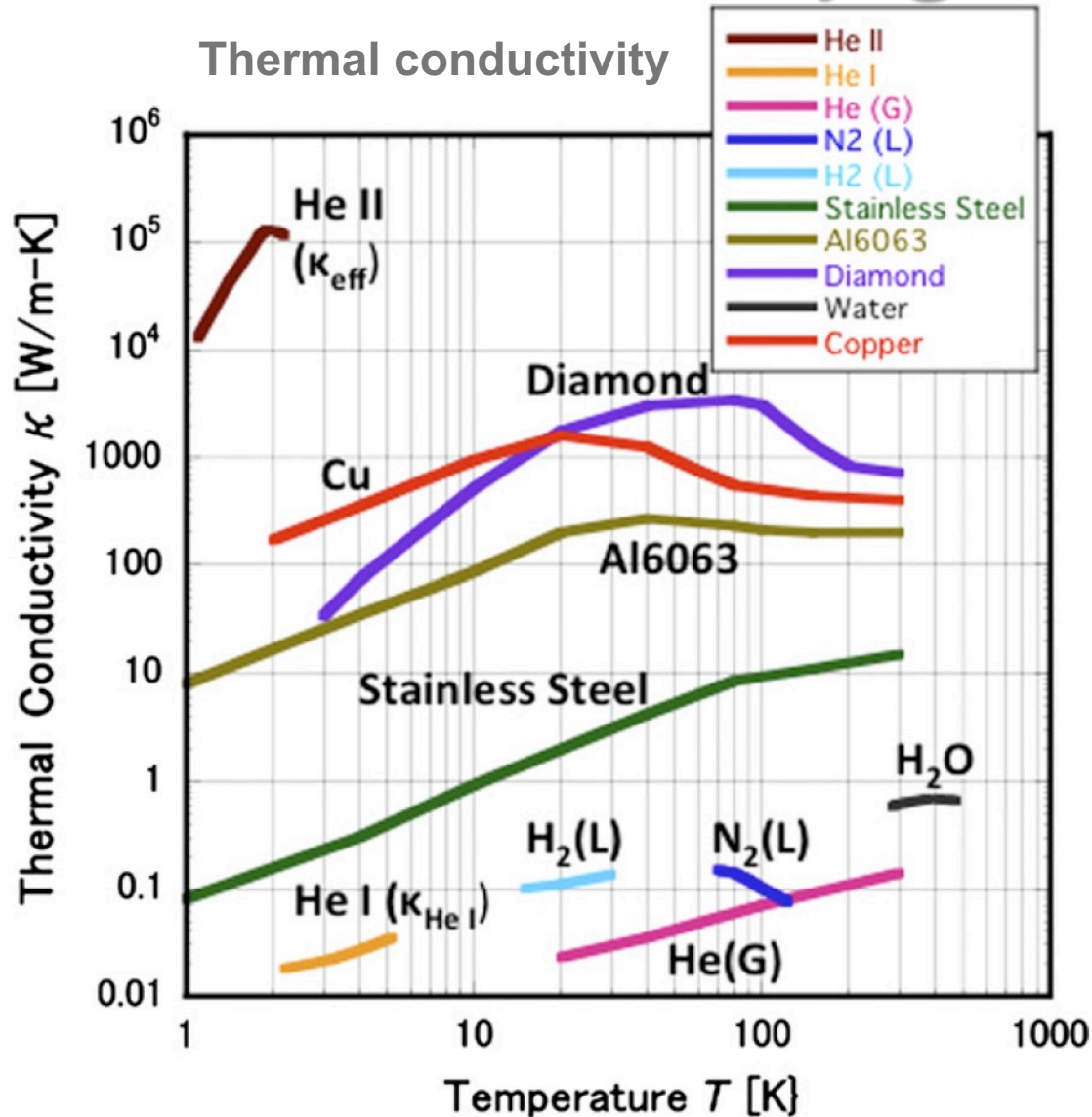


Schematic of film flow experiment



Ratio of normal and superfluid densities of He II
All pictures on this slide by: S.V. Van Sciver, Helium Cryogenics

Basic Cryogenics cont.



- The change in thermal conductivity in helium increases seven orders of magnitude at the lambda point
- At low temperatures many material properties can change very rapidly with temperature .
- e.g. heat capacity, electrical conductivity, vapour pressure

M. Murakami, Cryogenics, Volume 52, Issue 11, November 2012

SC vs. NC

For $T_1 = 300$ K and $T_2 = 4.2$ K, $\eta_c = 1/70$. The 'thermodynamic efficiency'

$$\eta_{td} = \dot{W}_c / \dot{W} \quad (4)$$

is the ratio of the power \dot{W}_c needed to operate the compressor in the ideal case to the 'real' power \dot{W} . The total cryogenic efficiency is

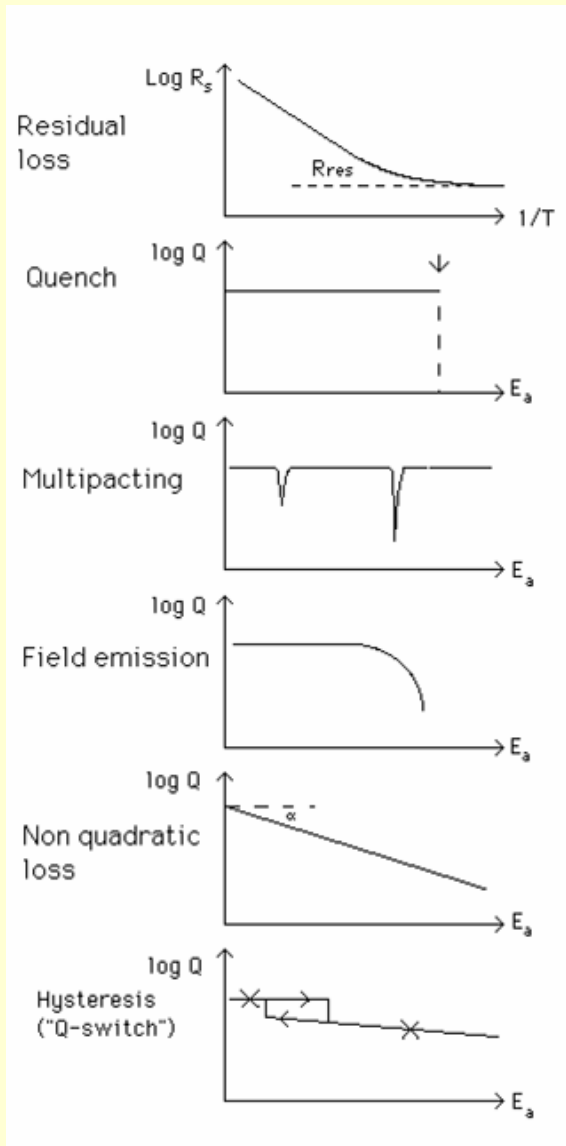
$$\eta_{cr} = Q_2 / \dot{W} = (Q_2 / \dot{W}_c) (\dot{W}_c / \dot{W}) = \eta_c \eta_{td} . \quad (5)$$

With $\eta_{td} \approx 0.3$ for large units the total cryogenic efficiency is $\eta_{cr} = 4.5 \times 10^{-3}$. Unavoidably, in an sc accelerator some power P_{cr} flows into the liquid He, even in the absence of RF (standby heat load of cryostat). The efficiency η for a sc accelerator of RF-to-beam power conversion is then

$$\eta = [1 + (P_c + P_{cr}) / (P_b \eta_{cr})]^{-1} . \quad (6)$$

As an example, for the sc cavity and cryostat for LEP with $P_c = 50$ W, $P_b = 50$ kW and $P_{cr} = 25$ W, we obtain a total efficiency of $\eta = 0.75$, which is larger by a factor of 5 than for a conventional RF system (Table 1).

Anomalous losses

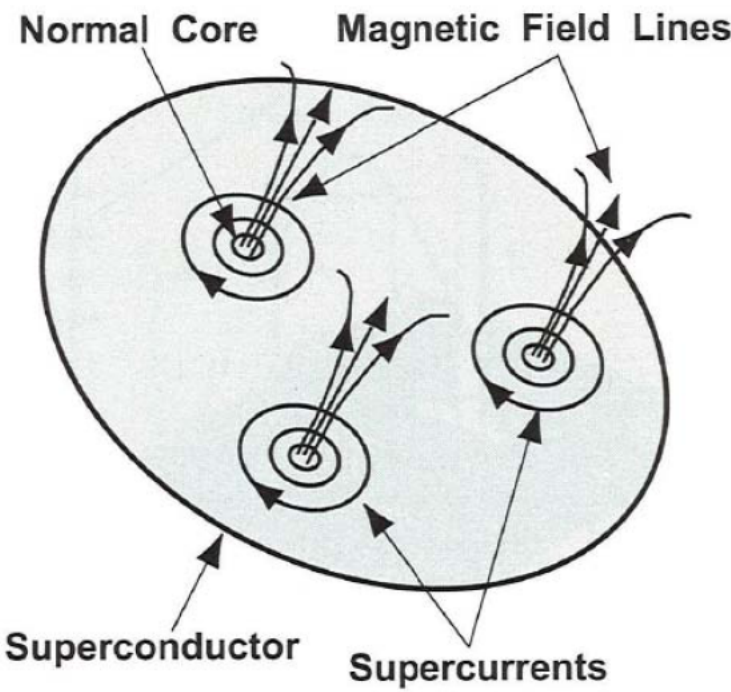


So-called « anomalous losses » account for all contributions to the RF losses that are not described by the intrinsic parameters of the superconducting material (critical temperature, critical field, BCS (or two fluid) surface resistance R_s , etc.).

These anomalous losses show up as heat and are visible in the $R_s(T)$ and $Q_0(E_a)$ plots, as well as in the « temperature maps ».

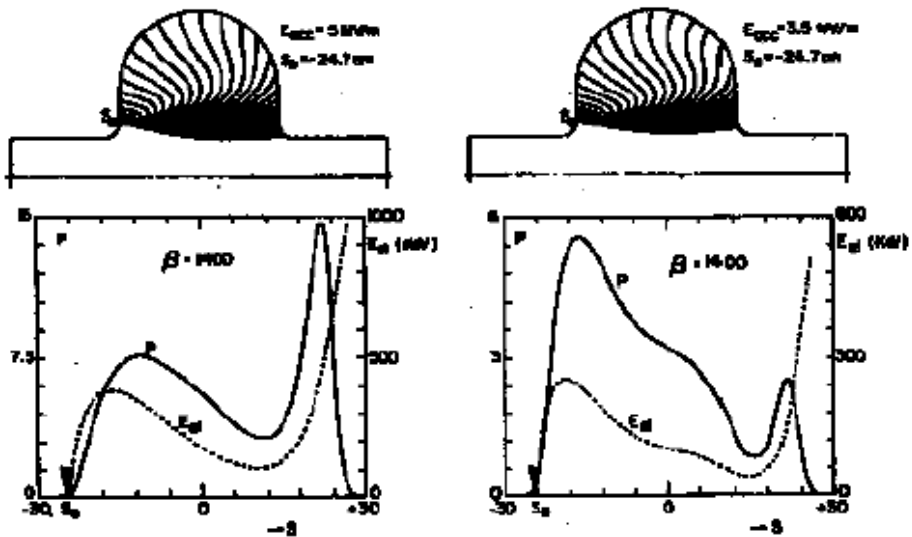
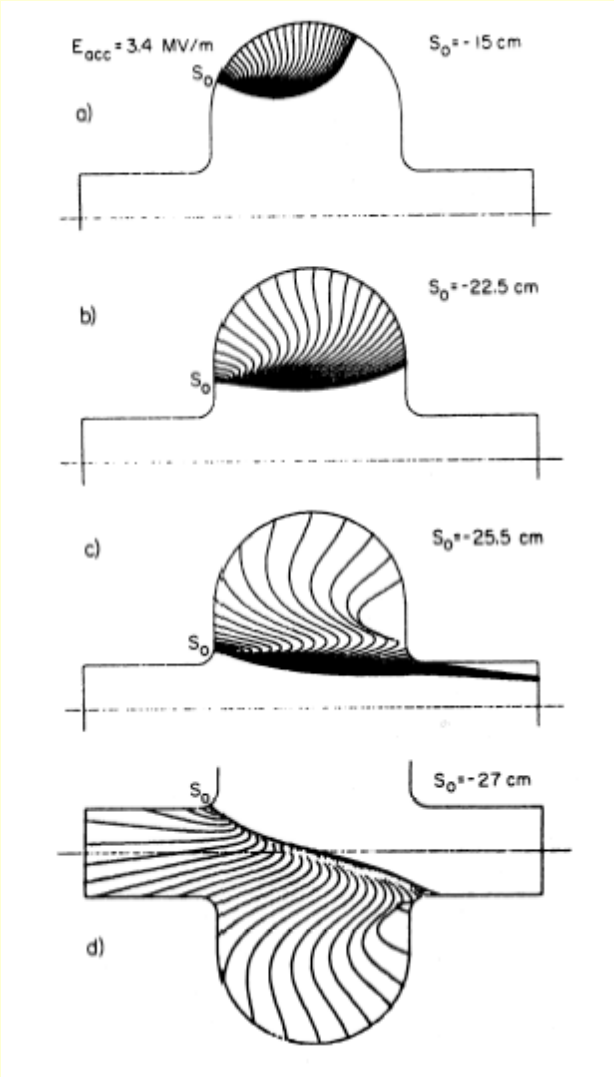
Magnetic shielding

- Why do we need a magnetic shielding?


$$R_{mag} = \frac{H_{ext}}{2H_{c2}} R_n$$
$$R_{mag} [n\Omega] = 3H_{ext} [\mu T] \sqrt{f [GHz]}$$

Tobias.Junginger@quasar-group.org

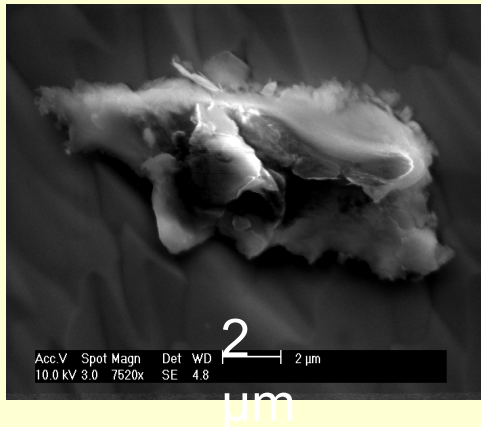
Electron field emission 1/4



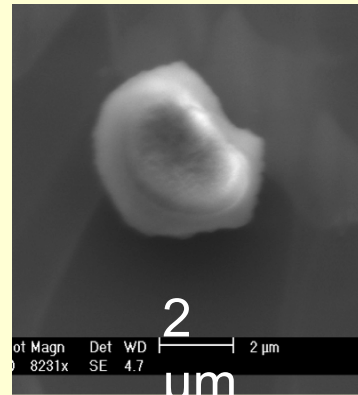
Impact energy and differential heat load

Electron field emission 2/4

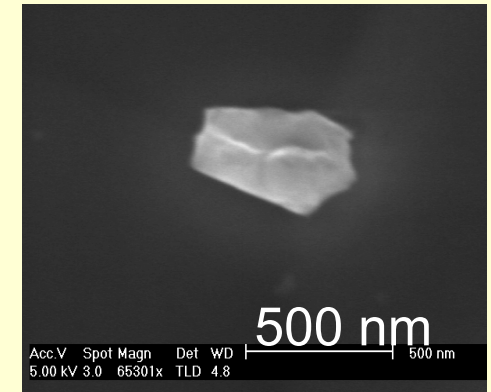
- Typical particulate emitters containing impurities



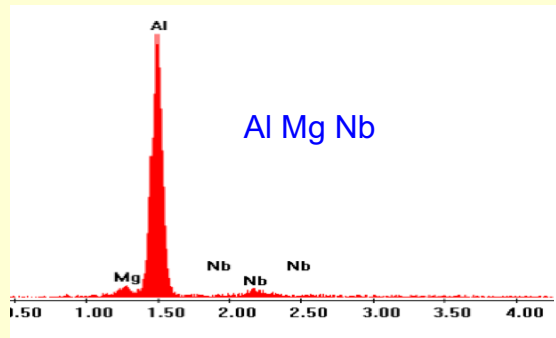
$E_{on}(2nA) = 140 \text{ MV/m}$
 $\beta = 31, S = 6.8 \cdot 10^{-6} \mu\text{m}^2$



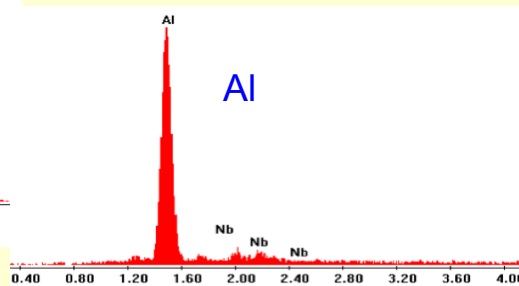
$E_{on}(2nA) = 132 \text{ MV/m}$
 $\beta = 27, S = 7 \cdot 10^{-5} \mu\text{m}^2$



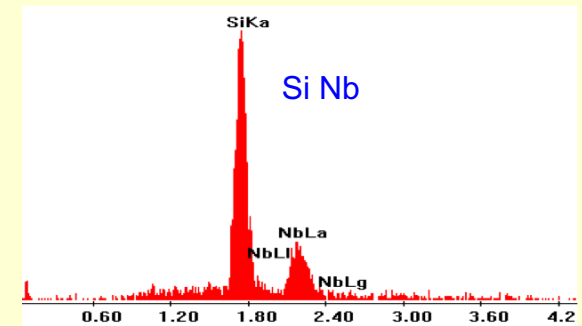
$E_{on}(2nA) > 120 \text{ MV/m}$
 $\beta = 46, S = 6 \cdot 10^{-7} \mu\text{m}^2$



Al Mg Nb



Al



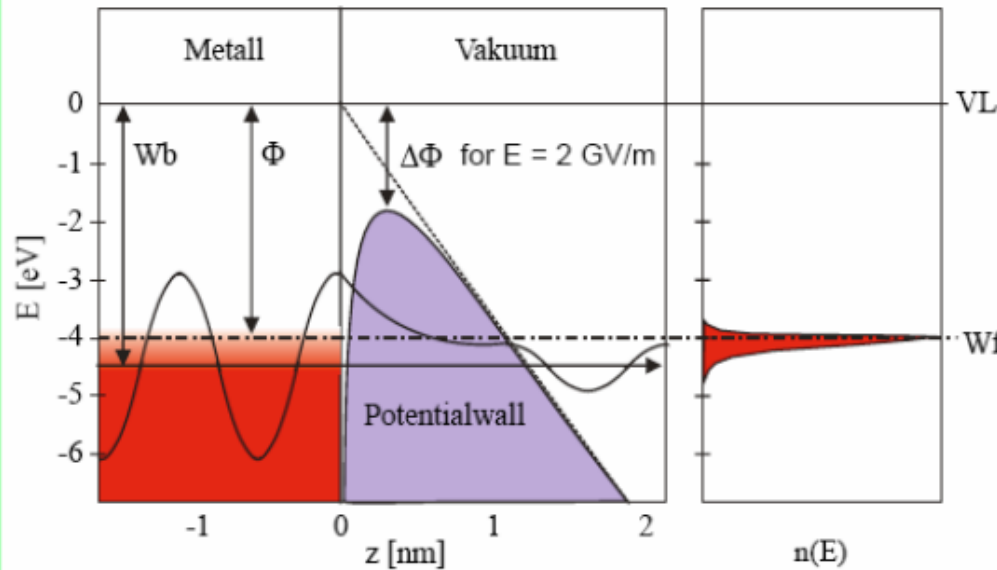
Si Nb

Electron field emission 3/4

- Fowler Nordheim theory

Field emission of electrons from flat metal surfaces

Electron waves of bound states in a metal can tunnel through the potential barrier $V(z)$ at the solid surface into vacuum by means of the quantum mechanical tunnelling effect



$$V(z) = -e \cdot E \cdot z - \frac{e^2}{16\pi\epsilon_0 \cdot z}$$

work function Φ of metal
 applied field E on surface
 image charge correction
 $\Delta\Phi = \left(\frac{e^3 E}{4\pi\epsilon_0}\right)^{1/2}$

Calculation of the current density $j(E)$ within the Fowler-Nordheim theory results in

$$j(E) = \frac{AE^2}{\Phi t^2(y)} \exp\left(-\frac{B\Phi^{3/2} v(y)}{E}\right)$$

with constants $A=154$ and $B=6830$ and slight correction functions $t(y)$ and $v(y)$
 $\Phi=4\text{eV}$ at $E=2000\text{ MV/m} \Rightarrow j=1\text{ nA}/\mu\text{m}^2$

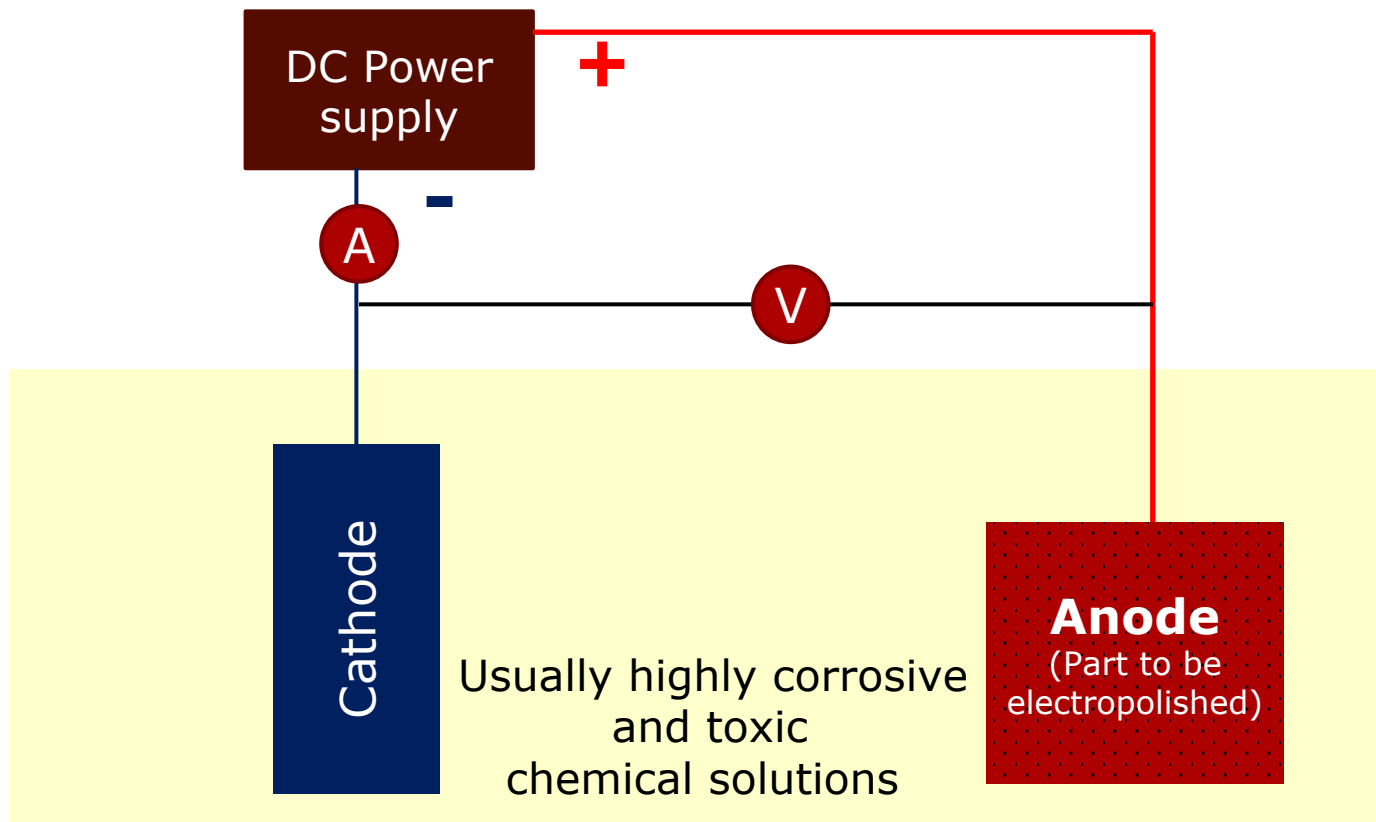
Electron field emission 4/4

- Clean room preparation mandatory



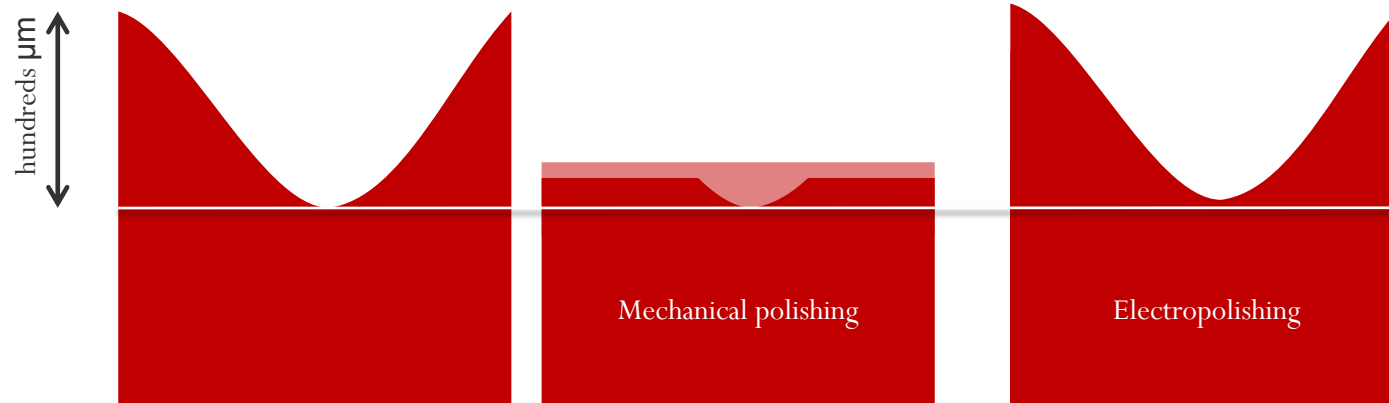
Electropolishing: How it works

- The metal is immersed in an electrolyte and subjected to direct current. The metal part to be treated is made anodic and under certain conditions, a controlled dissolution of the metal is achieved.



Electropolishing vs Mechanical based polishing

- Final roughness is function of initial surface finishing and removed thickness



- Usually highly corrosive and/or toxic solutions
 - Handling;
 - Process equipment;
 - Installation to process extracted fumes;
 - Installation to process waste water.

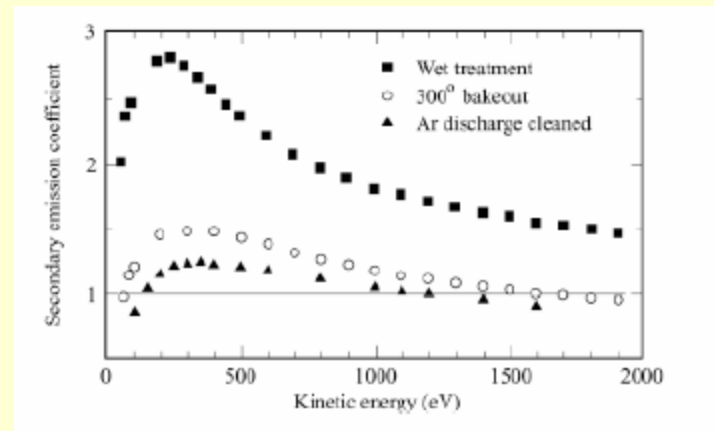
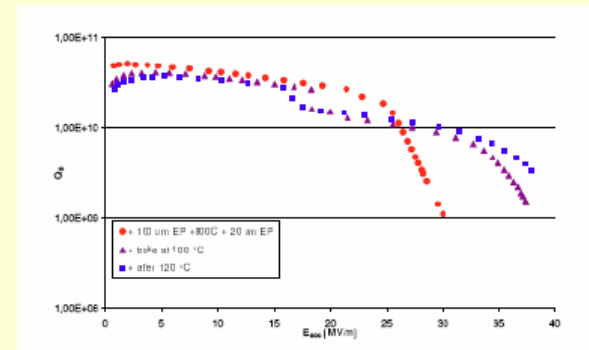
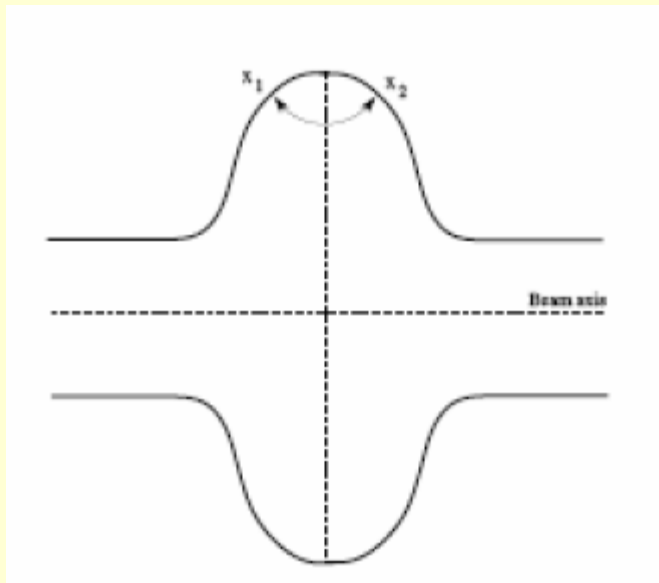
Disadvantages

Electron multipacting

Localized heating by multiple impact from electron current due to secondary emission in resonance with RF field.

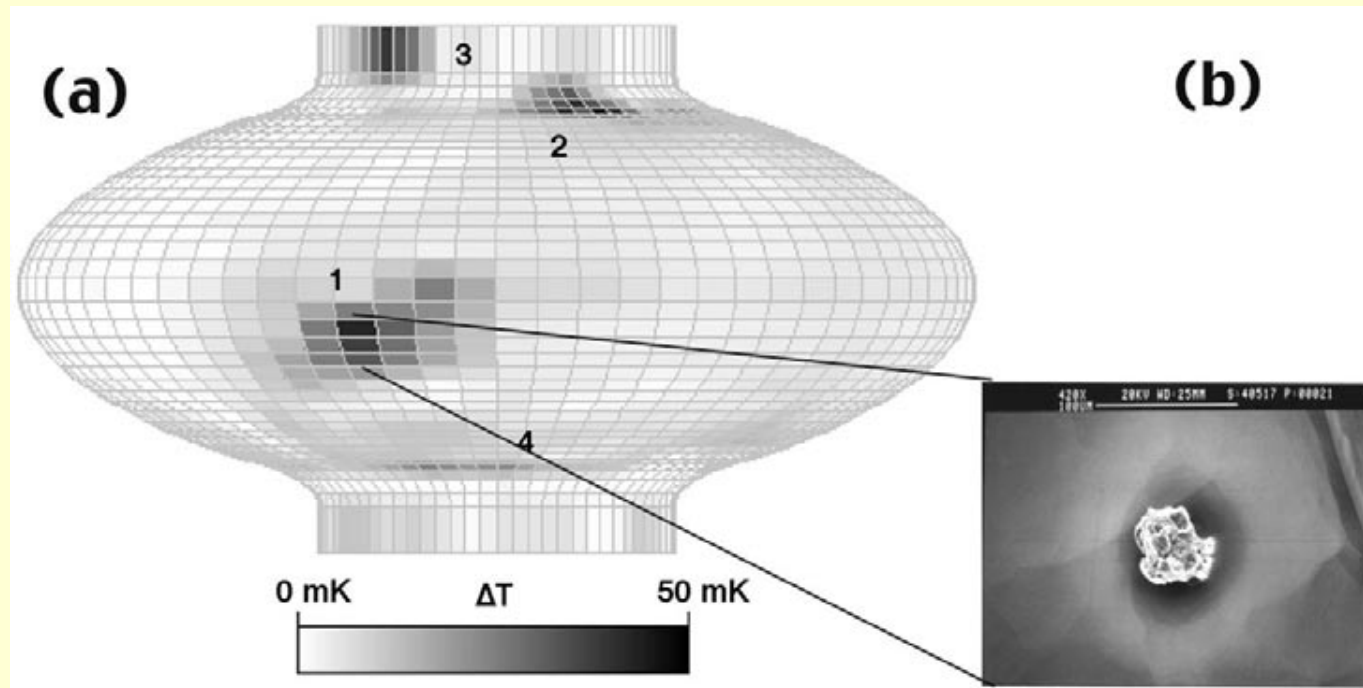
Historically this phenomenon was a severe limitation for the performance of SC cavities.

The invention of the “circular” shape opened up the avenue for higher gradients.



Field limitations – thermal breakdown

- Occurs at sub mm size defects with high resistance
- RF currents flow through the defects
- Defects heat up due to ohmic losses
- Area surrounding the defect is heated as well
- Thermal breakdown occurs if the surrounding area is heated above T_c



From H. Padamsee: CERN -2004 - 008

Heat removal

- Thermal Improvement of thermal conductivity for Niobium sheets

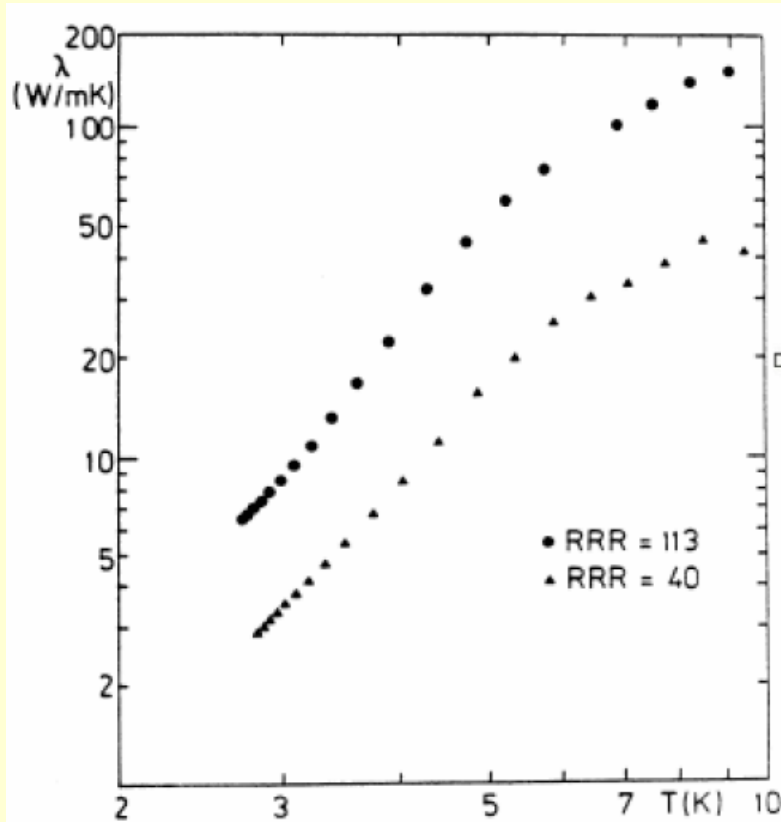
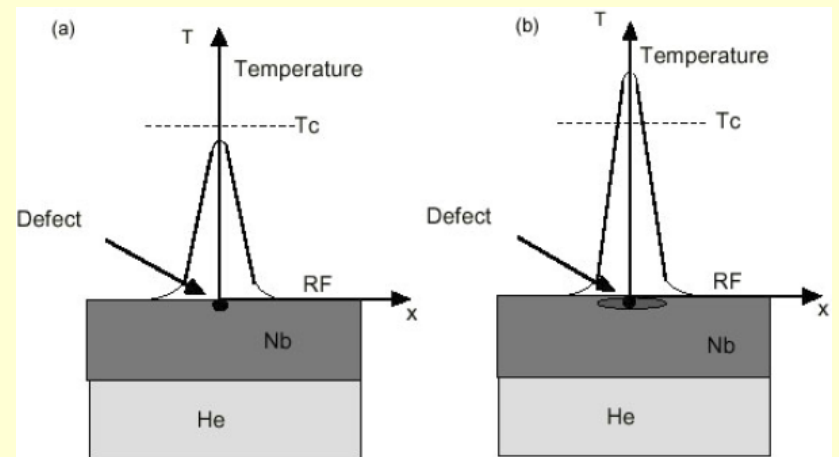


Fig. 1: Thermal conductivity of reactor grade niobium (RRR=40) and niobium of higher purity (RRR=113)

Cause for “quench”:

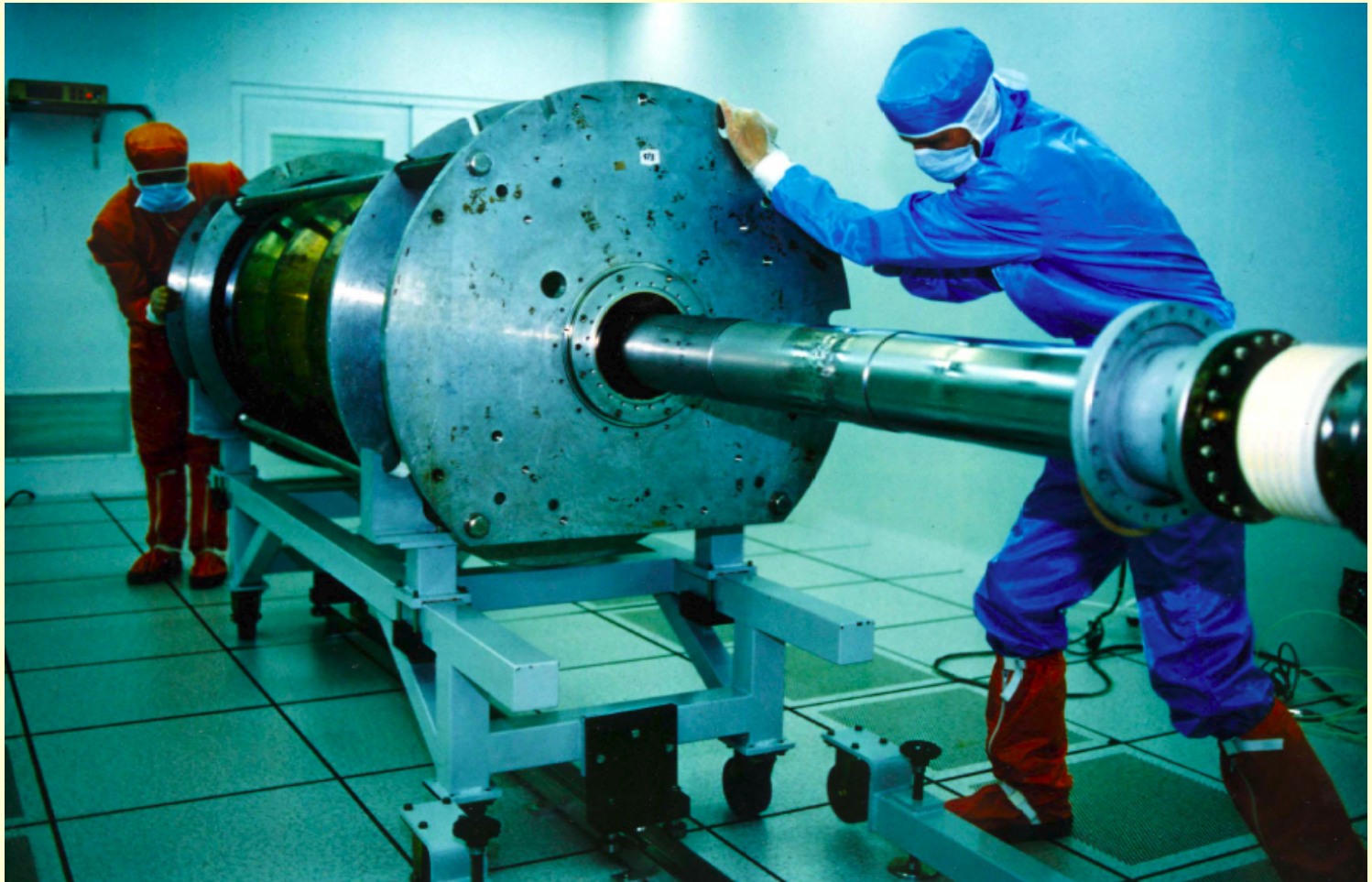


$$H_{\max} \approx \sqrt{4(T_c - T_B)\lambda / (R_n r)} .$$

RRR... residual resistance ratio

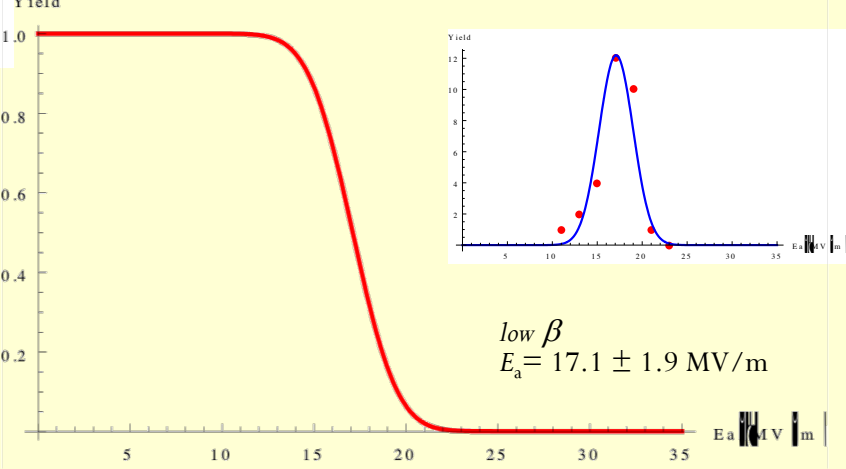
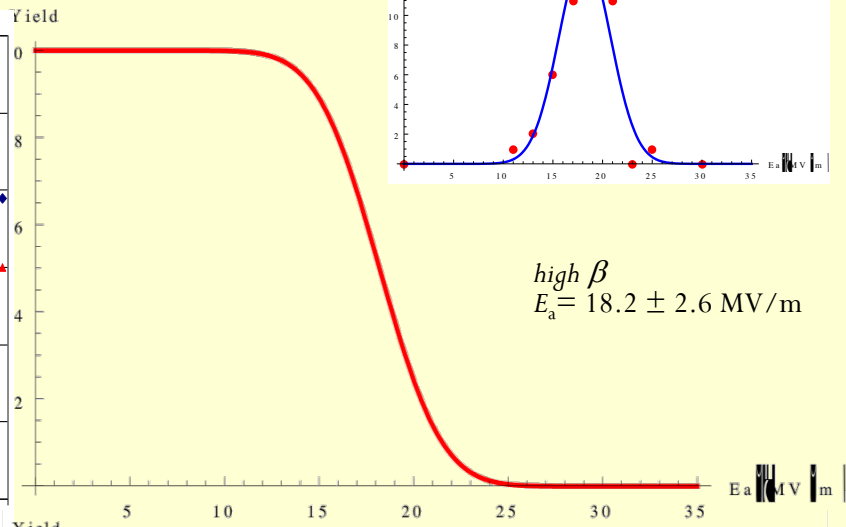
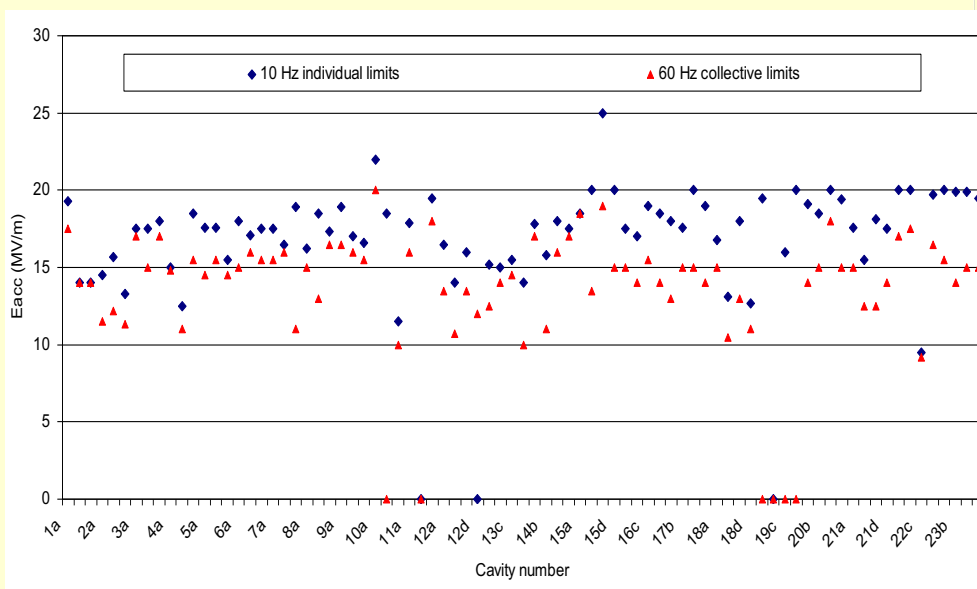
Thin film Nb coating

- Coating a copper cavity with a thin Nb film
- Important role of high thermal conductivity substrate (Nb/Cu cavity)



Improvement of quality assurance efforts: ORNL/JLAB results

Nevertheless, in spite of all technological efforts, performance of sc cavities is often stochastic



Source: I. E. Campisi and S.-H. Kim, **SNS Superconducting Linac operating experience and issues**,
 Accelerator Physics and Technology Workshop for Project X, November 12-13, 2007
<http://projectx.fnal.gov/Workshop/Breakouts/HighEnergyLinac/agenda.html>

Stochastic parameters

Influencing quantity	Impact quantity	Physical explanation	Cure
Field emission sites (foreign particles sticking to the surface, size, density)	Q – value / acc. gradient γ radiation HOM coupler quench	Modified Fowler-Nordheim-theory	Electro-polishing Assembling in dust-free air Rinsing with ultrapure water (control of resistivity and particulate content of outlet water) and alcohol High pressure ultrapure water rinsing (ditto) “He- processing” Heat treatment @ 800 – 1400 °C
Secondary emission coefficient δ	Electron-multipacting	Theory of secondary electron emission	Rounded shape of cavity Rinsing with ultrapure water Bake-out RF - Processing
<i>Unknown</i>	Q – slope / Q-drop (Q – value / acc. gradient)	<i>Unknown</i>	Annealing 150 °C Electro-polishing
Metallic normal-conducting inclusions in Nb	Acc. gradient	Local heating up till critical temperature of Nb	Inspection of Nb sheets (eddy current or SQUID scanning) Removal of defects ($\approx 1 \mu\text{m}$) Sufficiently large thermal conductivity (30 - 40 [W/(mK)])
Residual surface resistance	Q – value / acc. gradient	<i>Unknown to large extent</i>	Quality assurance control of a multitude of parameters

	WHY	COMMENTS
Forming		
EB Welding	Clean welding	Nb = getter material. If RRR/ 10 @ welding => $Q_0/10$
Ti purification	RRR enhancement	RRR 300-400 now commercially available
Chemical etching 100-200 μm	Remove contamination and damage layer	Limitation : BCP ~ 30MV/m; EP => >40 mV/m but lack of reproducibility
Annealing 800°C, 2h (or 600°C, 10h)	Get rid of hydrogen	Source of H: wet processes H segregates near surface in form of hydrides (= bad SC)
Chemical etching 5-20 μm	Remove diffusion layer (O, C, N)	Diffusion layer < ~1 μm in bulk, a little higher at Grain Boundaries
Specific rinsing	e.g. remove S particles due to EP	Under evaluation HF, H ₂ O ₂ , ethanol, degreasing, ...
High pressure rinsing (HPR)	Get rid of dust particles	Not always enough (recontamination during assembly)
Assembling	Ancillaries : antennas, couplers, vacuum ports...	In clean room, but recontamination still possible
Baking, 120°C, 48h	Decrease high field losses (Q-drop)	Unknown mechanism, first 10 nm of the surface in concern.
Post processing	Get rid of "re-contamination" ?	Under evaluation: dry ice cleaning, plasma
Test RF	Cavity's performance	First naked cavity in vertical cryostat, then dressed in horizontal cryostat/ accelerating facility
He processing, HPP	Decrease field emission	RF power with/ without He to destroy field emitters (dust particles) NB field emission : principal practical problem in accelerators

Improvement of cavity performance

Lilje & Schmueser

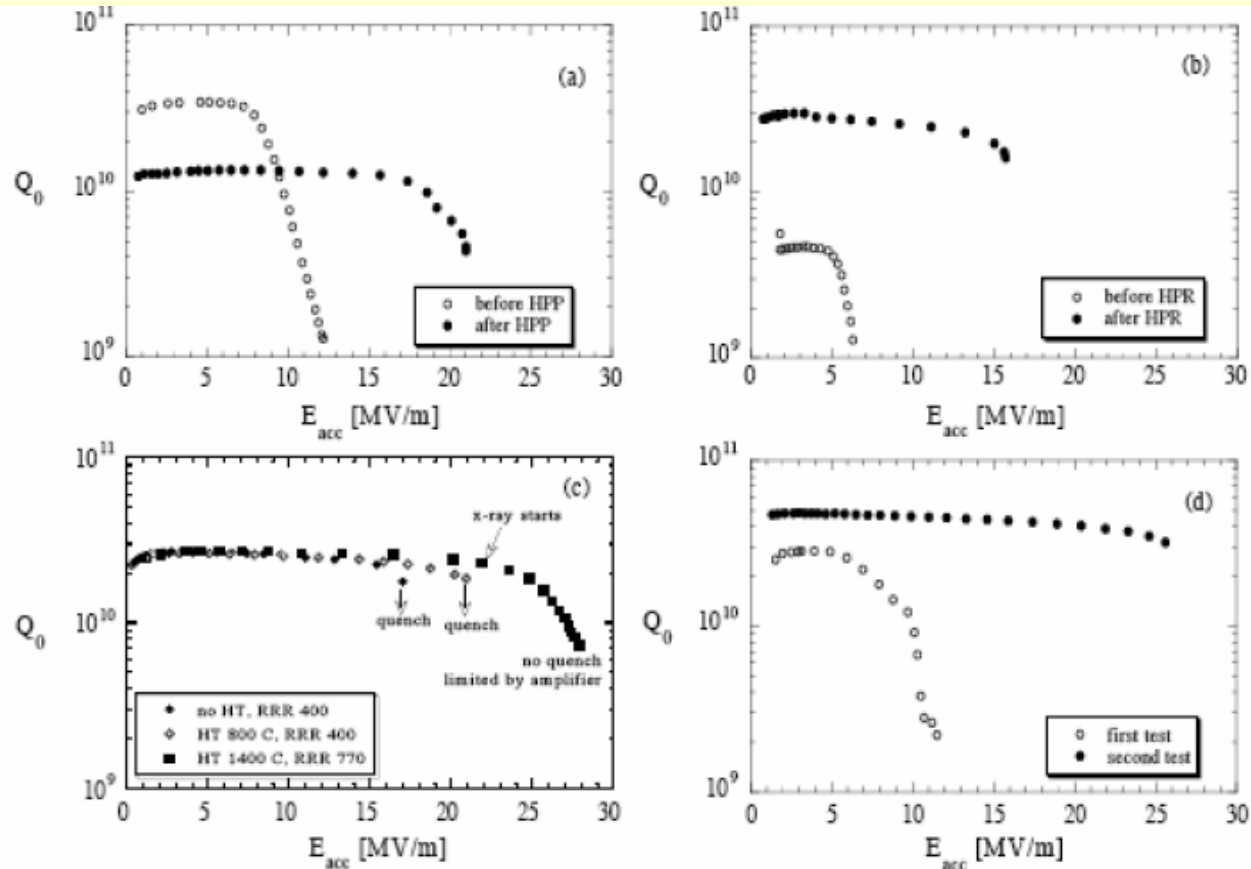


Figure 27: Improvement in cavity performance due to various treatments: (a) high power processing, (b) high pressure water rinsing, (c) successive application of 800°C and 1400°C heat treatment, (d) removal of surface defects or titanium in grain boundaries by additional BCP. All tests were done at 1.8 K [Aune et al. 2000].

Summary

- The choice of the technology (normal conducting vs. superconducting) depends on a variety of parameters: mass of accelerated particle, beam energy, beam current, mains power consumption, etc.
- If superconducting, the typical interval of RF frequencies is between 300 MHz and 3 GHz.
- The technically most suitable superconducting material being niobium, choosing lower frequencies allows operation at 4.2 – 4.5 K, the boiling temperature of lHe, higher frequencies request operation at 1.8 – 2 K. However, the cryogenic installation is much more demanding.
- The production of sc cavities requests careful application of quality control measures during the whole cycle of assembly in order to avoid the degradation of performance by « anomalous losses ».
- The « anomalous losses » contribute to an extra heat load, which is expensive to cool and which may limit the performance.

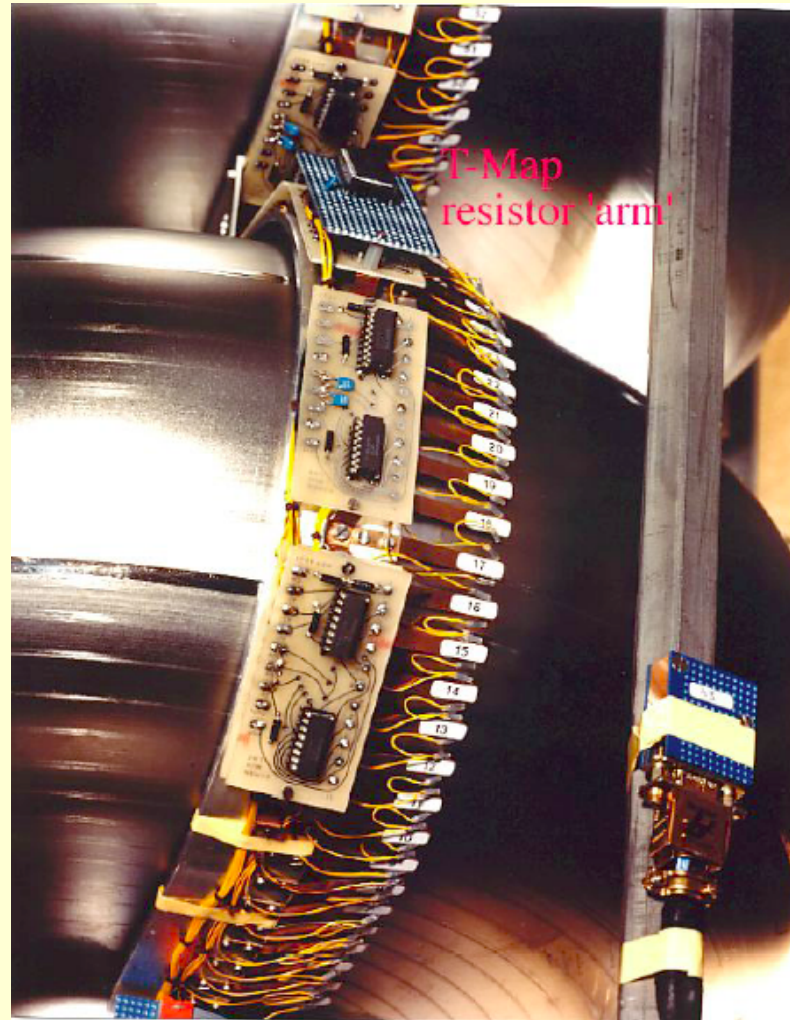
Diagnostics ^{1/8}

- Many features of the cavity can be tested by RF-measurements.
- But losses, which occur in the form of localized heat can only be detected by additional diagnostics.
- The classical approach is temperature mapping.



Diagnostics 2/8

- Temperature mapping equipment (~ 1980)



Diagnostics ^{3/8}

- Temperature mapping results (today)

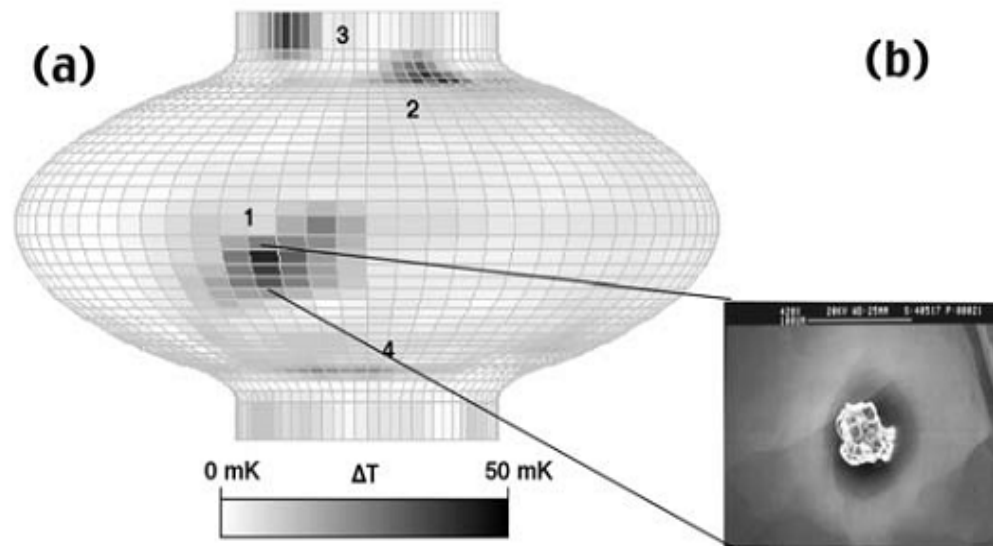


Fig. 16 (Left) Temperature map at 400 Oe of a 1.5 GHz, single cell cavity showing heating at a defect site, labelled #1 and field emission sites labelled #2, 3, and 4. (b) SEM micrograph of the RF surface taken at site #1 showing a copper particle [5].

From H. Padamsee: CERN -2004 - 008

Diagnostics 4/8

- T-mapping for the diagnosis of anomalous losses

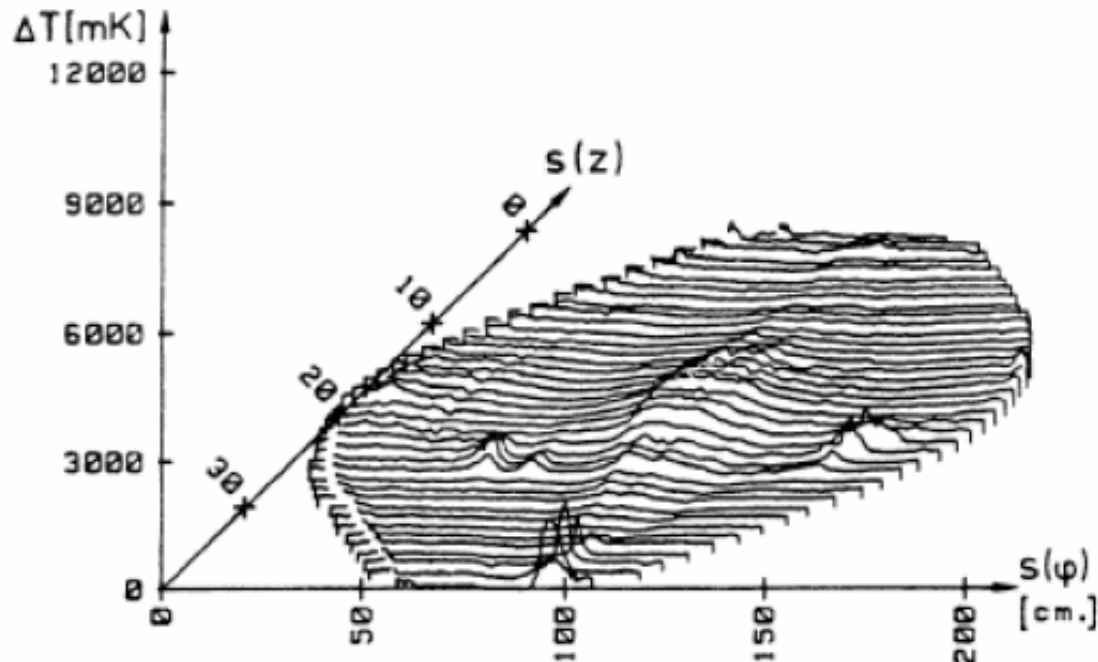
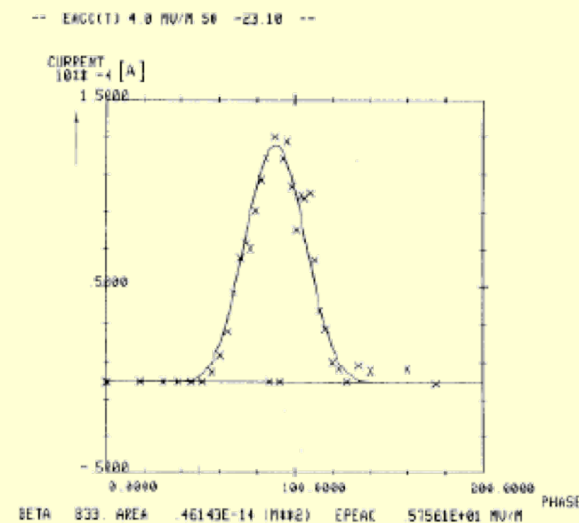
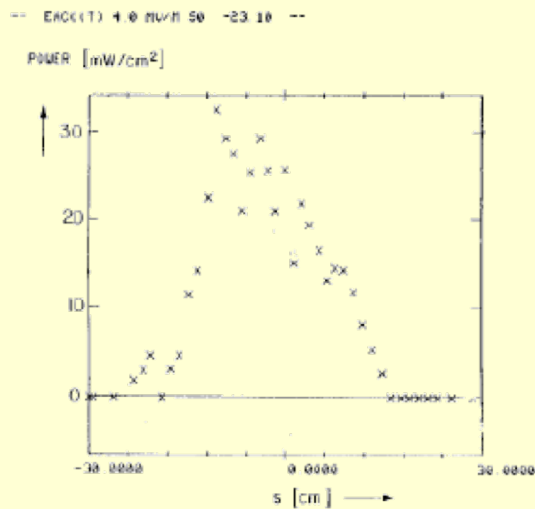
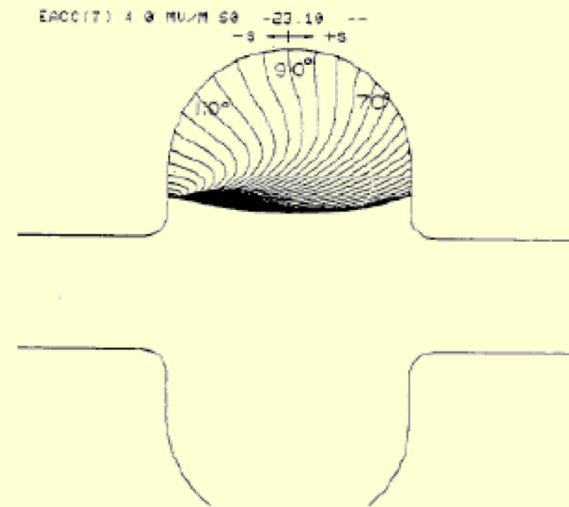
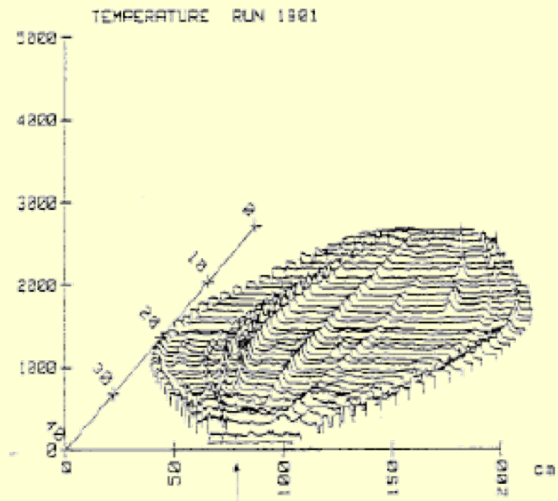


Fig. 4: Temperature map of a 500 MHz cavity at $E_{acc} = 12.5$ MV/m. The temperature increase ΔT of the outer cavity surface is plotted against the surface coordinates $s(z)$ and $s(\phi)$ (z =length in arbitrary units along a meridian, ϕ = azimuthal location)

Diagnosics 5/8

- T-mapping for electron field emission diagnosis

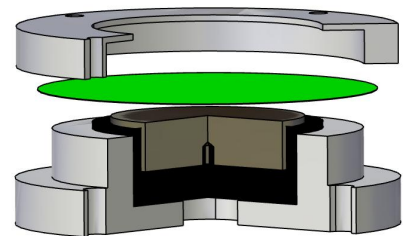
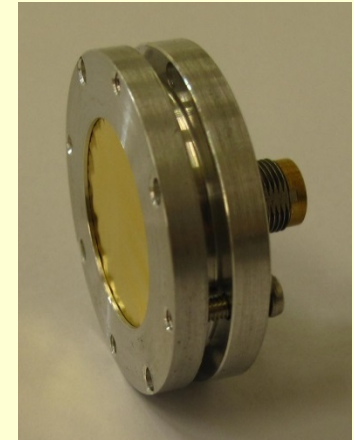
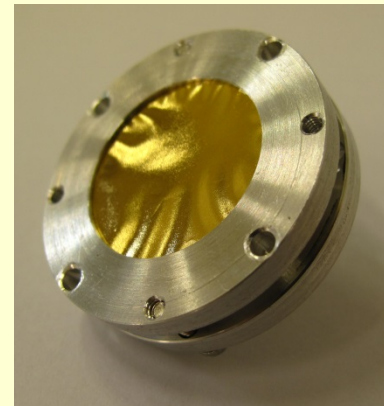
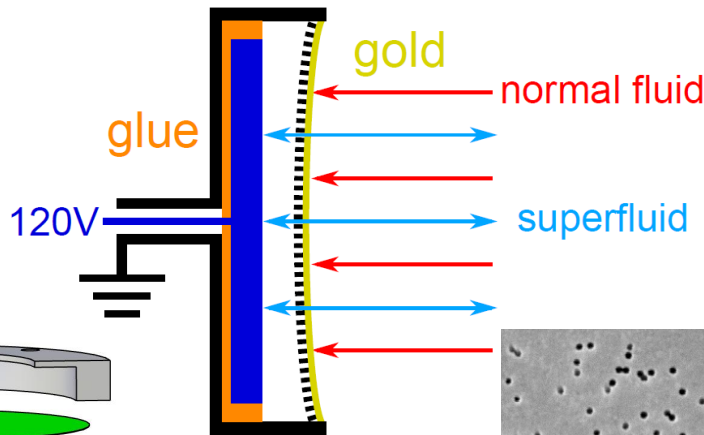


Diagnosics 6/8 an Introduction to OSTs

- Second sound in superfluid helium

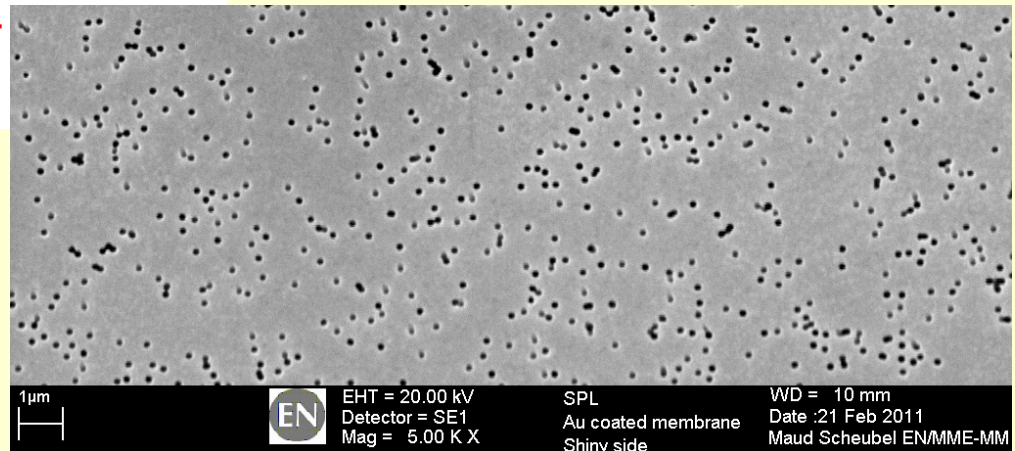
First used by K. Shepard at Argonne NL for detecting the quench location in split ring resonator

OST



Mohammed Fouaidy

Hannes Vennekate



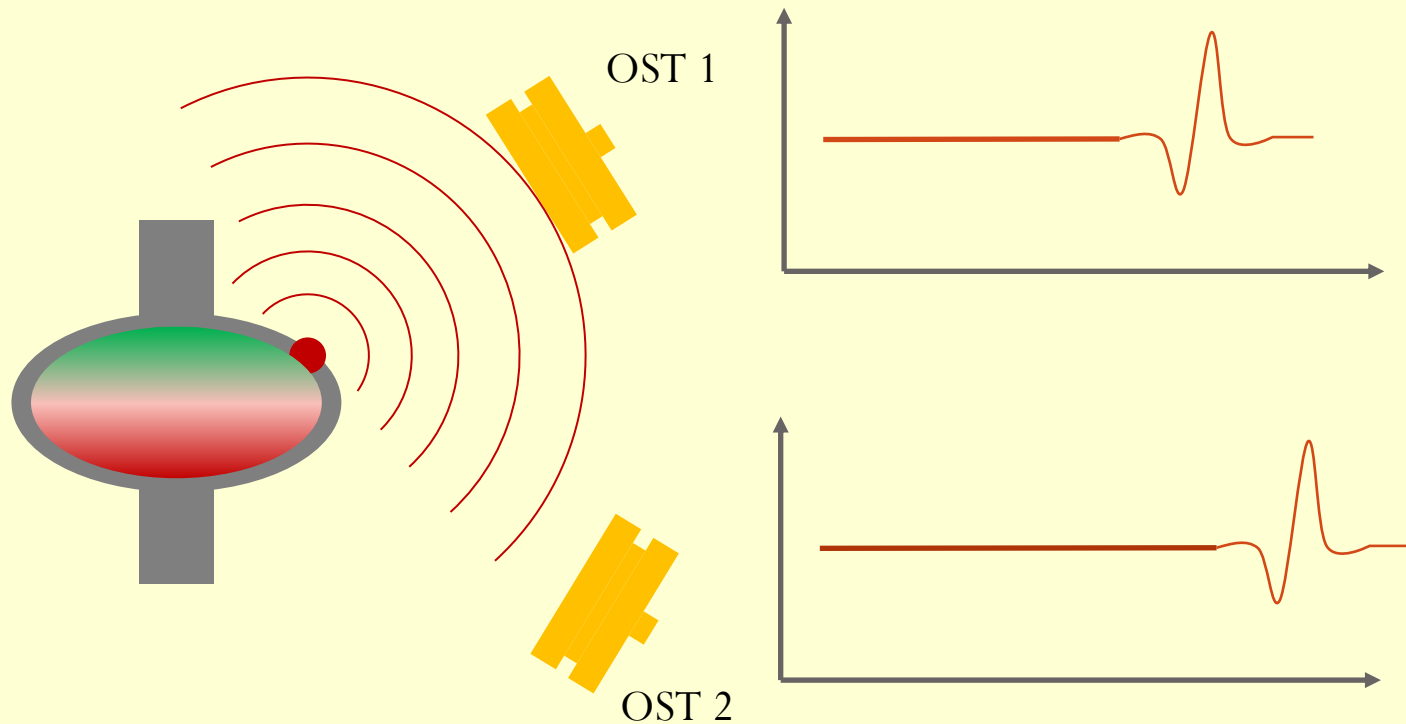
EN EHT = 20.00 kV
Detector = SE1
Mag = 5.00 K X

SPL
Au coated membrane
Shiny side

VWD = 10 mm
Date :21 Feb 2011
Maud Scheibel EN/MME-MM

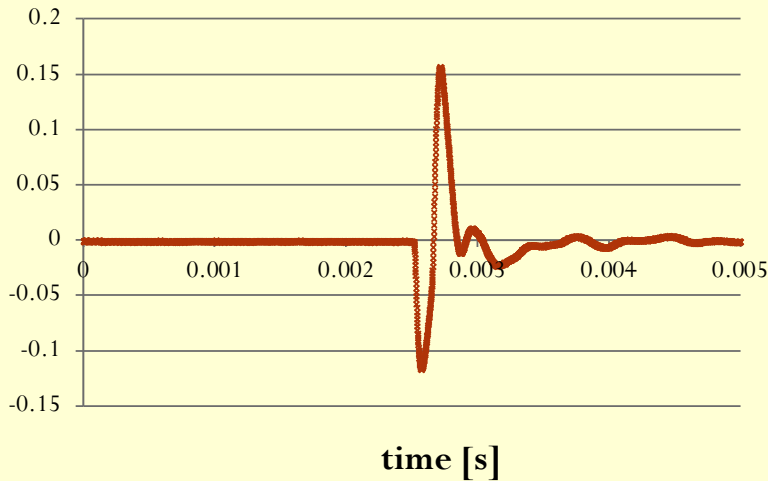
Diagnostics 7/8

- Detection and localisation of quenches on superconducting RF cavities by the measurement of the second sound with OSTs
- The localisation of a quench can be done with a relatively small number of sensors

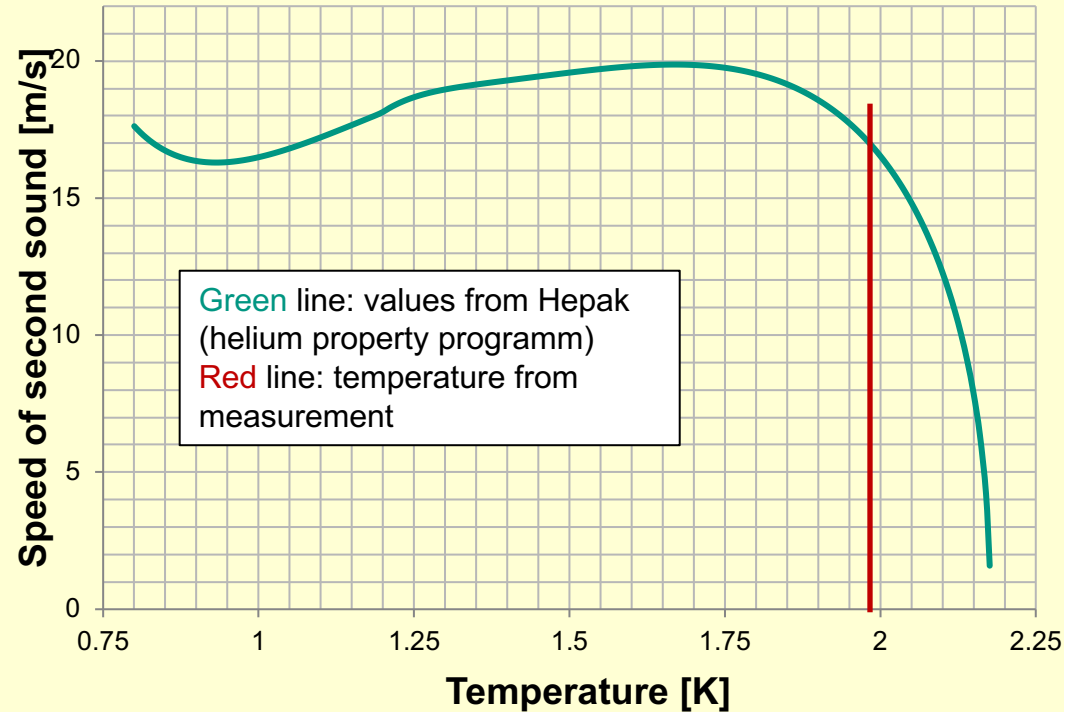


Diagnostics 8/8

OST signal



Speed of second sound in helium



- This measurement was done at 1.977 K
- $v_2(1.977 \text{ K}) = 17.14 \text{ m/s}$
- Signal of the measurement at $t = 2.52 \text{ ms}$
- Distance to heater $v_2 t = 4.32 \text{ cm}$

State of the art SRF research

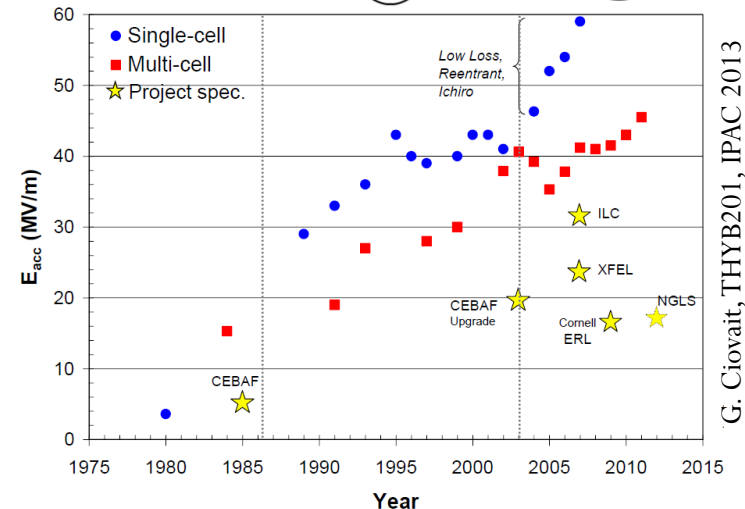
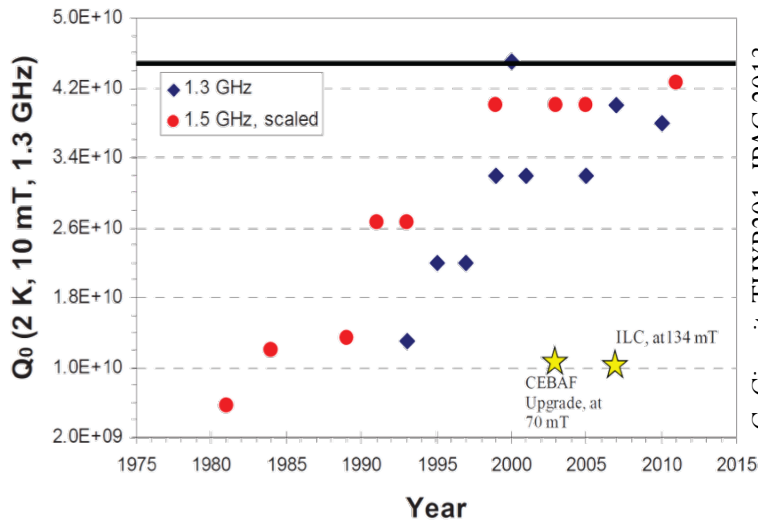
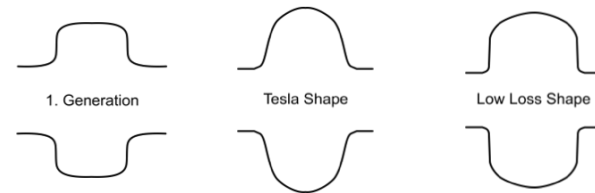
- Reaching ultimate performance with bulk Nb cavities
 - Maximizing the quality factor Q_0
 - Reaching high accelerating gradients E_{acc}
- Beyond Niobium: New materials
 - High temperature superconductors
 - Low temperature superconductors: Nb based materials

High Q versus high E_{acc}

- High Q is crucial for cw applications (e.g. light sources)
 - moderate E_{acc} (12 – 20 MV/m)
 - Cryogenics is cost driver
 - High Q reduces cryogenic load

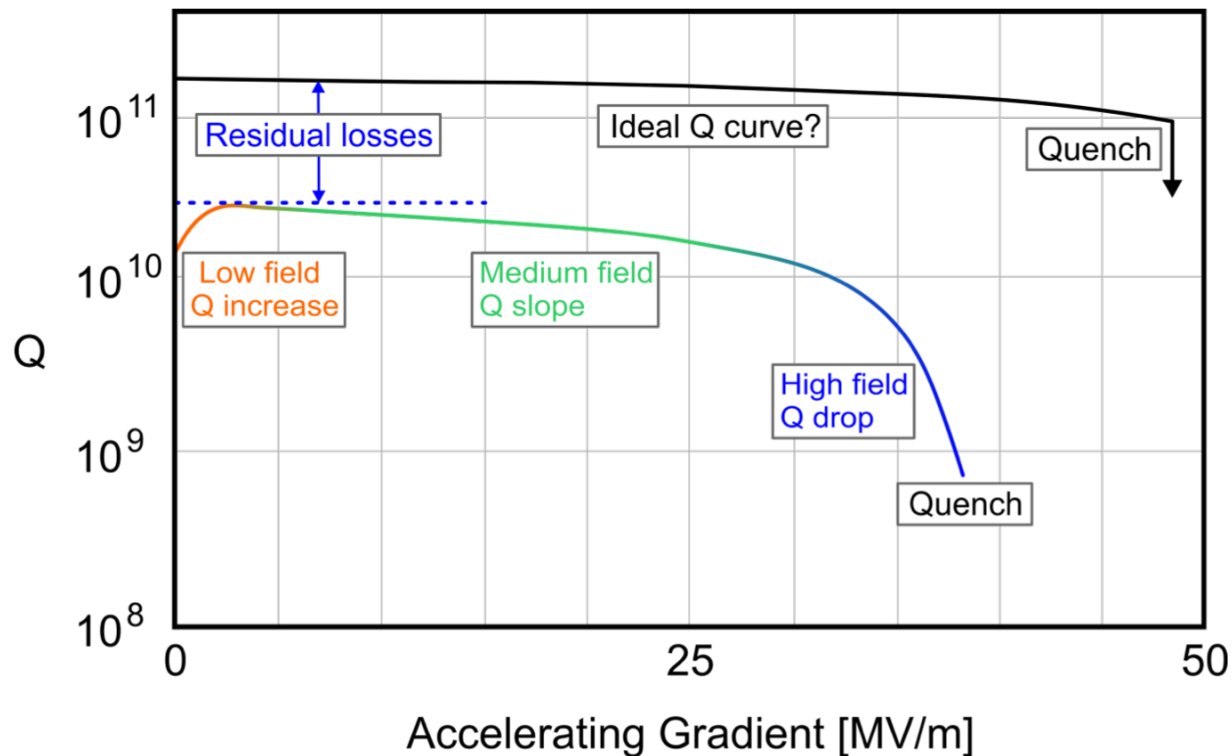
$$(P_{diss} \sim E_{acc}^2 / Q)$$

- High E_{acc} is crucial for pulsed applications (e.g. particle physics)
 - Machine size is cost driver.



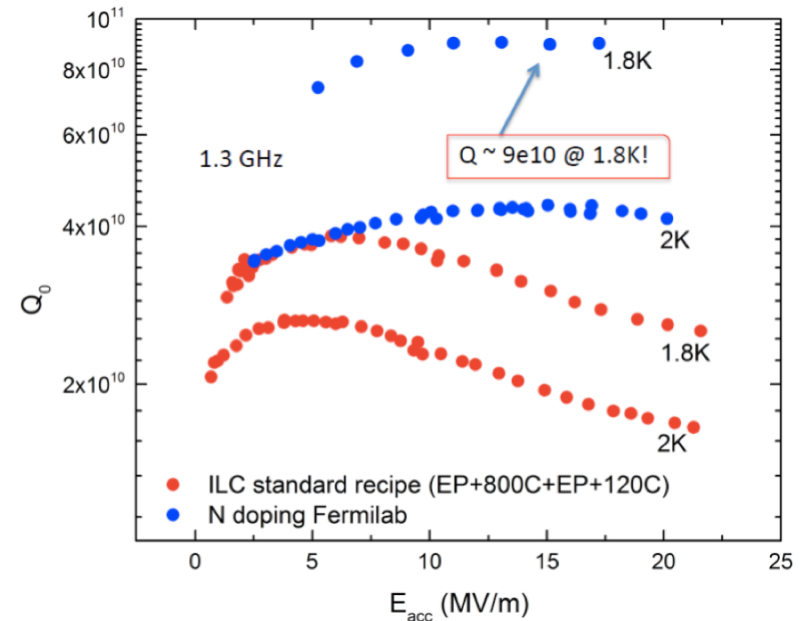
Maximizing Q: Ideal and Reality

- In the ideal case: Is Q constant up to the theoretical limit?
- Recent theoretical calculations yield increasing Q for increasing rf field. [See B.P. Xiao et al., Physica C 490 (2013)]



Maximizing Q: Improving treatments

- Baking at 800°C with injection of N₂ degrades cavity performance.
- After the removal of several μm by EP, the performance increases and exceeds baseline.
- Q slope reverses to “anti Q slope”.
- Comparison with Argon suggest interstitial effect instead of NbN formation.

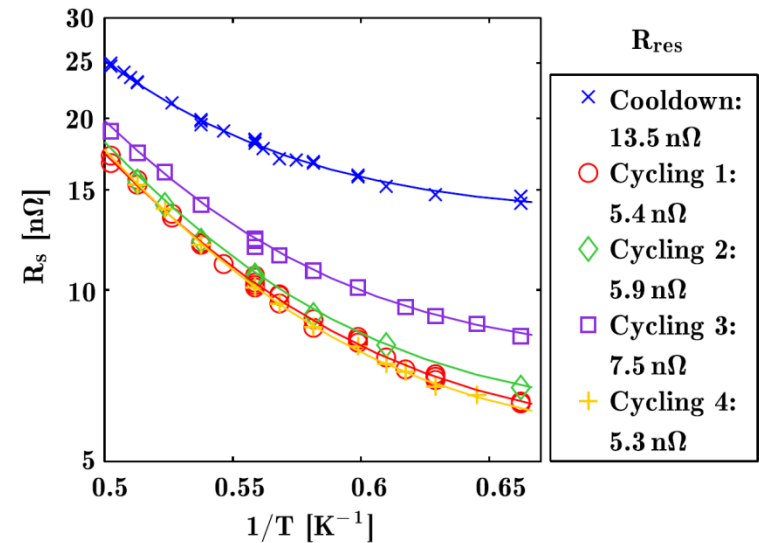


A. Grassellino, TUOAO3, SRF 2013

- Experimental data in good agreement with B.P. Xiao’s field dependent model.

Maximizing Q: Improving cooling procedures

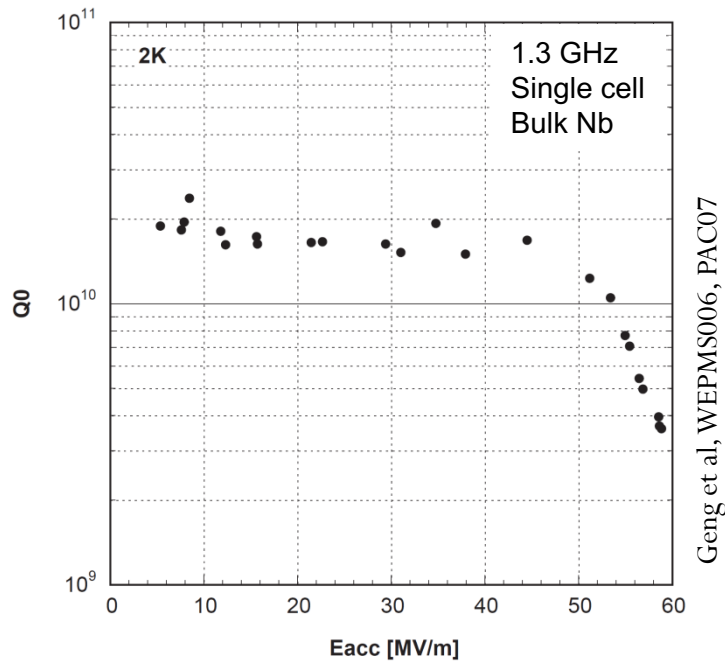
- Cooling speed through T_c and spatial temperature gradients impact the residual resistance.
- Measurements of the ambient field suggest that changes in flux trapping and the creation of thermal currents cause changes in R_{res} .



Vogt et al, PRST-AB 16.102002 (2013)

Achieving maximal gradients

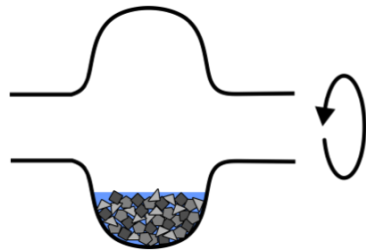
- World record $E_{\text{acc}} = 59 \text{ MV/m}$
($Q = 4 \cdot 10^9$)



- High performing cavities are limited by field emission or quench
- Avoiding emission sites by
 - Centrifugal barrel polishing: grinds larger defects
 - Improved Electro-polishing: smoothens surface on sub- μm scale
 - Cleaner handling: avoid (re-)contamination

Surface Preparation

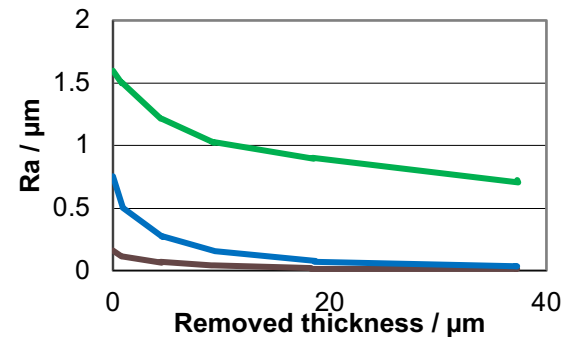
- Centrifugal barrel polishing:
 - Mechanical removal and smoothing of the surface with abrasive “stones”.



P. Michelato,
SRF Tutorials, 2013

- Produces a new damage layer that need to be etched.

- Electro-Polishing:
 - *Best* surface finish for cavities
 - Final roughness depends on initial surface finish



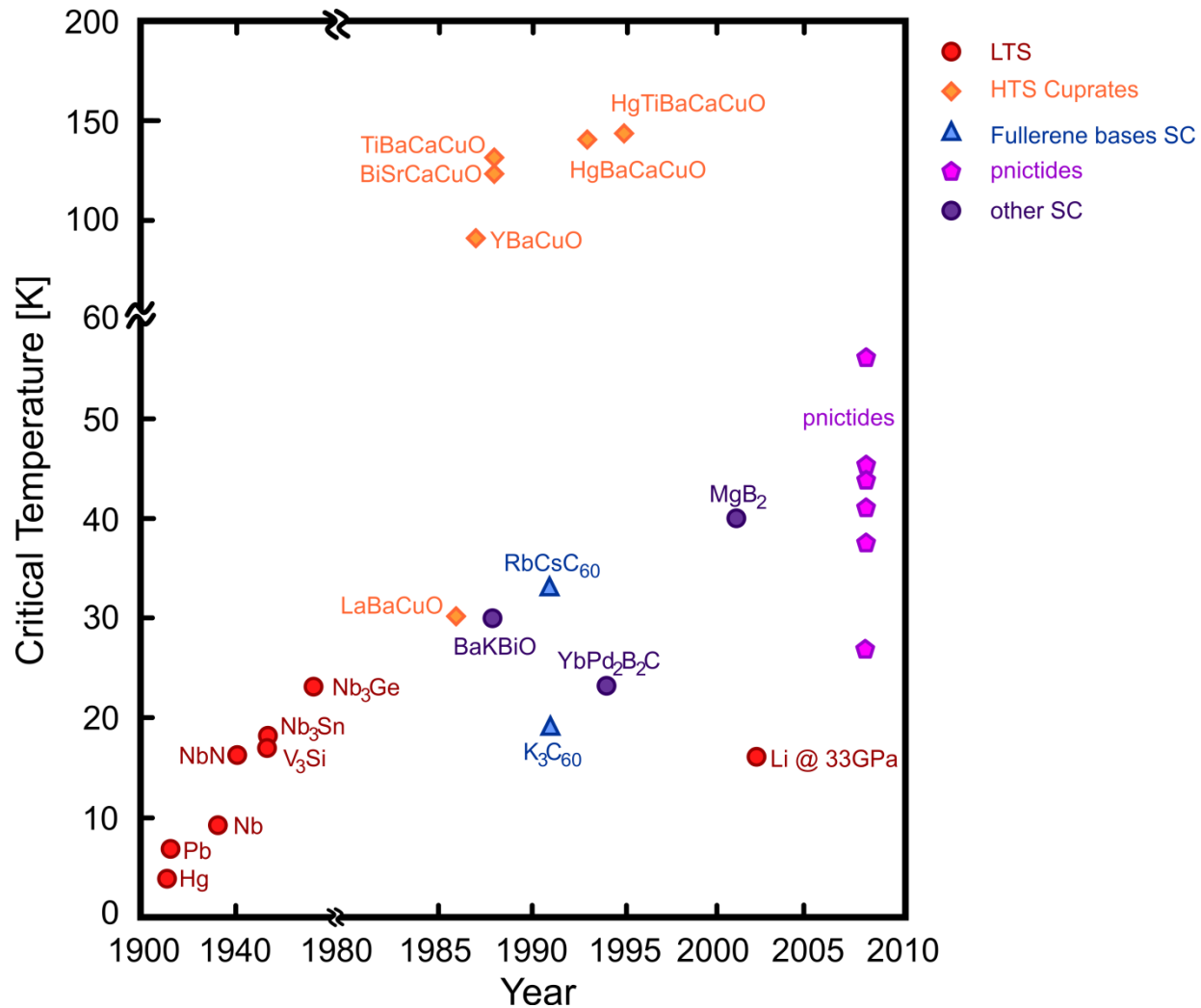
from: L. Ferreira,
B2FiftyTwo Seminar
Jan 2014

- Clean handling:
 - Any preparation of the surface and the final assembly needs to be done in a clean room (ISO 4).
 - Re-contamination has to be avoided.

Materials beyond Nb: Potential Benefits

- Higher Q due to lower BCS surface resistance:
 - Reduces cryogenic dynamic losses (operation costs)
 - Allows operation at higher temperature (reduces cryogenic static losses)
- Higher accelerating gradients:
 - Reduces installation costs due to more compact accelerators
- Reduced materials costs
 - Inexpensive materials, well formable, high thermal conductivity
- Simplified fabrication and assembly
 - Separating cavity shape from rf surface (Coatings)
 - More flexibility in design of cryomodules

Zoo of Superconductors



Materials beyond Niobium: Requirements

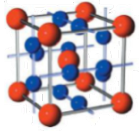
- High critical temperature T_c : $R_{BCS} \propto e^{(-\Delta/kT)}$; $T_c \propto \Delta$
 - Small penetration depth λ : $R_{BCS} \propto \lambda^3$
 - High critical field H_c : Operation at high gradient
 - High thermal conductivity: prevent quenches
-
- Compound phase should be stable over a broad composition range
 - Compound phase needs to be stable from 2 – 300 K
 - Material should be inert and formable

Classes of superconductors

	Nb	Low Temp. SC	MgB ₂	YBCO
T _c [K]	9.2	10 - 20	39	> 90
λ [nm]	40	60-180	140	150-1000
H _c [mT]	200	200-600	430	1400
κ	0.8	20-130	40	100
remarks			2 sc gaps	Ceramic, anisotropic

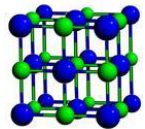
- High temperature superconductors are not suitable for srf applications
- Not all parameters are known for all potential candidates.

LTS: A15 & B1 compounds



A15 structure A_3B

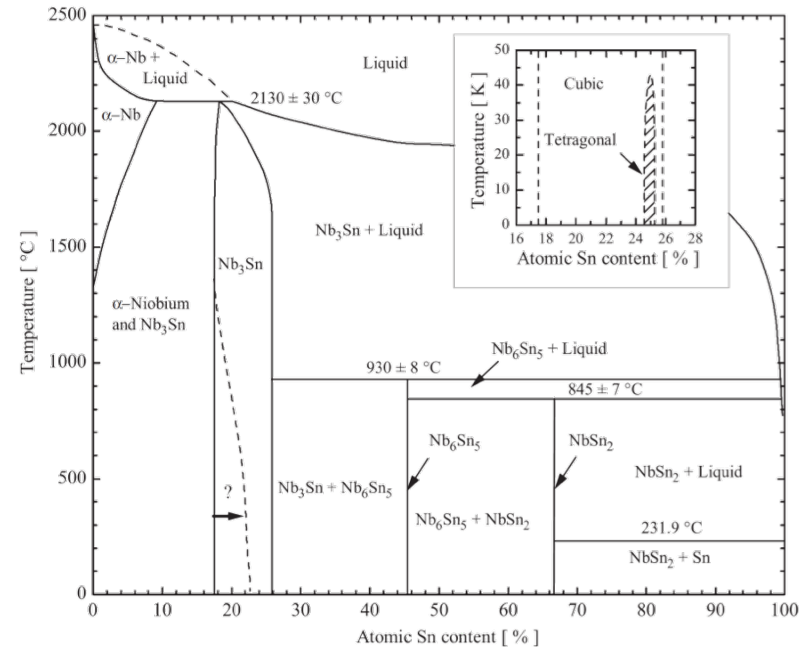
- A atoms: transition elements
- B atoms: non transition or transition elements
- Stable and high T_c : Nb_3Sn , V_3Ga , V_3Si , Mo_3Re
- A15 compounds are not formable due to extreme brittleness



B1 structure AB

- A atoms: metallic
- B atoms: non-metallic
- Stable and high T_c : NbC , NbN

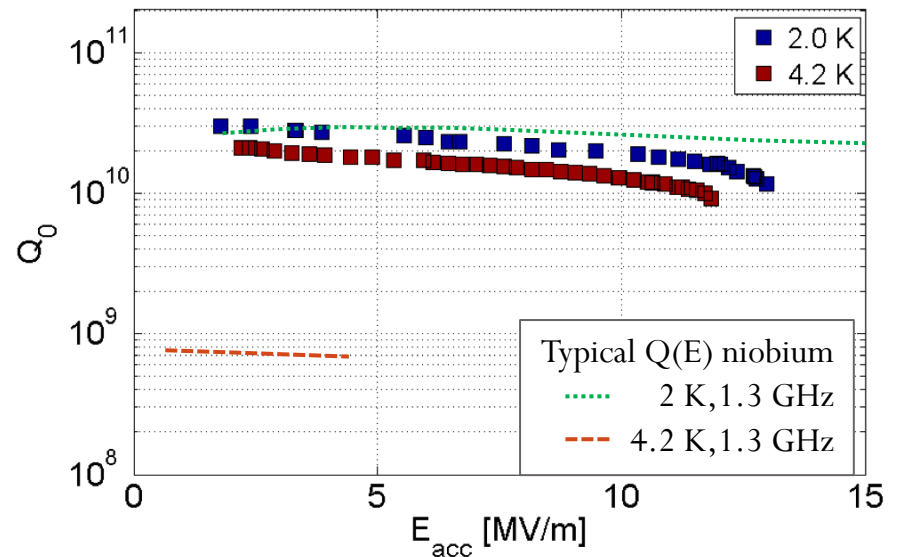
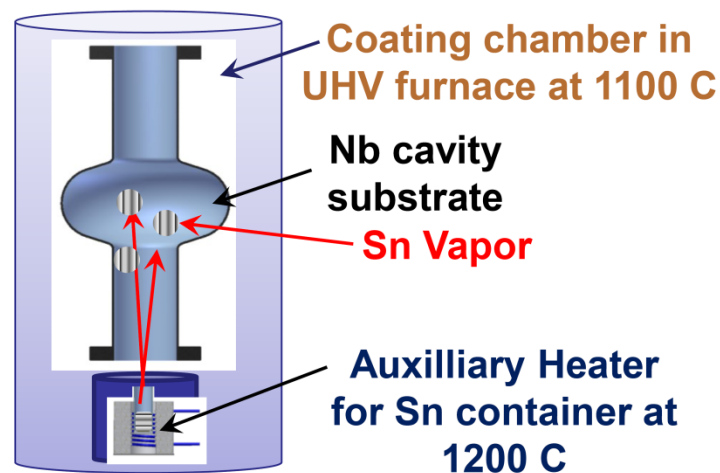
Phase diagram of the Nb-Sn system



A Godeke, Supercond. Sci. Technol. **19** (2006)
R68-R80

A15 compounds: Nb₃Sn

- Low thermal conductivity would favor coating a copper cavity with Nb₃Sn.
- Only successful fabrication so far: Sn vapor diffusion into Nb cavity, alloying Nb₃Sn (Wuppertal 1985, Cornell 2013)



Both pictures from: *Nb3Sn for SRF Application*
M. Liepe (Cornell), WEIOA04, SRF 2013

Summary

- For now, only high Q at moderate E_{acc} or high E_{acc} at moderate Q can be achieved.
- The high Q research tries to understand loss mechanisms and develops new recipes to minimize the residual resistance.
- Maximum E_{acc} can only be achieved by high-end surface preparation. Improving polishing and cleaning procedures is mandatory for multicell cavities and serial production.
- New materials have lower BCS surface resistance (higher Q) and/or higher critical field (higher E_{acc}).
- HTS are not suitable for rf applications.
- Nb_3Sn is the most promising alternative material so far.

ACKNOWLEDGMENT

- A lot of ‘material’ from CERN will be used but this does not mean that ‘material’ from other institutions is considered inferior.
- Other material was taken from contributions to the CERN Accelerator Schools, CAS ¹ (CERN-2006-002, CERN-2005-03, CERN-2005-04, CERN-2004-08, CERN-1996-03, CERN-1992-03, as well as earlier ones and other sources mentioned).
 - R. P. Feynman et al., Lectures on Physics Vol. II
 - P. Schmüser et al.; The Superconducting TESLA Cavities; Phys. Rev. Special Topics - AB 3 (9) 092001
 - A. W. Chao & M. Tigner, Handbook of Accelerator Physics and Engineering, World Scientific
 - Alexey Ustinov, Lecture on superconductivity, University Erlangen-Nürnberg (from which I used some slides w.r.t. Superconductivity)
- (http://www.pi.uni-karlsruhe.de/ustinov/group_hp/fluxon.physik.uni-erlangen.de/pages/lectures/WS_0708/Superconductivity-2007-01.pdf)
- and an excellent textbook of the field: H. Padamsee, J. Knobloch, and T. Hays, RF Superconductivity for accelerators & H. Padamsee, RF Superconductivity, Weinheim 2008, resp.

¹ <http://cdsweb.cern.ch/collection/CERN%20Yellow%20Reports>

Last but not least I thank my colleagues E. Haelbel and J. Tuckmantel for many discussions, clarifications, and presentation material.

BACKUP SLIDES

Surface tension at nc-sc interface 1/2

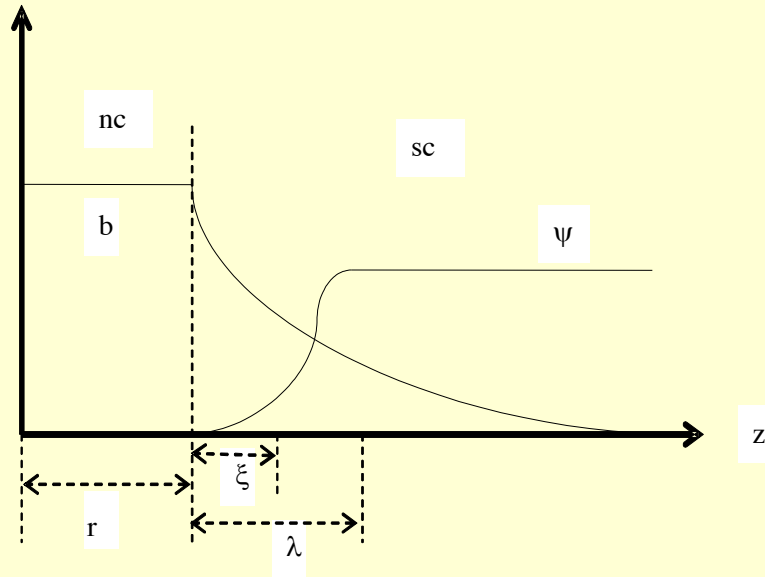


Fig. 1: Interface between normal to superconducting metal for a type II superconductor with $\lambda > \xi$. b denotes the (microscopic) magnetic field and ψ describes the wave function of the superconducting condensate.

Inspecting Fig. 1, the energy balance ΔE between the condensation energy E_c and the diamagnetic energy E_B for a planar interface area A and an applied magnetic field B , is

$$\begin{aligned} \Delta E &= \Delta E_c - \Delta E_B = \\ &= \frac{1}{2\mu_0} B_{th}^2 A(r + \xi) - \frac{1}{2\mu_0} B^2 A(r + \lambda) \end{aligned}$$

Surface tension at nc-sc interface 2/2

For a type II superconductor, as the penetration of magnetic fields starts from small filaments of cylindrical shape located parallel to the interface, a more realistic way to describe the energy balance is based on a small half-cylinder of radius r instead of a plane, which will become normal:

$$\Delta E = \Delta E_c - \Delta E_B = \frac{1}{2\mu_0} \cdot B_{th}^2 \cdot \frac{\pi}{2} \cdot (r + \xi)^2 - \frac{1}{2\mu_0} \cdot B^2 \cdot \frac{\pi}{2} \cdot (r + \lambda)^2 < 0 ,$$

from which the threshold B_{c1}^* of the magnetic field for penetration is defined as

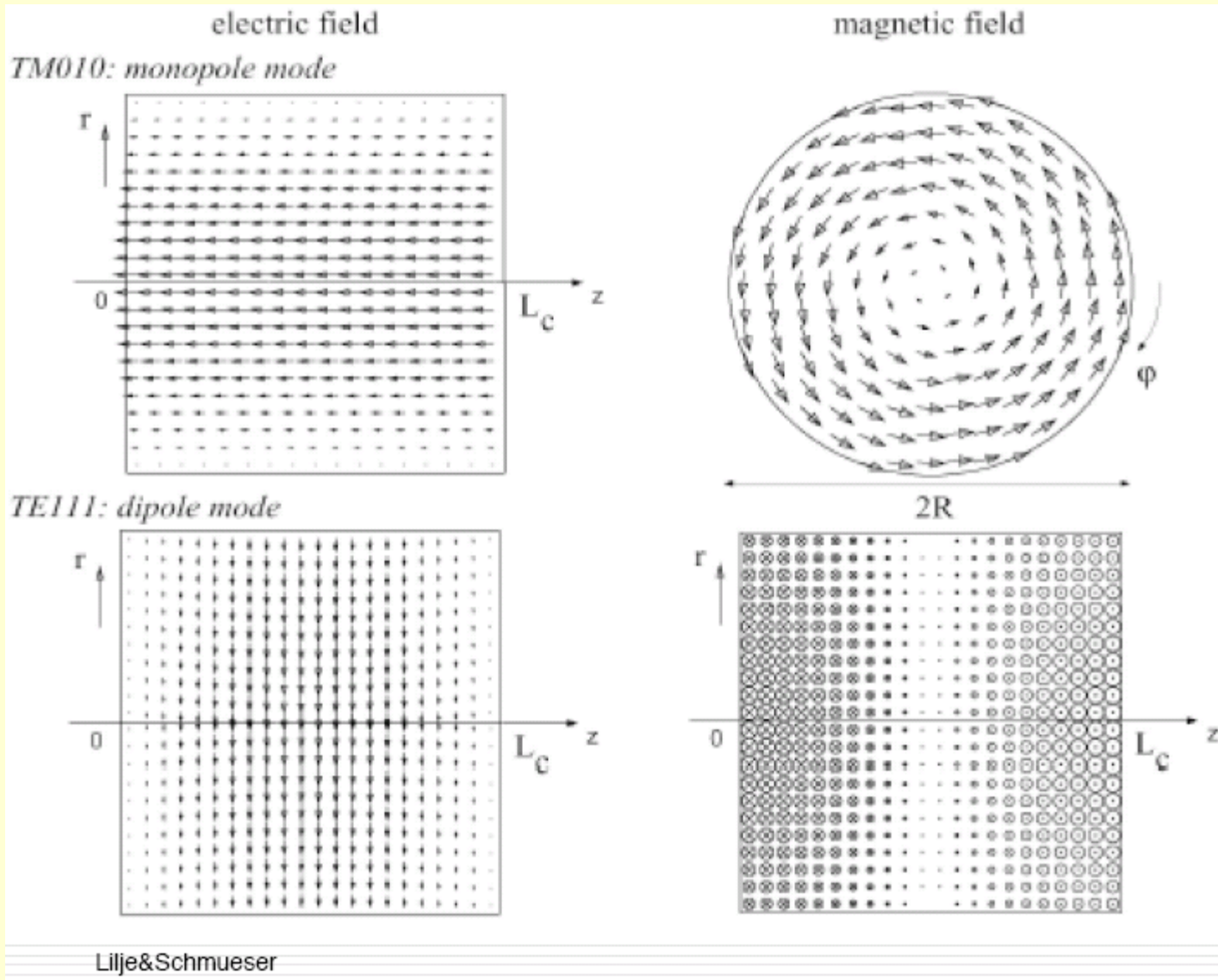
$$B_{c1}^* \geq \frac{r + \xi}{r + \lambda} \cdot B_{th} \xrightarrow{r \rightarrow 0} \frac{\overset{1/\kappa}{\xi}}{\lambda} \cdot B_{th} = \frac{1}{\kappa} \cdot B_{th} .$$

In a type II superconductor, the lowest value of the applied magnetic field B which induces penetration as filaments of magnetic field into the bulk is called the lower critical field B_{c1} , for which the microscopic theory gives as exact result:

$$B_{c1} = \frac{\ln \kappa}{\sqrt{2} \cdot \kappa} \cdot B_{th} ,$$

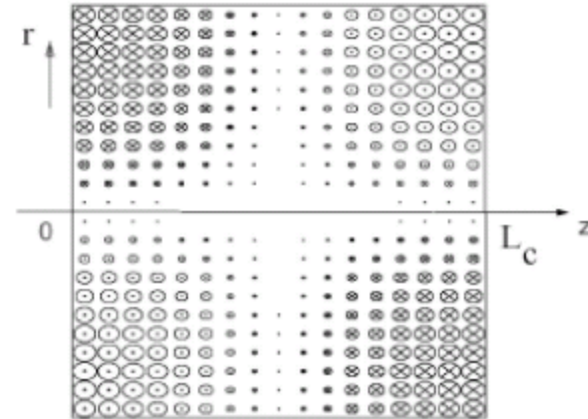
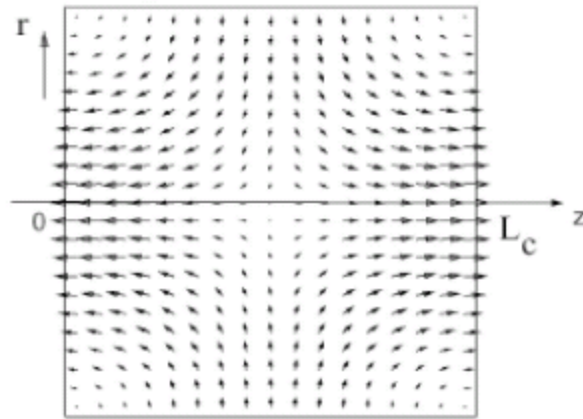
very close to the previous one. In a type I superconductor, the lowest value of the applied magnetic field B which induces bulk penetration of magnetic field is called the thermodynamic critical field B_{th}

Different mode families $1/2$



Different mode families 2/2

TM₀₁₁: monopole mode



TM₁₁₀: dipole mode

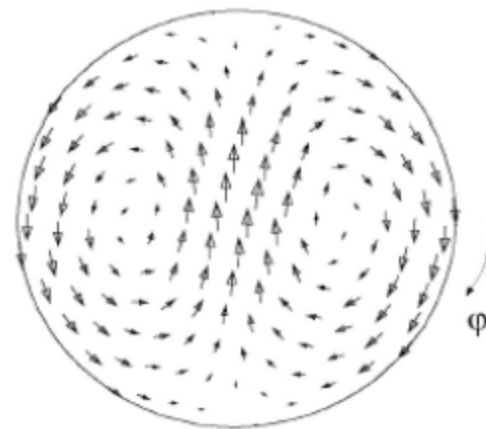
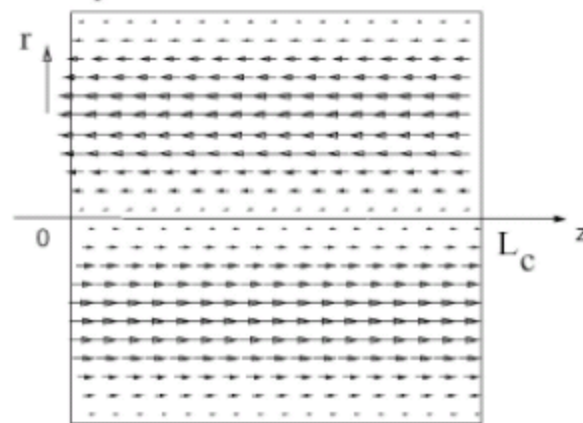
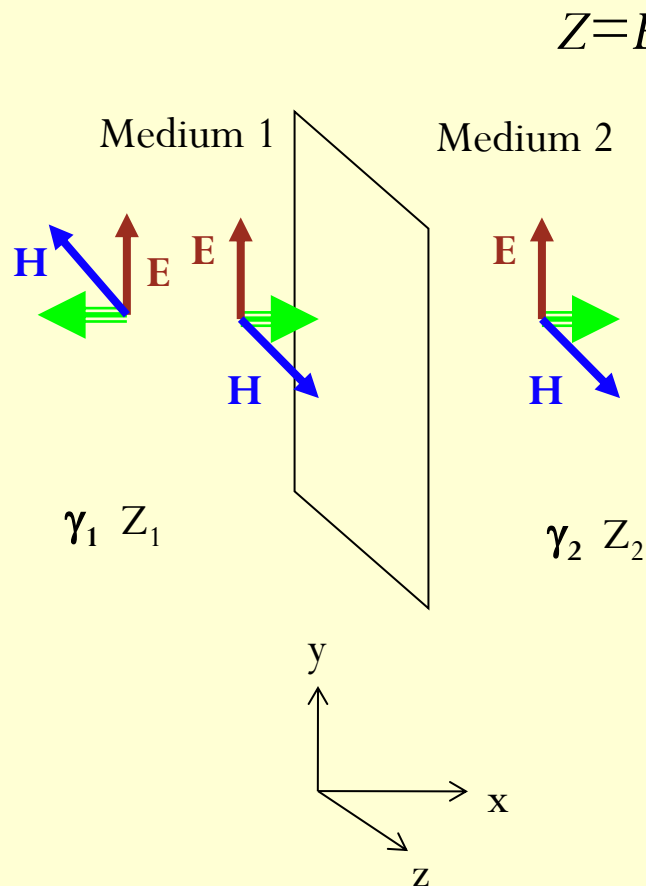


Figure 1: Electric and magnetic field in a pillbox cavity for several resonant modes (Courtesy of M. Liepe).

Lilje&Schmueser

Transmission line 1/2

Introduction of the notion of reflection and transmission factors.



$$Z = E_y / H_z$$

$$E_{yi} = \hat{E} e^{-\gamma_1 x} e^{i\omega t}$$

$$H_{zi} = \frac{\hat{E}}{Z_1} e^{-\gamma_1 x} e^{i\omega t}$$

$$E_{yr} = \rho \hat{E} e^{\gamma_1 x} e^{i\omega t}$$

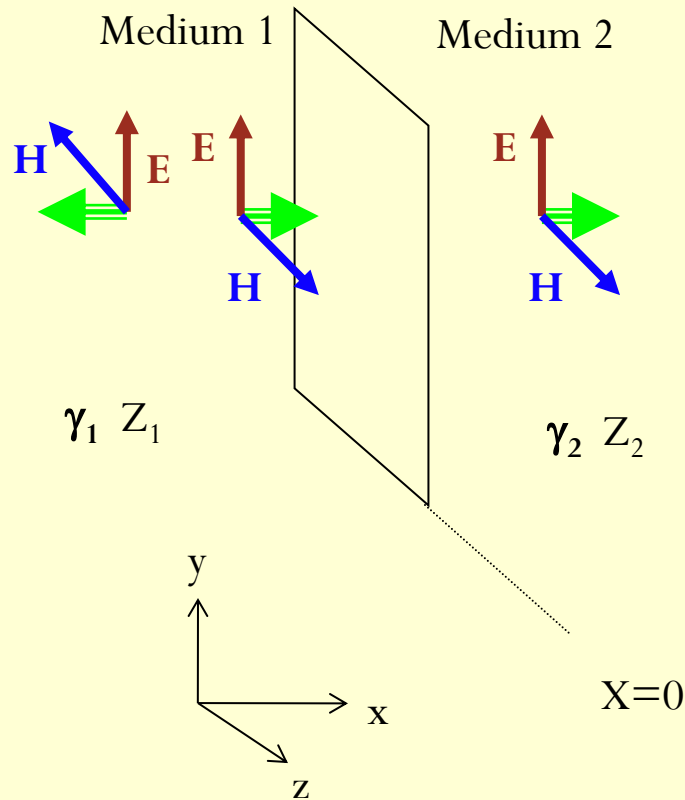
$$H_{zr} = -\rho \frac{\hat{E}}{Z_1} e^{\gamma_1 x} e^{i\omega t}$$

$$E_{yt} = \tau \hat{E} e^{-\gamma_2 x} e^{i\omega t}$$

$$H_{zt} = \tau \frac{\hat{E}}{Z_2} e^{-\gamma_2 x} e^{i\omega t}$$

Transmission line 2/2

From continuity at the interface:
$$\left. \begin{aligned} E_{yi} + E_{yr} &= E_{yt} \\ H_{zi} + H_{zr} &= H_{zt} \end{aligned} \right\} x = 0$$



$$1 + \Gamma = \tau$$

$$\frac{1}{Z_1} - \Gamma \frac{1}{Z_1} = \tau \frac{1}{Z_2}$$

$$\frac{Z_2}{Z_1} (1 - \Gamma) = \tau$$

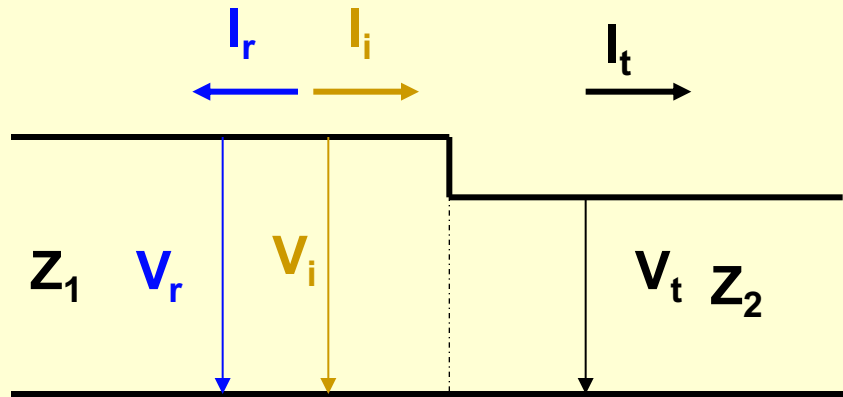
$$1 + \Gamma = \frac{Z_2}{Z_1} (1 - \Gamma)$$

$$\Gamma = \frac{Z_2 - Z_1}{Z_2 + Z_1}$$

$$\tau = \frac{2Z_2}{Z_2 + Z_1}$$

Response of a cavity to RF ^{1/5}

- Apply transmission line theory (to a one-port impedance):



$$V_t = V_i + V_r$$

$$I_t = I_i - I_r$$

$$V_t = \tau \cdot V_i$$

$$V_r = \Gamma \cdot V_i$$

$$V_r = Z_1 \cdot I_i$$

$$V_t = Z_2 \cdot I_t$$

Reflexion factor ρ

Transmission factor τ

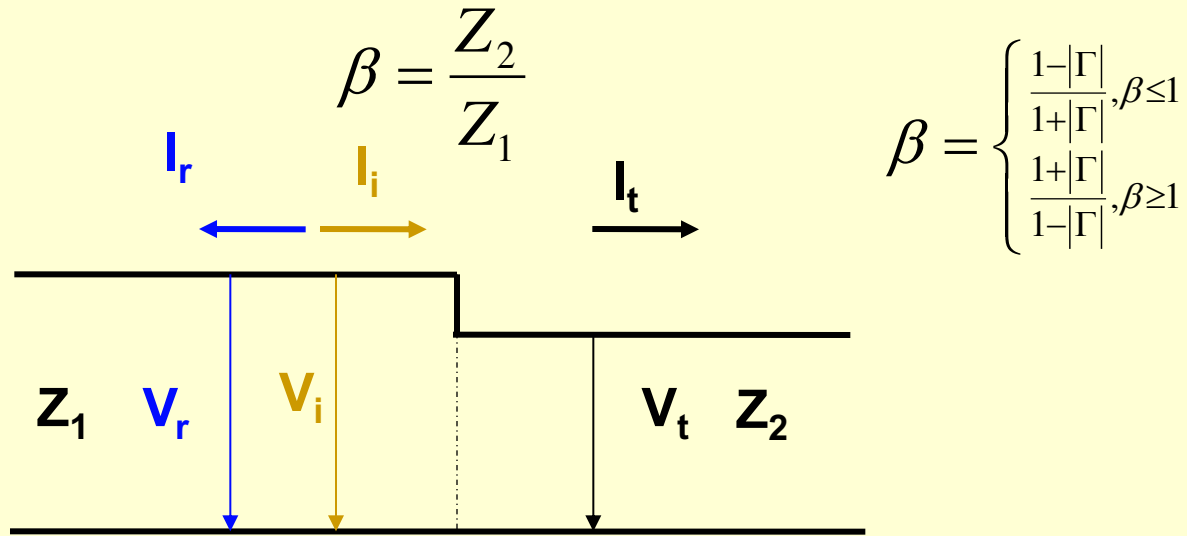
$$\Rightarrow \Gamma = \frac{Z_2 - Z_1}{Z_2 + Z_1}$$

$$\Rightarrow \tau = \frac{2 \cdot Z_2}{Z_2 + Z_1}$$

$$\tau - \Gamma = \frac{2 \cdot Z_2 - (Z_2 - Z_1)}{Z_1 + Z_2} = 1$$

Response of a cavity to RF 2/5

- Reflexion factor Γ depends on position, the coupling factor β does not:



$$|\Gamma| = \left| \frac{Z_2 - Z_1}{Z_2 + Z_1} \right| = \left| \frac{Z_2/Z_1 - 1}{Z_2/Z_1 + 1} \right| = \begin{cases} \frac{\beta-1}{\beta+1}, \text{if } \beta \geq 1 \\ \frac{1-\beta}{1+\beta}, \text{if } \beta \leq 1 \end{cases}$$

$$|\tau| = |1 + \Gamma|_{\rho \geq 0} = 1 + |\Gamma| = 1 + \frac{\beta-1}{\beta+1} = \frac{2\beta}{1+\beta} \quad |\tau| = |1 - \Gamma|_{\rho \leq 0} = 1 - |\Gamma| = 1 - \frac{1-\beta}{1+\beta} = \frac{2\beta}{1+\beta}$$

Response of a cavity to RF ^{3/5}

- Determination of Q_0 and accelerating voltage/gradient

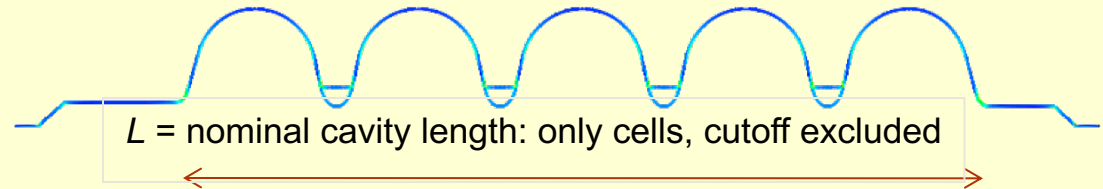
$$V_t = \tau \cdot V_i = \frac{2\beta}{1+\beta} V_i \Rightarrow V_t^2 = \frac{4\beta^2}{(1+\beta)^2} V_i^2 = \frac{8\beta^2}{(1+\beta)^2} \cdot \underbrace{Z_1}_{(R/Q)Q_0/\beta} \cdot \underbrace{\frac{V_i^2}{2Z_1}}_{P_i} \quad 1)$$

$$\Rightarrow V_t = \sqrt{\frac{8\beta}{(1+\beta)^2} \cdot (R/Q) \cdot Q_0 \cdot P_i}$$

$$\frac{1}{Q_L} = \frac{1}{Q_0} + \frac{1}{Q_{ext}} = \frac{1 + \frac{Q_0}{Q_{ext}}}{Q_0} \Rightarrow Q_0 = \left(1 + \frac{Q_0}{\underbrace{Q_{ext}}_{=\beta}} \right) \cdot Q_L = (1 + \beta) \cdot \underbrace{Q_L}_{\omega\tau}$$

$$\beta = \begin{cases} \frac{1-|\Gamma|}{1+|\Gamma|}, & \beta \leq 1 \\ \frac{1+|\Gamma|}{1-|\Gamma|}, & \beta \geq 1 \end{cases}$$

$$E_{acc} = V_t / L$$

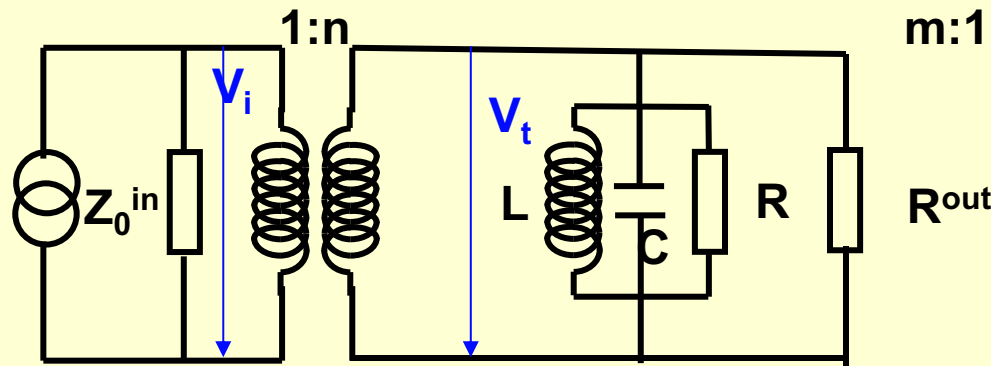
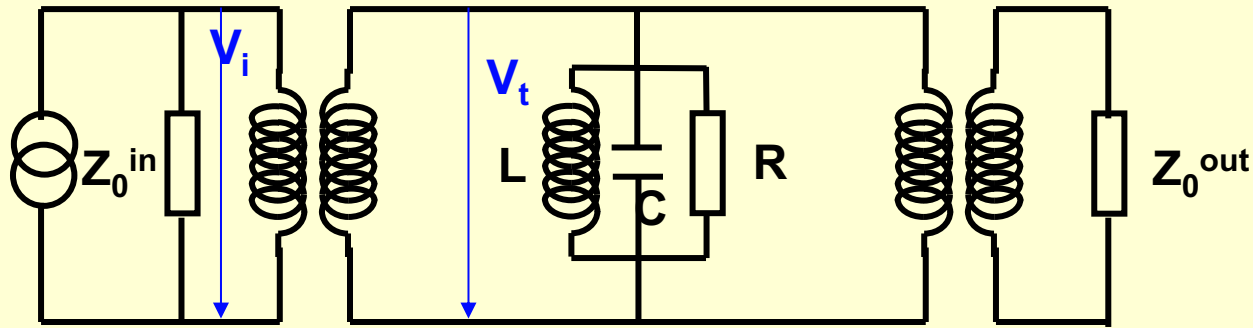


1) Remember

$$Z_1 = \frac{Z_1}{\underbrace{Z_2}_{1/\beta}} \cdot Z_2 = \frac{Z_2}{\beta} = \frac{R}{\beta} = \frac{1}{\beta} \cdot \frac{R}{\underbrace{V_c^2/2}_{P_c}} \cdot \omega U \cdot \frac{V_c^2}{2\omega U} = \frac{1}{\beta} \cdot \frac{\omega U}{\underbrace{P_c}_{Q_0}} \cdot \frac{V_c^2}{\underbrace{2\omega U}_{R/Q}} = \frac{(R/Q) \cdot Q_0}{\beta}$$

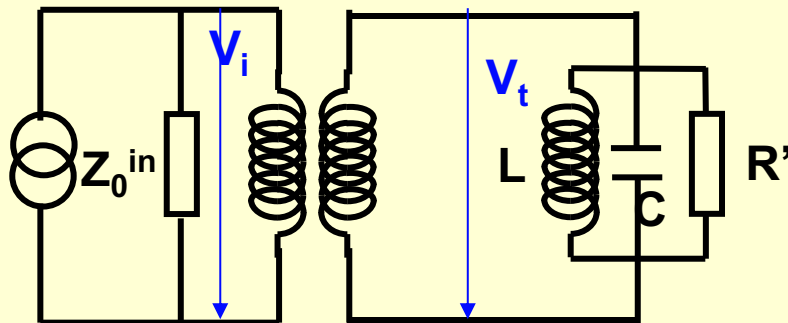
Response of a cavity to RF 4/5

- The response of a **two port cavity** is equivalent to that of a one-port cavity



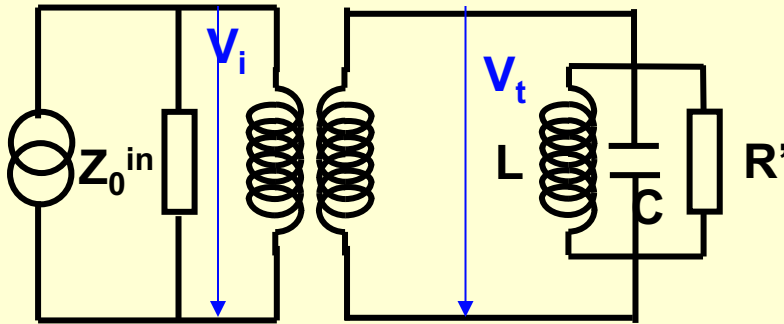
$$R^{out} = m^2 Z_0^{out}$$

$$m^2 = \frac{(R/Q) \cdot Q_{ext}^{out}}{Z_0^{out}}$$



$$\frac{1}{R'} = \frac{1}{R} + \frac{1}{R^{out}}$$

Response of a cavity to RF 5/5



$$V_t = \tau \cdot V_i = \frac{2\beta'}{1 + \beta'} V_i \Rightarrow V_t^2 = \frac{4\beta'^2}{(1 + \beta')^2} V_i^2 = \frac{8\beta'^2}{(1 + \beta')^2} \cdot \underbrace{Z_0^{in}}_{(R/Q)Q_0'/\beta'} \cdot \underbrace{\frac{V_i^2}{2Z_0^{in}}}_{P_i}$$

$$\Rightarrow V_t = \sqrt{\frac{8\beta'}{(1 + \beta')^2} \cdot (R/Q) \cdot Q_0' \cdot P_i}$$

$$Q_0' = (1 + \beta') \cdot \underbrace{Q_L}_{\omega\tau}$$

$$E_{acc} = V_t / L$$

$$\beta' = \begin{cases} \frac{1 - |\Gamma|}{1 + |\Gamma|}, \beta' \leq 1 \\ \frac{1 + |\Gamma|}{1 - |\Gamma|}, \beta' \geq 1 \end{cases}$$

$$\frac{1}{Q_0} = \frac{1}{Q_0'} - \frac{1}{Q_{ext}^{out}}$$

$$Q_{ext}^{out} = \frac{\omega U}{P_{out}} = \frac{V^2}{2 \cdot (R/Q) \cdot P_{out}}$$

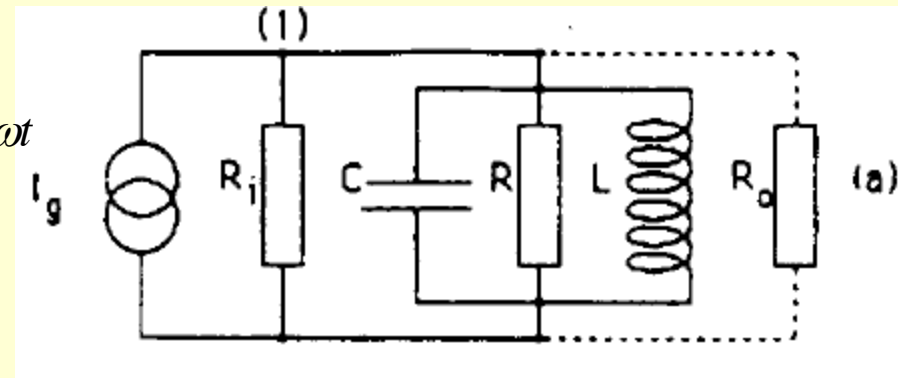
Transient Response 1/2

1. Apply Kirchhoff's current law at node (1)

$$\frac{V}{R_i} + \frac{1}{L} \int V(t) + C \frac{dV}{dt} + \frac{V}{R} = I_{g0} \cdot \cos \omega t$$

2. Differentiate and transform lumped circuit elements into cavity parameters by using preceding "Table 7"

$$\frac{d^2 V}{dt^2} + \frac{\omega_0}{Q_L} \frac{dV}{dt} + \omega_0^2 V = -I_{g0} \cdot \left(\frac{R}{Q} \right) \cdot \omega \cdot \omega_0 \cdot \sin \omega t$$



3. Find the general solution of the homogeneous differential equation

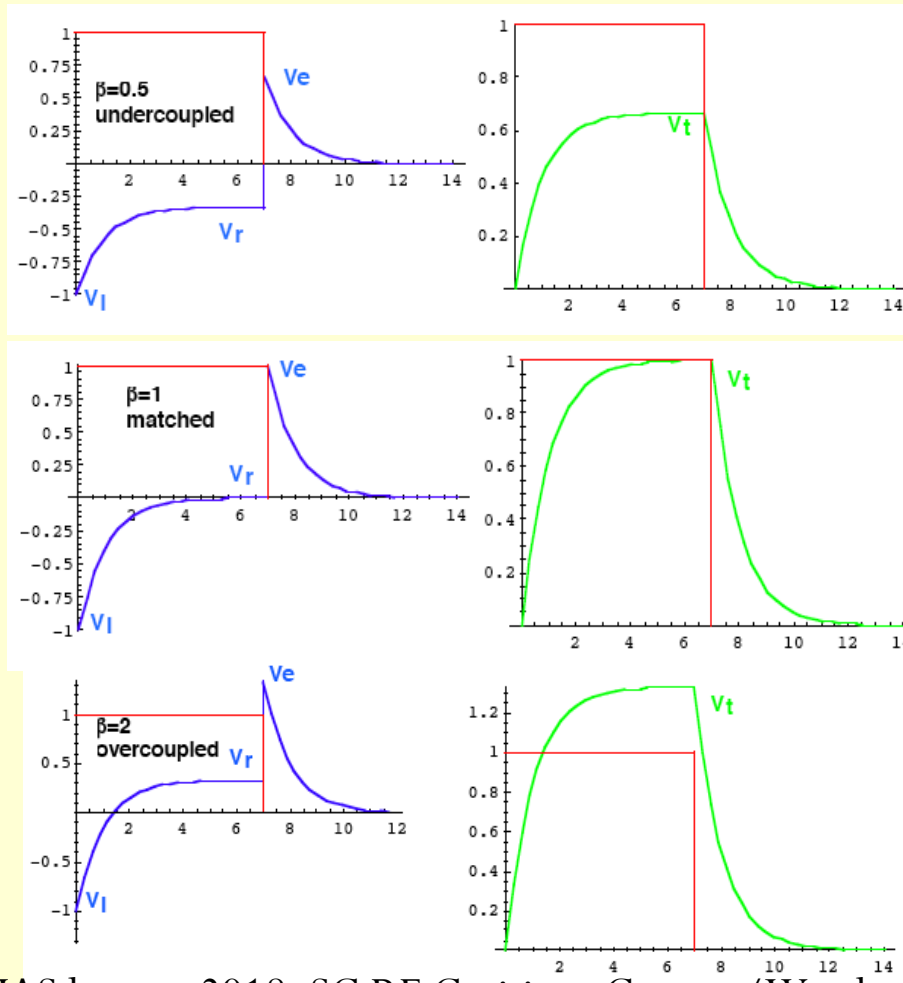
$$V(t) = e^{-\frac{\omega_0 t}{2Q_L}} \cdot \left(c_1 \cdot e^{i\sqrt{1-1/(2Q_L)^2} \cdot \omega_0 t} + c_2 \cdot e^{-i\sqrt{1-1/(2Q_L)^2} \cdot \omega_0 t} \right)$$

4. Find the solution of the inhomogeneous differential equation

$$V(t) = V_0 \cdot \cos \omega_0 t \cdot \left\{ 1 - e^{-\frac{\omega_0 t}{2Q_L}} \right\}$$

Transient response 2/2

- Determination of Q_0 and accelerating voltage/gradient (2)
- Oscilloscope signal for voltage measurement



$$V_t = V_i + V_r$$

Remember: $V_e = V_i + V_r$

$$|\rho| = \left| \frac{V_r}{V_i} \right| \Rightarrow 1^{\text{st}} \text{ method:}$$

$$\beta = \frac{1 - \left| \frac{V_r}{V_i} \right|}{1 + \left| \frac{V_r}{V_i} \right|} = \begin{cases} \frac{|V_i| - |V_r|}{|V_i| + |V_r|}; \beta \leq 1 \\ \frac{|V_i| + |V_r|}{|V_i| - |V_r|}; \beta \geq 1 \end{cases}$$

$$2^{\text{nd}} \text{ method: } \beta = \frac{1 - \left| \frac{V_r}{V_i} \right|}{1 + \left| \frac{V_r}{V_i} \right|} = \frac{1 - \left| \frac{V_i - V_e}{V_i} \right|}{1 + \left| \frac{V_i - V_e}{V_i} \right|} =$$

$$= \frac{|V_e|}{2 \cdot |V_i| - |V_e|} = \frac{1}{2 \cdot \left| \frac{V_i}{V_e} \right| - 1}$$